R81-16

OSP 89809
OSP 89964

SIMULATION OF RANDOM FIELDS WITH THE TURNING BANDS METHOD

by
ARISTOTELIS MANTOGLOU
and
JOHN L. WILSON

RALPH M. PARSONS LABORATORY
HYDROLOGY AND WATER RESOURCES SYSTEMS

Department of Civil Engineering
Massachusetts Institute of Technology

Report No. 264

Prepared with the partial support of the Office of Surface Mining, Department of Interior through M.I.T.'s Mining and Mineral Resources Research Institute, and the Agency for International Development, Department of State, through M.I.T.'s Technology Adaptation Program

July 1981

DEPARTMENT
OF
CIVIL
ENGINEERING

SCHOOL OF ENGINEERING
MASSACHUSETTS INSTITUTE OF TECHNOLOGY
Cambridge, Massachusetts 02139

R81-16

OSP 89809
OSP 89964

SIMULATION OF RANDOM FIELDS WITH THE TURNING BANDS METHOD

by
ARISTOTELIS MANTOGLOU
and
JOHN L. WILSON

RALPH M. PARSONS LABORATORY
HYDROLOGY AND WATER RESOURCES SYSTEMS

Department of Civil Engineering
Massachusetts Institute of Technology

Report No. 264

Prepared with the partial support of the Office of Surface Mining, Department of Interior through M.I.T.'s Mining and Mineral Resources Research Institute, and the Agency for International Development, Department of State, through M.I.T.'s Technology Adaptation Program

July 1981

ABSTRACT

SIMULATION OF RANDOM FIELDS WITH THE TURNING BANDS METHOD

by

Aristotelis Mantoglou and John L. Wilson

This report presents and extends the Turning Bands Method (TBM) for the synthetic simulation of random fields. Originally introduced by G. Matheron (1973) of the Ecole des Mines de Paris, the TBM can be applied to stationary or non-stationary fields.

For two and three dimensional stationary isotropic fields the general TBM equations are derived with particular emphasis on the two dimensional case. In a new approach the unidimensional line process is generated by a simple spectral method, a technique which can be generally applied for any two dimensional covariance function and is easily extended to anisotropic processes. In a second approach the line process is generated as a moving average process for which corresponding one dimensional equivalents are derived for special two dimensional covariance functions. The convergence properties of the TBM with the number of lines is described mathematically and by example, and guidelines are presented for the selection of model parameters. The TBM is compared to other methods in terms of cost and accuracy, demonstrating that the TBM is as accurate and far less expensive than any other existing technique.

Using the unidimensional spectral method the TBM is extended to the direct generation of stationary anisotropic processes. Examples of this generation are given with a comparison between theoretical and sample statistics.

Equations are derived giving the covariance function and the spectral density function for the process of areal averages of stationary processes. It is observed that reduced covariance between areas can damp out quickly, relative to the size of the areas, suggesting the possibility of approximating areal average covariance by point covariance in some instances. The areal average process is, in general, anisotropic. Thus the anisotropic TBM is applied for direct generation of the areal average process. The comparison of the theoretical and sample statistics is excellent.

The Turning bands method for the simulation of nonstationary random fields (IRF) is presented, using a Wiener-Levy process for line generation as suggested by Matheron (1973). Examples are given for IRF's of zero, first and second order.

ACKNOWLEDGEMENTS

This work was supported in part by funds from the Office of Surface Mining, Department of Interior, under Grant No. G5105071 through M.I.T.'s Mining and Mineral Resources Research Institute (OSP 89809); and from the Agency for International Development, Department of State through M.I.T.'s Technology Adaptation Program (OSP 89964). Any opinions, findings, and conclusions or recommendations expressed in this report are those of the authors and do not necessarily reflect the views of the sponsors.

This report essentially constitutes, with a few later additions, the work presented by the first author as a Master's Thesis to the Department of Civil Engineering in January 1981. The thesis was supervised by the second author.

The contribution of Professor Rafael Bras, particularly in the first stages of this work, as well as his support in the publication of this report, is greatfully acknowledged.

We would also like to thank the following Graduate Research Assistants of the Parsons Laboratory for their helpful suggestions. Mr. Konstantine Georgakakos participated in many discussions and reviewed the original material making several valuable suggestions. Mr. Carlos Puente and Mr. Lloyd Townley participated in useful discussions, while Mr. Pedro Restrepo-Posada provided computer consulting during some difficult moments.

Ms. Carole Solomon typed the original version of the report with skill and patience.

TABLE OF CONTENTS

LIST OF FIGURES

LIST OF PRINCIPAL SYMBOLS

$A(\underline{u})$	Region of area A corresponding to vector $\underline{u}$
$a_{\underline{h}}(\underline{\omega})$	A characteristic function of two regions at vector distance $\underline{n}$
$a_{\underline{u}}(\underline{\omega})$	A characteristic function of a region at point $\underline{u}$
a	Parameters of some covariance function
b	Normalizing parameter of some covariance functions
$C(\cdot)$	Two or three dimensional covariance functions
$C_1(\cdot)$	One dimensional covariance function corresponding to the two or three dimensional covariance function C( )
$C_A(\cdot)$	Covariance function of the areal average process
c_ω	Circle of radious ω
$d\underline{x}$	Differential of the vector $\underline{x}$ defined as: $d\underline{x} = dxdy$ in two dimensions
$\Delta X, \Delta Y$	Discretization distances of a rectangular grid
$E[\ ]$	Expectation operator
$Ei(\cdot)$	Exponential integral function
$f(\omega)$	Radial spectral density function of a two dimensional isotropic process
$f_{\underline{u}}(\underline{x})$	Probability density function of the vector $\underline{x}$ uniformly distributed on region $A(\underline{u})$
$f_o(\underline{w})$	Probability density function of the vector $\underline{\omega}$ uniformly distributed on region A(0)

$f(w)$	A weighting function in the moving average process
$\tilde{f}(w)$	Transpose of the function f defined by $f(\ ) = f(-\ )$
$H(\underline{\omega})$	Characteristic function of the geometry and rotation of a region
$H_o(\underline{\omega})$	Characteristic function of a region depending only on the geometry of the region
$\lvert H(\underline{\omega}) \rvert$	Absolute value of $H(\underline{\omega})$
$\underline{h}$	Vector distance between two points
$I_o(\cdot), I_1(\cdot)$	Bessel functions of order zero and one respectively
$I_o(\cdot)$	A Bessel function of order zero
k_{max}	Number of summation elements in the moving average process
$K(\cdot)$	Generalized covariance (GC) function of an IRF
$K_1(\cdot)$	A modified Bessel function of order 1; A GC for a unidimensional process
L	Number of lines in the turning bands method
Lx, Ly	Sides of a rectangular area
$L_o(\cdot), L_1(\cdot)$	Modified Strube functions of order o and 1 respectively
M	Number of harmonics used in the generation of the line process
$m(x)$	Mean of a random function of point x
NX, NY	Number of columns and rows in a rectangular grid
N	Total number of points simulated in a rectangular grid given by $N = NX \cdot NY$
NS	Number of simulations
$r(\cdot)$	Correlation function of a random function
R^n	n-dimensional space
$S(\omega)$	Spectral density function of a two dimensional isotropic process

$S_1(.)$ Spectral density function of the corresponding one dimensional process

$S_A(\underline{\omega})$ Spectral density function of the areal average process

ζ_{Ni} Inner product of vectors $\underline{x}_N$ and $\underline{u}_i$

T Random variable unformly distributed moving zero mean and variance 1

$\underline{u}_i$ Unit vector on line i

$\Delta\zeta$ Discretization distance along the turning bands lines

$\underline{x}_N$ Vector corresponding to point N in space

y_i Value at point i of one dimensional simulation using a moving average process

$Z(\cdot)$ Two or three dimensional random processes

$Z_A(\cdot)$ Process of areal averages

$Z_i(\cdot)$ One dimensional process corresponding to line i

$z_s(\ )$ Obtained from simulation realizations of the random field

α Discretization length of the process T

β Angle of rotation of a region

$\Delta\omega$ Discretization of the unidimensional spectral density function

$\delta\omega$ Small random frequency uniformly distributed between $-\Delta\omega'/w$ and $\Delta\omega'/2$

$\Delta\omega'$ Small frequency such that $\Delta\omega' << \Delta\omega$

θ Angle formed between a turning bands line and the x axis, in a two dimensional process

μ An integer defined by the ratio $\mu = \Delta\zeta/\alpha$

σ^2 Variance of a process

$\underline{\omega}$ Frequency vector of a two dimensional anisotropic process

ω Frequency distance of a two dimensional isotropic process or a unidimensional process

Ω Maximum frequency where we cut the spectrum

CHAPTER 1

INTRODUCTION

The theory of random fields has been recently applied in mining (e.g., Matheron, 1973; Journel, 1974; Delfiner, 1976; Chiles, 1977; Journel and Huijbregts, 1978), groundwater hydrology (e.g., Delhomme, 1979; Wilson, 1979; Smith and Freeze, 1979 a,b; Dettinger and Wilson, 1980), surface water hydrology (e.g., Mejia and Rodriguez-Iturbe, 1974; Renals and Rodriguez-Iturbe, 1974; Lenton and Rodriguez-Iturbe, 1974, 1977), oceanogrophy (e.g., Shinozuka and Jan, 1972), goetechnical engineering (e.g., Vanmarke, 1977) and other geophysical sciences. The theory is used to account for uncertainties introduced by the unpredictable nature of the process or by the scarceness of measurements. These many types of application are usually treated in a similar way, although some conceptual differences exist. For example rainfall is a spatial and time process, while ore body or aquifer properties present only spatial variations. From measurements of several realizations (e.g., yearly) of rainfall, or from measurements over space of ore body or aquifer properties, we can calculate the statistics of the underlying random field by means of statistical methods employing the ergodicity assumption.

Two approaches can be taken:

(a) Estimation approach: from measurements of one realization of the field (for example of the annual rainfall over an area in a given year, or of the existing ore body or aquifer realization)

we estimate the values of the same realization at unmeasured points of the areas (using Best Linear Unbiased Estimator, Kriging, etc.), such that we minimize some objective functions. This approach is useful in groundwater hydrology for calculation of the parameters used in deterministic groundwater models, and in mining for the estimation of ore reserves.

(b) Simulation approach: in this approach we generate realizations of the underlying random field. In the case of the rainfall model, these realizations represent possible rainfalls over the area and can be used in a rainfall-runoff model to predict the statistics of discharges, and other model outputs. In groundwater models, the realizations represent possible patterns of the aquifer properties, and can be used as inputs in aquifer models to yield the statistics of piezometric head, specific discharges and other outputs. In the latter case, it might be appropriate, depending on the number of the data points and the uncertainty in measurements, to perform conditional simulations, that is simulations which preserve the observed values at the data points. Conditional simulation of ore bodies is often performed in mining to test alternative mining sequences and sampling programs.

In this report we focus on the simulation approach primarily in the case of two dimensional fields.

1.1 Scope and objectives

The objective of this work is to present and extend a relatively new simulation method, the "Turning Bands Method" (TBM), for generation

of hydrologic random fields, and to develop strategies for using it efficiently in terms of accuracy and cost. The method is extended to the direct generation of anisotropic random fields and the process of areal averages. Finally a comparison of the existing simulation methods versus the TBM in terms of accuracy and cost is given.

In Chapter 2 we give basic definitions and derivations appropriate to random fields, and present some random field simulation methods from the literature. In Chapter 3 we present the turning bands method for the general case of stationary isotropic two or three dimensional fields. This method is extended for the two dimensional case, using spectral methods and moving average techniques for generation along the lines. Examples of generations are given and compared with other methods in terms of accuracy and cost. In Chapter 4 the turning bands method is extended to the generation of stationary anisotropic random fields, and and an example generation is given. In Chapter 5 we present areal averages of stationary processes, with an example of direct areal average simulation by the TBM. In Chapter 6 we present the TBM for the simulation of a category of non-stationary random fields, called intrinsic random fields. Chapter 7 summarizes the results and conclusions of this reprot, and gives recommendations for futher research.

CHAPTER 2

REVIEW OF THE PROPERTIES OF RANDOM FUNCTIONS AND SIMULATION TECHNIQUES

2.1 Introduction

The concept of a random function is a generalization of the concept of a random variable. If $\underline{x}$ represents a point in n dimensional space, R^n, and $Z(\underline{x})$ is a random variable corresponding to point $\underline{x}$, then we define a random function on R^n as the set $\{(\underline{x},Z(\underline{x}))\,|\,\underline{x}\epsilon R^n\}$. If the dimensionality n of the space R^n is 2 or 3 the random function is usually called a random field. When n=1 it is called a line process or unidimensional process. A random function is also called a stochastic process.

The theory of random fields has quite a few applications in hydrology. An example is the annual rainfall depth over an area,or the field of permeabilities in an aquifer system. In the latter case,although the field is deterministic (only one true realization), the theory of random functions is applied to account for imperfect knowledge of the field of permeabilities as a function of space.

The statistical properties of a random field under consideration can be estimated as averages over the ensemble of many realizations of the random field. This, of course, is possible if many realizations are available (as in the case of annual rainfall over an area). However, in many cases measurements of only one realization are available (as for the field of permeabilities in an aquifer system),

and we cannot estimate ensemble averages. It is then often necessary to assume that the random field is stationary and ergodic and that the one existing true realization is a "representative realization" (Gelb, 1974), i.e. it includes all the information of the random field. In this case we can substitute the ensemble averages with the space averages taken from the one available realization.

There are two problems of different type inherent with the above assumptions. The first problem is that we really don't know if the field is actually stationary and ergodic. One realization is simply insufficient to evaluate the properties of the underlying random field. As in the case of a random variable, one value of the variable is not enough to say anything about the underlying distribution from which the variable is drawn. Moreover we don't know if the available realization is a representative one. The second problem is of a different type. Even if the assumptions of stationarity, ergodicity and representative realization hold, an error is introduced in the approximation of the statistics of the random field taken from only one part of the realization. The ergodicity assumption gives the statistics of the underlying random field if the available realization is of infinite size. In practical applications the available measurements of the realization are within a region which is of small size, compared to some correlation length, so that a large error is expected if we estimate the statistics of the underlying random field from those data. To circumvert the above problems (in cases when only one realization is available) Matheron (1973) proposed a new theory introducing the concept of intrinsic random functions, in order to model processes that are not stationary

and ergodic or processes for which the nature of the underlying random field cannot be inferred from the available realization limited size.

Throughout this work it is assumed that the statistical properties of the random field are known. The calculation of those properties is an estimation problem and is out of the scope of this report.

In the remainder of this chapter we review some basic definitions and derivations pertinent to random fields and present briefly two state-of-the-art simulation models for the generation of realizations of random functions.

2.2 Second Order Stationary Random Fields

2.2.1 Basic definitions

In this section we are going to present some basic definitions and derivations pertinent to the concept of a random function. It is assumed that to each point $\underline{x} = (x_1 x_2 \ldots x_n)$ in R^n space, there corresponds a random variable $Z(\underline{x})$.

The mean function is defined as

$$m(\underline{x}) = E[Z(\underline{x})] \tag{2.1}$$

where $E[\ ]$ is the expectation operator. If $E[Z^2(\underline{x})]$ is finite for all $\underline{x}$ we can define the covariance function of the stochastic process as

$$C(\underline{x}_1,\underline{x}_2) = E[\{Z(\underline{x}_1)-m(\underline{x}_1)\}\{Z(\underline{x}_2)-m(\underline{x}_2)\}]$$

$$= E[Z(\underline{x}_1)Z(\underline{x}_2)]-m(\underline{x}_1)m(\underline{x}_2) \qquad (2.2)$$

where $\underline{x}_1,\underline{x}_2 \varepsilon R^n$. The correlation function of the process is defined as:

$$R(\underline{x}_1,\underline{x}_2) = \frac{C(\underline{x}_1,\underline{x}_2)}{[C(\underline{x}_1,\underline{x}_1)C(\underline{x}_2,\underline{x}_2)]^{1/2}} \qquad (2.3)$$

and the variance of the process at a point $\underline{x}$ is defined by:

$$\text{var}(\underline{x}) = C(\underline{x},\underline{x}) \qquad (2.4)$$

When $\underline{x}_1 \equiv \underline{x}_2$ (2.3) gives $R(x_1,x_1) = 1$.

A random process is called a "second-order stationary process" if the following conditions are satisfied:

-The mean is independent of the position of each point in space R^n:

$$E[Z(\underline{x})] = m(\underline{x}) = m \quad \forall\ \underline{x}\varepsilon R_n \qquad (2.5)$$

-The covariance function depends only on the vector difference $(\underline{x}_1-\underline{x}_2)$, and not on each particular vector $\underline{x}_1,\underline{x}_2$:

$$C(\underline{x}_1,\underline{x}_2) = C(\underline{x}_1-\underline{x}_2) = C(\underline{h}) \qquad (2.6)$$

where $\underline{h} = \underline{x}_1-\underline{x}_2$.

The terms second-order stationary, broad stationary, and wide sense stationary are interchangable. In the cases where $\underline{x}$ is a space parameter, the term broad homogeneity is often used instead.

A second order stationary process is called isotropic if the covariance function does not depend on the direction $\underline{h} = \underline{x}_1 - \underline{x}_2$ of the distance vector, but only on the vector length $|\underline{h}|$. Then we can write:

$$C(\underline{h}) = C(r) \tag{2.7}$$

where $r = |\underline{h}|$

2.2.2 Some common covariance functions

In order for a function to serve as a proper covariance function certain specific properties should be satisfied (Veneziano, 1978). The functions described here preserve these properties.

Two common one dimensional covariance models are mentioned here. The exponential type model is given by

$$C(x) = \sigma^2 e^{-bx} \qquad 0 \leq x < \infty \tag{2.8}$$

where x is the distance from the origin, σ^2 is the variance of the process, and b is a parameter. The parameter b^{-1} has units of length and is often called correlation distance. Another common one dimensional model is given by the "hole type funciton" defined as:

$$C(x) = \sigma^2(1 - bx)e^{-bx} \qquad 0 \leq x < \infty \tag{2.9}$$

where b^{-1} is the value of x for which covariance is zero, $C(x) = C(b^{-1}) = 0$. In this case for $x < b^{-1}$ correlation is positive, while for $x > b^{-1}$ correlation is negative.

The simplest two dimensional isotropic covariance function used in hydrology is of the exponential type written as:

$$C(r) = \sigma^2 e^{-br} \qquad r \geq 0 \tag{2.10}$$

where r is the distance bewteen any two points in R^2. Another type of two dimensional isotropic covariance used in hydrology (Mejia and Rodriguez-Iturbe, 1974) is of the Bessel type:

$$C(r) = \sigma^2 br\, K_1(br) \qquad r \geq 0 \tag{2.11}$$

where $K_1(\cdot)$ is a modified Bessel function of the second type of order 1. Other isotropic covariance functions used in mining and recently applied to hydrology (Delhomme, 1978) are of polynomial type. A simple polynomial type covariance function is the so called spherical model given by:

$$C(r) = \begin{cases} \sigma^2\left[1 - \frac{3}{2}\frac{r}{\alpha} + \frac{1}{2}\left(\frac{r}{\alpha}\right)^3\right] & r \leq \alpha \\ 0 & r > \alpha \end{cases} \tag{2.12}$$

For completeness we mention here the double exponential type model which has been used to model three dimensional covariance functions mainly, but has been used as a two dimensional model as well. The covariance function of this model is given by:

$$C(r) = \sigma^2 e^{-b^2 r^2} \qquad 0 \leq r < \infty \tag{2.13}$$

In three dimensional fields the above mentioned exponential and spherical models have been used as well as the double exponential model. Some other models exist in the literature (e.g., Veneziano, 1978; Matern, 1960; Vanmarcke, 1977; Rhenals, 1974).

2.2.3 Spectral analysis of a second order stationary stochastic process

One dimensional process

If the covariance function C(r) of a unidimensional process is decreasing rapidly such that the integral $\int_{-\infty}^{+\infty}|C(r)|dr$ is bounded, the covariance function C(r) can be represented by a Fourier integral as:

$$C(r) = \int_{-\infty}^{+\infty} e^{i\omega r} S(\omega)d\omega \tag{2.14}$$

The function $S(\omega)$ is called the spectral density function of the process. Correspondingly $S(\omega)$ is written as:

$$S(\omega) = \frac{1}{2\pi}\int_{-\infty}^{+\infty} e^{-i\omega r} C(r)dr \tag{2.15}$$

The functions C(r) and $S(\omega)$ form a Fourier transform pair.

For r=0 (2.14) gives:

$$C(0) = \sigma^2 = \int_{-\infty}^{+\infty} S(\omega)d\omega \tag{2.16}$$

If the process is real then both C(r) and $S(\omega)$ are real and symmetric functions. In addition $S(\omega) \geq 0$ for all ω. Then we can write:

$$C(r) = 2\int_{0}^{\infty} \cos(\omega r) S(\omega)d\omega \tag{2.17}$$

$$S(\omega) = \frac{1}{\pi}\int_{0}^{\infty} \cos(\omega r) C(r)dr \tag{2.18}$$

Two dimensional process (see Matern, 1960)

If the two dimensional covariance function $C(\underline{h})$ is continuous and tends to zero fast enough as $|\underline{h}| \to \infty$, then $C(\underline{h})$ can be expressed as a Fourier integral given by:

$$C(\underline{h}) = \int_{R^2} e^{i\underline{h}\cdot\underline{\omega}} S(\underline{\omega}) d\underline{\omega} \tag{2.19}$$

where $\underline{\omega} = [\omega_1, \omega_2]$,

$$d\underline{\omega} = d\omega_1 d\omega_2 \tag{2.20}$$

and $(\underline{h}\cdot\underline{\omega})$ is the inner product of the vectors $\underline{h}$ and $\underline{\omega}$. The function $S(\underline{\omega}) = S(\omega_1, \omega_2)$ is called spectral density function of the two dimensional process. For real fields $C(\underline{h}) = C(-\underline{h})$ and $S(\underline{\omega}) = S(-\underline{\omega})$; equation (2.19) then gives:

$$C(\underline{h}) = \int_{R^2} \cos(\underline{h}\cdot\underline{\omega}) S(\underline{\omega}) d\underline{\omega} \tag{2.21}$$

The function $S(\underline{\omega})$ is a non-negative function and is given by the inverse transform of $C(\underline{h})$ as:

$$S(\underline{\omega}) = \frac{1}{(2\pi)^2} \int_{R^2} C(\underline{h}) e^{-i\underline{h}\cdot\underline{\omega}} d\underline{h} \tag{2.22}$$

For real fields again we get:

$$S(\underline{\omega}) = \frac{1}{(2\pi)^2} \int_{R^2} C(\underline{h}) \cos(\underline{h}\cdot\underline{\omega}) d\underline{h} \tag{2.23}$$

If the field is isotropic we have, from (2.7),

$$C(\underline{h}) = C(r) \tag{2.24}$$

where $r = |\underline{h}|$, and from (2.23)

$$S(\underline{\omega}) = S(\omega) \tag{2.25}$$

where $\omega = |\underline{\omega}|$. In polar coordinates ω,θ the differential in (2.21) is written as:

$$d\underline{\omega} = \omega d\theta d\omega$$

and, since the field is isotropic, it is valid to write (using a coordinate translation and rotation)

$$\underline{h} = [h_1, h_2] = [r, 0]$$

so that

$$C(r) = \int_0^{\infty} \left[\int_0^{2\pi} \cos(\omega r \cos\theta) d\theta \right] S(\omega) \omega d\omega \tag{2.26}$$

The integral inside the brackets is given by (Gradshteyn and Ryzhik, 1965):

$$\int_0^{2\pi} \cos(\omega r \cos\theta) d\theta = 2\pi J_o(\omega r) \tag{2.27}$$

where J_o is a Bessel function of first kind of order zero. Substituting (2.27) into (2.26) gives:

$$C(r) = 2\pi \int_0^{\infty} J_o(\omega r) S(\omega) \omega d\omega \tag{2.28}$$

We introduce here the concept of the radial spectral density function $f(\omega)$ of an isotropic process with spectral density function $S(\omega)$. In the two dimensional field define:

$$f(\omega) = \frac{1}{\sigma^2}\int_{c_\omega} S(\omega)d\underline{\omega} = \frac{1}{\sigma^2} S(\omega) \int_{c_\omega} d\underline{\omega} = \frac{2\pi\omega S(\omega)}{\sigma^2} \tag{2.29}$$

where c_ω is a circle of radius ω and $d\underline{\omega}$ is the differential length on circle c_ω. Equation (2.28) then is written as (Shoenberg, 1938):

$$C(r) = \sigma^2 \int_0^\infty J_o(\omega r)f(\omega)d\omega \tag{2.30}$$

Taking the Hankel transform of the above integral gives

$$f(\omega) = \frac{\omega}{\sigma^2}\int_0^\infty C(r)J_o(\omega r)rdr \tag{2.31}$$

Determination of $f(\omega)$ for some two dimensional isotropic covariance functions (Matern, 1960)

If the two dimensional covariance function $C(r)$ is known we can use equation (2.31) to calculate the corresponding radial spectral density function $f(\omega)$:

(a) Exponential type: $C(r) = \sigma^2 e^{-br}$ Gradshteyn and Ryzhik, (1965):

$$f(\omega) = \frac{\omega}{b^2[1 + \frac{\omega^2}{b^2}]^{3/2}} \tag{2.32}$$

(b) Bessel type: $C(r) = \sigma^2 br K_1(br)$

$$f(\omega) = \frac{2\omega}{b^2[1 + \omega^2/b^2]^2} \tag{2.33}$$

(c) Double exponential: $C(r) = \sigma^2 e^{-b^2 r^2}$

$$f(\omega) = \frac{\omega}{2b^2} \exp\left[-\frac{\omega^2}{4b^2}\right] \tag{2.34}$$

We note here that we can define the spectral density function of random fields in higher dimension than 2, but the general formulas are not presented here because they are not used in this report.

2.3 Non-stationary Random Fields

Often the assumption of stationarity may not be justified. An example of a non-stationary random field is the field of precipitation in an orographic region. In that case there is an obvious trend in the mean of the process. Higher precipitation occurs (on the average of many realizations of the field) at higher latitudes. In these cases where many realizations of the field $Z(x)$ are available the mean variance, etc., can be evaluated at each point of the field. If the obtained statistics show that the field is not stationary a new field $Z'(\underline{x})$ given by:

$$Z'(\underline{x}) = \frac{Z(\underline{x}) - m(\underline{x})}{\sigma(\underline{x})} \tag{2.35}$$

can be defined. The field $Z'(\underline{x})$ is stationary in the mean and variance and often the assumption of second order stationarity can be applied in the new field $Z'(\underline{x})$.

When only one realization is available, as in the case of ore body or aquifer properties, it is then not possible to estimate the means, variances, etc. at each point. Only one value of the field is available at the points. The assumptions of second order stationarity and ergodicity then is sometimes made in order to make it possible to calculate the statistics of the underlying random field. This assumption cannot be justified in most cases and other techniques for analyzing the properties of the field have to be sought. One of these is to assume a functional approximation for the mean $m(\underline{x})$ obtained from the values of the field at the data points, and from physical considerations of the process. In this case with "known" mean a new process can be defined by:

$$Z'(\underline{x}) = Z(\underline{x}) - m(\underline{x}) \tag{2.36}$$

This new process has a constant mean and could be assumed to be second order stationary, although the assumption of constant mean does not guarantee this.

To circumvent the above mentioned problems in cases where one only realization is available and the process is not (or we do not know if it is) stationary and ergodic, G. Matheron and his group at the Ecole des Mines de Paris developed the theory of Intrinsic Random Functions (IRF). This theory is described in an excellent paper published several years ago (Matheron, 1973). In this paper Matheron proposes that for estimation and simulation problems we don't need to actually know the mean. In the estimation problem (Kriging) the mean is filtered out by taking appropriate differences (as in time series analysis). In the simulation problem the mean is inherently in the data points (condition simulation).

An intrinsic random function of order k (IRF-k) is a non-stationary random function for which its k + 1 order differences (as defined in Delfiner, 1976) produce a stationary field. A simple example os an IRF is that of a random function of the form: $Z(\underline{x}) = Z_o(\underline{x}) + P_k(\underline{x})$ where $Z_o(\underline{x})$ is a zero mean stationary random function with covariance function $C(\underline{h})$, and $P_k(\underline{x})$ is a polynomial of k^{th} degree with random (unknown) coefficients. The random function $Z(\underline{x})$ is then in IRF or order k. A function $K(\underline{h})$, called a Generalized Covariance function of order k (GC - k), can be defined on the random function $Z(\underline{x})$ (Matheron, 1973). In the example above, where the remaining field $Z_o(\underline{x})$ is stationary with

covariance $C(\underline{h})$, then $K(\underline{h}) = C(\underline{h})$. However, the class of IRF as defined in Matheron (1973) is larger than this simple example (which was obtained by the superposition of a stationary process to a polynomial function). Consequently the class of admissible generalized covariance functions is larger than the class of covariance functions of stationary processes. In fact polynomial covariance functions (with certain limitations on the coefficients) are admissible as GC.

Polynomial GC functions are easily applied to estimation or simulation problems, and so are commonly used in practice. The order, ℓ, of the polynomial GC-k function $K(\underline{h})$ is a function of the order, k, of the underlying polynomial $P_k(\underline{x})$ [or the order of the differences required to produce stationarity in the mean, k+1], and is given by $\ell = 2k + 1$. The general form of admissible polynomial isotropic GC-k is given in Matheron (1973) as:

$$K_n(r) = \sum_{p=o}^{k} (-1)^{p+1} \frac{\alpha_p \beta_{np} r^{2p+1}}{(2p+1)!} \tag{2.37}$$

where $r = |\underline{h}|$, n is the dimensionality of the field and

$$\beta_{np} = \frac{p!\ \Gamma(n/2)}{\sqrt{\pi}\ \Gamma\{p+\frac{1}{2}(1+n)\}} \tag{2.38}$$

$\Gamma(\ )$ is the gamma function. The coefficients α_p should satisfy the inequality

$$\sum_{p=o}^{k} \alpha_p \chi^{2(k-p)} \geq 0 \tag{2.39}$$

for all real χ.

These models are not bounded in R^n ($K_n(r) \to \infty$ as $r \to \infty$). By replacing

$$a_p = \frac{\alpha_p \beta_{np}}{(2p+1)!} \tag{2.40}$$

we get:

$$K_n(r) = \sum_{p=o}^{k} (-1)^{p+1} a_p r^{2p+1} \tag{2.41}$$

a form we will use latter in Chapter 6. In two diminstions, n=2 the parameter $\beta_{np} = \beta_{2p}$ (2.38) reduces to

$$\beta_{2p} = \frac{p!}{\sqrt{\pi}\ \Gamma(p+3/2)} \tag{2.42}$$

For this case the GC-k (2.37) is written as

$$K_2(r) = \sum_{p=o}^{k} \frac{(-1)^{p+1} \alpha_p}{(2p+1)!} \frac{p!\ r^{2p+1}}{\sqrt{\pi}\ \Gamma(p+3/2)} \tag{2.43}$$

For k=0, 1, 2 we have the most useful models which wriiten in the form of Equation (2.41) are:

$$k = 0 \quad K_2(r) = -a_o r \tag{2.44a}$$

$$k = 1 \quad K_2(r) = -a_o r + a_1 r^3 \tag{2.44b}$$

$$k = 2 \quad K_2(r) = -a_o r + a_1 r^3 - a_2 r^5 \tag{2.44c}$$

Because of inequality (2.39) the coefficients a_p(2.40) becomes:

$$a_o \geq 0 \ ; \quad a_1 \geq -\frac{10}{3} \sqrt{a_o\ a_2} \ ; \quad a_2 \geq 0 \tag{2.44d}$$

The function defined by $Z_o(\underline{x}) = Z(\underline{x}) - P_k(\underline{x})$, where $P_k(\underline{x})$ is the mean function and $Z(\underline{x})$ is a representation of the IRF-k, is stationary only in the mean! The variance of $Z_o(\underline{x})$ tends to infinity as $|\underline{x}| \to \infty$.

2.4 Simulation of Random Fields

We often wish to generate realizations of a random field. In the case of rainfall the realizations might represent rainfall events over a region or annual rainfall depths. In the case of an aquifer or mining system the realizations may represent possible patterns of the aquifer or ore body properties (hydraulic conductivity, transmissivity, porosity, ore grade, etc). These realiztions or simulations should have the statistical properties of the underlying random field, that is, for the stationary case they should preserve the means, variances, and covariances as well as the histogram of the underlying random field. Otherwise, the realizations are biased. Sometimes we wish to generate fields which also preserve observations at given points. We then talk about conditional simulations which, for example, are useful for the generation of aquifer (Delhomme, 1979), or ore body (Journel and Huijbregts, 1978) properties. In the case of the simulation of future rainfall events the unconditional simulation approach would be more appropriate.

In the (second order) stationary case the problem of unconditional simulation involves the construction of realizations which have a given mean, variance, covariance function, and histogram. Quite often the histogram of the process is of the normal or lognormal type. In the latter case a logarithmic transformation could be made to yield a process

with a normal pdf. If $Z(\underline{x})$ is the original log-normal process then the process $Z'(\underline{x}) = \ell n[Z(\underline{x})]$ is normal. After realizations of this process $z'_s(\underline{x})$ are obtained by using the simulation model (subscript s represents simulation result), realizations of the original field can be obtained through the inverse transformation: $z_s(\underline{x}) = \exp(z'_s(\underline{x}))$. Care must be taken to insure that the covariance function of the field $z_s(\underline{x})$ preserves the theoretical covariance function, because the simulation model preserves only the covariance function of $Z'(\underline{x})$.

The problem of unconditional simulations in the non-stationary case with known mean and variance can be resolved easily if the process $Z'(\underline{x}) = [Z(\underline{x})-m(\underline{x})]/\sigma(\underline{x})$ is stationary in the covariance (obviously this process has zero mean and unit variance). In that case simulations of the stationary field $z'_s(\underline{x})$ are obtained and the simulated values of the original field are given by: $z_s(\underline{x}) = \sigma(\underline{x})\ z'(\underline{x}) + m(\underline{x})$.

In all the above mentioned cases the simulation problem is transformed to the problem of simulation of a stationary random field with a normal pdf. Existing spectral methods for generations of this type are described in Section 2.5 of this chapter, while the turning bands method for stationary fields is presented in Chapter 3.

We are sometimes interested in performing conditional simulations, i.e. simulations that preserve observations at the data points. Those simulations are intended to mimic the spatial variability of the real phenomenon. Obviously, the mean of the simulated fields at the data points is the measured values obtained from the real field, and the variance at those points is zero (unless there is a nugget effect). Conditional simulations can be obtained easily in this case by using Kriging.

(Delfiner, 1975; Journel, 1974; Journel and Huijbregts, 1978; Delhomme, 1979). The conditionally simulated values of the field are given by

$$z_{cs}(\underline{x}) = z^*(\underline{x}) + [z_s(\underline{x}) - z_s^*(\underline{x})] \qquad (2.45)$$

where $z_{cs}(\underline{x})$ is the conditional simulation of the field at point $\underline{x}$, $z^*(\underline{x})$ is the Kriged value of the field based on measurements at the data points, $z_s(\underline{x})$ the unconditionally simulated value of the field and $z_s^*(\underline{x})$ the Kriged value of the unconditionally simulated field taken at the data points. The field defined above has the desired properties (Delfiner, 1975). Obviously, conditional simulation involves as a first step the unconditional simulation of the field.

In the case of only one available realization, and if the stationarity and ergodicity properties are not justified, then the mean and covariance functions cannot be obtained. In that case we can estimate from the available realization a generalized covariance function $K(\underline{h})$ (usually polynomial) and then perform first unconditional and then conditional simulations using this generalized covariance function. Realizations of a zero mean IRF $Z_o(\underline{x})$ can be easily obtained, as will be illustrated later (Chapter 6) with the turning bands method. A polynomial $P_k(\underline{x})$ of order k with random coefficients can be added to obtain other representations of the intrinsic random function $Z(\underline{x})$. Usually conditional simulations are performed, so the addition of $P_k(\underline{x})$ becomes meaningless as it is subtracted during the conditioning step. The mean of the process enters in the simulations through the Kriging of the original data.

2.5 Review of Two Simulation Models From the Stationary Case

In the simulation models it is assumed that the statistical characteristics of the random field (such as mean, variance, covariance function, etc.) are known. The simulation model uses those characteristics and the obtained realizations should preserve those statistics. In practice though, because of discretization or other reasons, a small error is introduced which we call model error. A certain model becomes more accurate as it becomes more expensive.

In the following, two simulation models are reviewed. In both models the random function is simulated by a series of cosine functions. In the first model (Mejia and Rodriguez-Iturbe, 1974) the cosine functions have the same amplitude and random frequency vectors are sampled from the spectral density function of the process (a type of Monte-Carlo integration of the spectral density function), while in the second model (Shinozuka and Jan, 1972), the cosine functions have weighted amplitudes and evenly spaced frequencies (a type of numerical integration).

Model of Mejia and Rodriguez-Iturbe (1972)

The simulated field is expressed by a series of cosine functions of the same amplitude as:

$$z_s(\underline{x}) = \sigma\left(\frac{2}{N}\right)^{1/2} \sum_{k=1}^{N} \cos(\underline{\omega}_k \underline{x} + \phi_k) \qquad (2.46)$$

where the subscript s on z_s indicates the simulated realizations of the field, σ^2 is the variance of the process, ϕ_k is a random angle uniformly distributed between 0 and 2π, and $\underline{\omega}_k$ is an independent random vector with probability density function equal to the normalized spectral

density function $S(\underline{\omega})/\sigma^2$. For one dimensional processes (2.46) is written as:

$$z_s(x) = \sigma(\frac{2}{N})^{1/2} \sum_{k=1}^{N} \cos(\omega_k x + \phi_k) \qquad (2.47)$$

where ω_k is an independent random variable with probability density function $S(\omega)/\sigma^2$. In two dimensional isotropic random fields we use the radial spectral density function instead and (2.46) is written as:

$$z_s(\underline{x}) = \sigma(\frac{2}{N})^{1/2} \sum_{k=1}^{N} \cos[\omega_k(x_1\cos\theta_k + x_2\sin\theta_k) + \phi_k] \qquad (2.48)$$

where ω_k is an independent random variable with probability density function equal to the radial spectral density function, and θ_k, ϕ_k are independent random vectors uniformly distributed between 0 and 2π. The fields defined by (2.46), (2.47) or (2.48) preserve the mean and variance of the process, but are asymptotically ergodic only for $N\to\infty$. The standard deviation of the model covariance function estimated as a space average is given by:

$$\sigma_\varepsilon = \sqrt{\frac{\sigma^2 C(2r) - 2C^2(r) + \sigma^4}{2N}} \qquad (2.49)$$

This equation shows that the model covariance function tends to the theoretical one vary slowly as $(1/\sqrt{N})$.

Model of Shinozuka and Jan (1972)

It is assumed $S(\underline{\omega})$ is negligible outside the rectangle:

$$\{\underline{\omega}: -\infty < -\Omega_i < \omega_i < \Omega_i < +\infty \quad ; \quad i = 1,2...n\}$$

where n is the dimension of the field and $\{\Omega_1,\Omega_2...\Omega_n\}$ is a given

vector with positive elements. We denote $\Delta\omega_i = \frac{2\Omega_i}{N_i}$ as an interval along the ith frequency axis, where N_i is the number of intervals on that axis. The nth dimensional process then can be simulated by the series:

$$z_s(\underline{x}) = \sqrt{2} \sum_{k_1=1}^{N_1} \sum_{k_2=2}^{N_2} \cdots \sum_{k_n=1}^{N_n} [S(\omega_{1k_1}, \omega_{2k_2}, \ldots \omega_{nk_n}) \Delta\omega_1 \Delta\omega_2 \ldots \Delta\omega_n]^{1/2} \cdot$$

$$\cdot \cos(\omega'_{1k_1} x_1 + \omega'_{2k_2} x_2 + \ldots + \omega'_{nk_n} x_n + \phi_{k_1 k_2 \ldots k_n}) \qquad (2.50)$$

where:

$\phi_{k_1,\ldots k_n}$ = an independent random angle uniformly distributed between 0 and 2π.

$\omega_{ik_i} = -\Omega_i + (k_i - 1/2)\Delta\omega_i \quad k_i = 1,2\ldots N_i \; ; \; i = 1,2,\ldots,n$

$\omega'_{ik_i} = \omega_{ik_i} + \delta\omega_i \quad k_i = 1,2\ldots N_i \; ; \; i = 1,2,\ldots,n$

In the above $\delta\omega_i$ is a small random frequency added in order to avoid periodicities, and is uniformly distributed between $-\Delta\omega'_i/2$ and $\Delta\omega'_i/2$ with $\Delta\omega'_i << \Delta\omega_i$.

In one dimension (2.50) is written as

$$z_s(x) = \sqrt{2} \sum_{k=1}^{N} [S(\omega_k)\Delta\omega]^{1/2} \cos(\omega'_k x + \phi_k) \qquad (2.51)$$

This equation is used extensively for the generation of one dimensional processes and was proposed by Rice (1954).

The process defined by (2.50) is ergodic but has a covariance function which is slightly different from the associated theoretical one which we want to preserve. This model error (bias) tends to zero as the number of harmonics used tends to infinity ($N_i \to \infty \; \forall i$), while the discretization frequencies $\Delta\omega_i$ tend to zero.

Discussion

For n = 1 (one dimensional process) Shinozuka and Jan (1972) prove that the process defined by (2.51) approaches the theoretical covariance function as $\frac{1}{N^2}$ while the process defined by (2.47) converges as $\frac{1}{\sqrt{N}}$.

In practical applications the parameter N of Mejia's model is finite. The same is true for parameters N_i of Shinozuka and Jan's model; moreover, in this method $\Delta\omega_i$ is finite. That means that there is some error in both methods and depends on the values N or N_i, $\Delta\omega_i$ that are chosen. A more expensive model is more accurate. In an application we should choose the parameters N or N_i, $\Delta\omega_i$ of one model such that we have sufficient accuracy and less cost.

In practical hydrologic or mining applications in two dimensional fields, it should be sufficient in Shinozuka's method to take: $N_1 = N_2 = 20$ (400 harmonics). In Mejia's model we generate frequency vectors randomly on the plane, and in order to describe the whole frequency spectrum accurately, the number of harmonics should be quite large. For practical purposes a number of harmonics N = 500 should give a good approximation.

In the next chapter the turning bands method is presented. The advantage of this method over those mentioned above, as we will see, is that for the same levels of accuracy its cost is much less, particularly when the number of the simulated points is large.

CHAPTER 3

THE TURNING BANDS METHOD FOR SIMULATION OF STATIONARY ISOTROPIC RANDOM FIELDS

3.1 Introduction

In Section 5 of the previous chapter we gave a brief review of two multi-dimensional simulation methods proposed by Mejia and Rodriguez-Iturbe (1974) and Shinozuka and Jan (1972). Both of those methods are based on the representation of random process as a weighted integral of the spectral density function of the process. They differ in that the method of Mejia and Rodriguez-Iturbe is based on random smapling from the spectral density function (Monte Carlo integration), while the method of Shinozuka and Jan is based on the discretization of the spectral density function (numerical integration). In both of these methods each simulated point value of the field is calculated as the sum of a large number of weighted cosine functions. The cost of simulation is proportional to the number of generated point values. In many applications it is necessary to describe the entire field, which means that we must generate at many points. Consequently, both of these simulation methods are very expensive, especially when a large number of simulations are performed.

In this chapter we are going to present the turning bands method, which is a relatively new simulation technique. This method was first presented in a strict mathematical format by Matheron (1973) and was applied by his colleagues at the Ecole des Mines de Paris:

Journel (1974), Chiles (1977), Journel and Huijbregts (1978), and Delhomme (1979). The originality of this method is that it transforms the two or three dimensional simulation problem to a unidimensional one. The results of several line simulations are added to generate the point value of the two or three dimensional field. Through this transformation the cost of simulation increases proportionally to the square root of the number points in the field at which we generate. That means that when the number of points of the field is significant (in practice greater than 5-10) then the turning bands method is more efficient than the other methods.

The turning bands method has been used during the last few years in the simulation of three dimensional random fields in mining applications (Journel and Huijbregts, 1978) for different covariance functions. In two dimensional fields this method in its original form has been applied only to very special types of covariance functions (Chiles, 1977; Delhomme, 1979), which are not commonly used in hydrologic models.

This chapter presents the turning bands method for the case of generating point processes having second order stationary isotropic covariance functions. Since the three dimensional simulation problem has been treated sufficiently before our main focus will be on the two dimensional simulation problem. The main original contributions of this chapter are:

-A transformation of the two dimensional spectral density function to a corresponding one dimensional spectral density function is proposed for the first time. With this transformation we can

generate the unidimensional line process very easily, using spectral methods. The transformation is general and can be applied to any two dimensional covariance function if the corresponding spectral density function is known (Section 3.3).

-Some one dimensional covariance functions, corresponding to common two dimensional models used in hydrology, are calculated. Conversely, two dimensional covariance functions corresponding to some simple one dimensional covariance models are also calculated. Using these results we can generate the line process as a moving average process (Section 3.4).

-The rate of convergence of the covariance function obtained by the turning bands method towards the theoretical one is derived. The model covariance function is calculated for different numbers of lines and different sizes of the discretization length along the lines. The figures presented can be used in order to design the model we use in a particular case (Section 3.5).

-The turning bands method is compared to other simulation methods in terms of accuracy and cost (Section 3.6).

In the next section the turning bands method is presented in a general form for two or three dimensional fields. This presentation can be found in a different format in Matheron (1973), or in the case of three dimensional fields in Journel and Huijbregts (1978) and for two dimensional fields in Chiles (1977).

3.2 Transformation of the two or three dimensional simulation problem to a unidimensional problem

Instead of simulating the two or three dimensional field directly, in the turning bands method we perform simulations along lines in space. Then at each point of the region R^n a weighted sum of the corresponding values of the line processes is assigned.

It is assumed here that the process is second order stationary and isotropic. Without loss of generality it is also assumed that at each point the values of the field are normally distributed and have zero mean. If this is not the case we can usually make a transformation to Gaussian and then subtract the mean. It is also assumed that the covariance of the field we want to simulate is known.

First we are going to give a conceptual description of the turning bands method. Then we'll derive the basic equations governing the transformation of the two or three dimensional covariance functions to a one dimensional covariance function.

Let P represent the two or three dimensional field we want to simulate, by generating values at discrete points in space. A two dimensional example is shown in Figure 3.1. Choose an arbitrary origin and generate lines with random direction in two or three dimensions. Let i be one of those lines, forming an angle θ with the x axis. In the two dimensional example, if x is a fixed axis, the randomness of the direction of line i implies that the angle θ is uniformly distributed between 0 and 2π. Along each line i, generate a unidimensional process having zero mean and covariance function $C_1(\zeta)$,

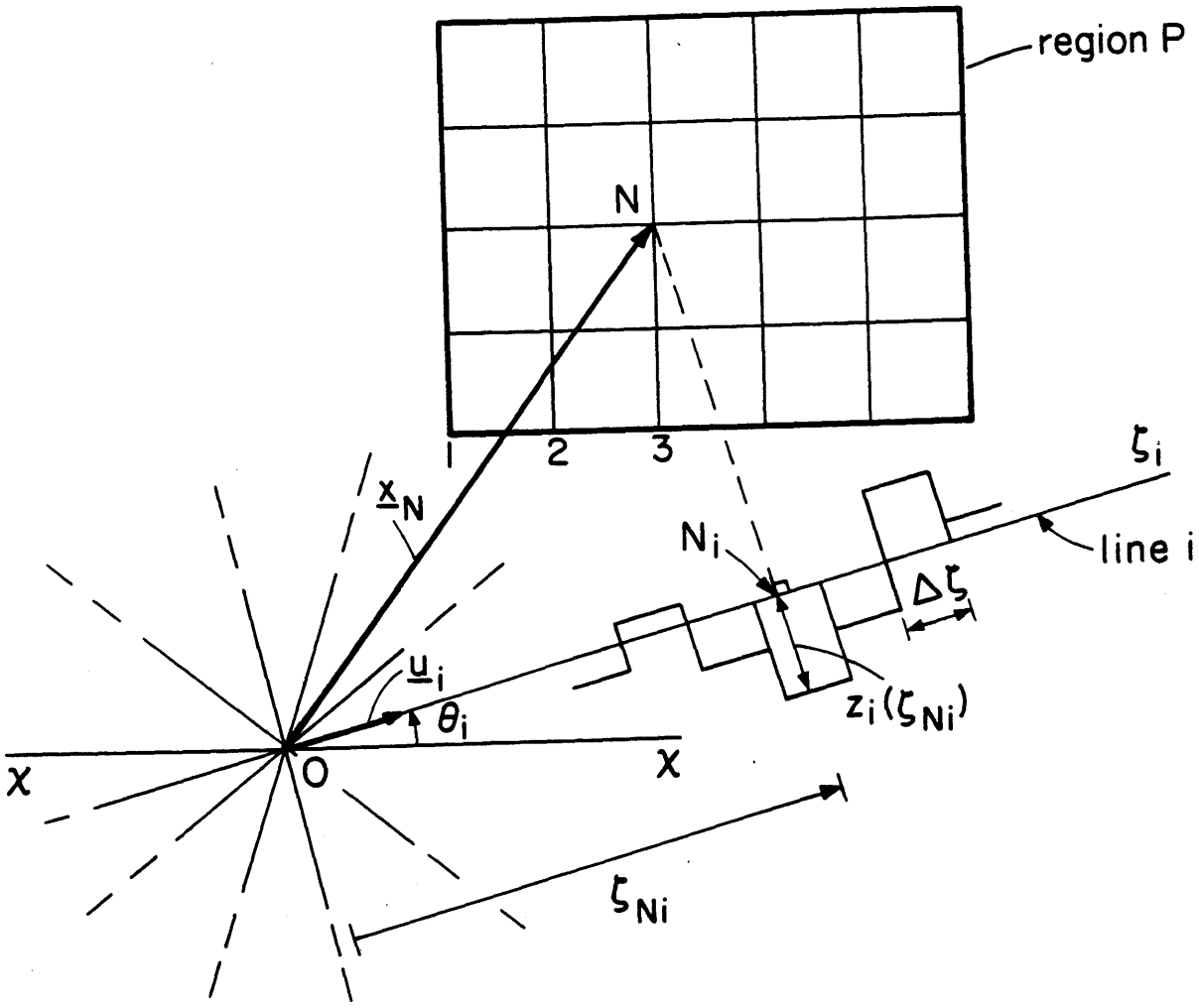

Figure 3.1 Schematic representation of the field and the turning bands lines.

where ζ is the coordinate along line i. We'll derive later $C_1(\zeta)$ as a function of two dimensional covariance function. Orthogonally project onto line i, those points in the field, where we want to generate values and assign to them the corresponding values of the one dimensional process. If N is a point of the region having location vector $\underline{x}_N$, then the assigned value from line i will be $z_i(\zeta_{Ni})$ where ζ_{Ni} is the projection of the vector $\underline{x}_N$ onto line i (see Figure 3.1). Let $\underline{u}_i$ be the unit vector on line i, giving $z_i(\zeta_{Ni}) = z_i(\underline{x}_N \cdot \underline{u}_i)$ where $\underline{x}_N \cdot \underline{u}_i$ represents the inner product of the vectors $\underline{x}_N$ and $\underline{u}_i$. Generate L lines such as i. For each line generate an independent realization using $C_1(\zeta)$ as the covariance function. Then at every point N of the region, there are L assigned values $z_i(\zeta_{Ni}) = z_i(\underline{x}_N \cdot \underline{u}_i)$, where i=1,...,L from the line simulations. Finally, assign to the point N the value $z_s(\underline{x}_N)$ given by:

$$z_s(\underline{x}_N) = \frac{1}{\sqrt{L}} \sum_{i=1}^{L} z_i(\underline{x}_N \cdot \underline{u}_i) \tag{3.1}$$

as the realization of the two or three dimensional random field. The subscript s represents the term "simulated" or "synthetic."

The field given by (3.1) has zero mean. The question that arises is "what should be the unidimensional covariance function $C_1(\zeta)$ so that the field defined by (3.1) has the imposed two or three dimensional covariance function C(r)?". In the following we are going to derive the relation between the covariance functions C(r) and $C_1(\zeta)$.

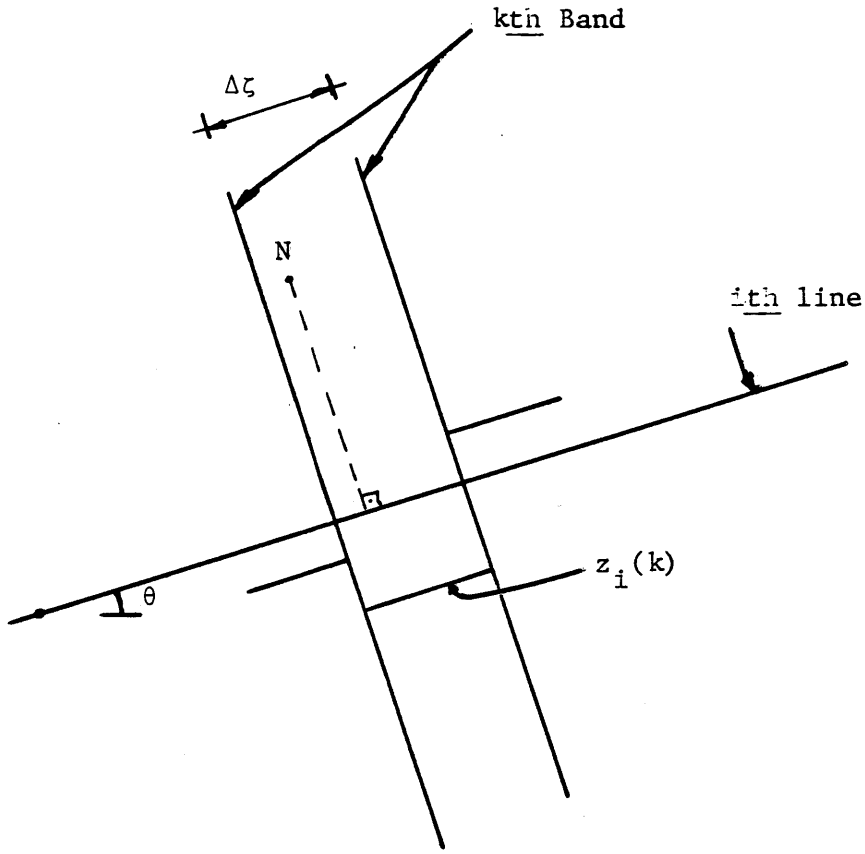

Figure 3.2 Definition of a band on a turning bands line.

Before we do so please note that the line process is generated discretely. If we draw lines or planes perpendicular to the line at the discrete ends of each discretized segment a set of bands is defined (Figure 3.2). As the lines turn the bands defined above also turn. Thus, the method was given the name "Turning bands method" (TBM) by Matheron (1973).

Take two points of the field having location vectors $\underline{x}_1$, $\underline{x}_2$ respectively, as shown in Figure 3.3. The simulated values corresponding to those points are given by (3.1) as:

$$z_s(\underline{x}_1) = \frac{1}{\sqrt{L}} \sum_{i=1}^{L} z_i(\underline{x}_1 \cdot \underline{u}_i) \tag{3.2}$$

and

$$z_s(\underline{x}_2) = \frac{1}{\sqrt{L}} \sum_{j=1}^{L} z_j(\underline{x}_2 \cdot \underline{u}_j) \tag{3.3}$$

Because the unidimensional process Z_i has zero mean, the process Z_s has zero mean, too. Between two points $\underline{x}_1$ and $\underline{x}_2$, the covariance function of the simulation is given by

$$C_s(\underline{x}_1,\underline{x}_2) = E\left[\left(\frac{1}{\sqrt{L}} \sum_{i=1}^{L} Z_i(\underline{x}_1 \cdot \underline{u}_i)\right)\left(\frac{1}{\sqrt{L}} \sum_{j=1}^{L} Z_j(\underline{x}_2 \cdot \underline{u}_j)\right)\right]$$

$$= \frac{1}{L} \sum_{i=1}^{L} \sum_{j=1}^{L} E[Z_i(\underline{x}_1 \cdot \underline{u}_i)\, Z_j(\underline{x}_2 \cdot \underline{u}_j)]$$

Because the unidimensional realizations along two different lines are independent, their expected value $E[Z_i(\underline{x}_1 \cdot \underline{u}_i)Z_j(\underline{x}_2 \cdot \underline{u}_j)]$ will be zero unless $i \equiv j$. Thus the equation for the covariance reduces to

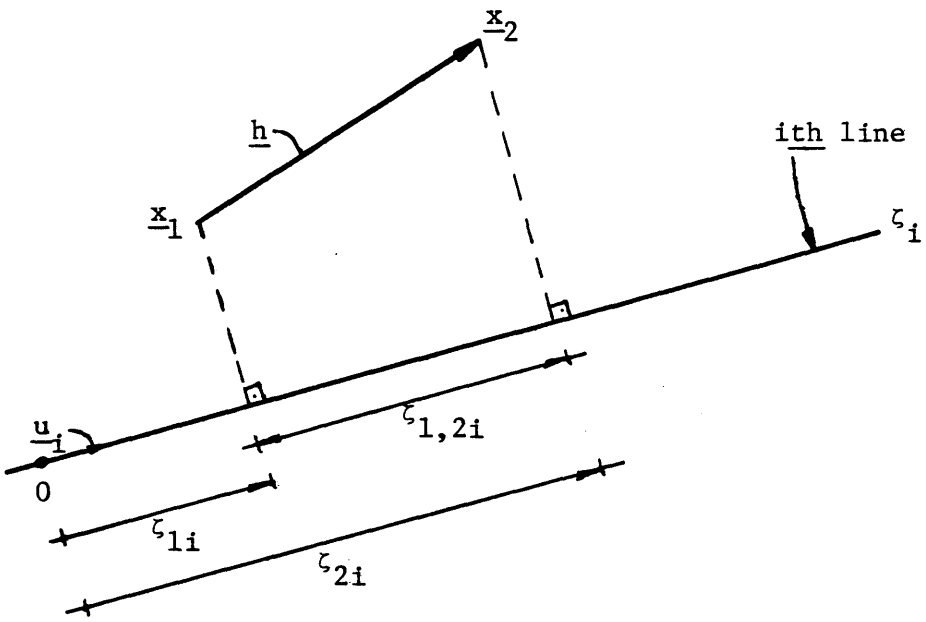

Fiugre 3.3 Projection of the vector $\underline{h}$ on a turning bands line.

$$C_s(\underline{x}_1,\underline{x}_2) = \frac{1}{L}\sum_{i=1}^{L} E[Z_i(\underline{x}_1\cdot\underline{u}_i)Z_i(\underline{x}_2\cdot\underline{u}_i)] \tag{3.4}$$

The expected value $E[Z_i(\underline{x}_1\cdot\underline{u}_i)Z_i(\underline{x}_2\cdot\underline{u}_i)]$ represents the covariance of the one dimensional process in line i between points $\underline{x}_1\cdot\underline{u}_i$ and $\underline{x}_2\cdot\underline{u}_i$ and can be written,

$$E[Z_i(\underline{x}_1\cdot\underline{u}_i)Z_i(\underline{x}_2\cdot\underline{u}_i)] = C_1(\underline{h}\cdot\underline{u}_i) \tag{3.5}$$

where $\underline{h} = \underline{x}_2-\underline{x}_1$. This equation assumes that the unidimensional processes are second order stationary. Substituting (3.5) into (3.4) gives

$$C_s(\underline{x}_1,\underline{x}_2) = \frac{1}{L}\sum_{i=1}^{L} C_1(\underline{h}\cdot\underline{u}_i) \tag{3.6}$$

Because the vector $\underline{u}_i$ is uniformly distributed over the unit circle or sphere, for two and three dimensions, respectively, the right-hand side of (3.6) is only a function of $|\underline{h}|$ for large L. This means that the obtained process is wide sense stationary and isotropic, so that we can write:

$$C_s(\underline{x}_1,\underline{x}_2) = C_s(\underline{h}) = C_s(r) = \frac{1}{L}\sum_{i=1}^{L} C_1(\underline{h}\cdot\underline{u}_i) \tag{3.7}$$

where $r = |\underline{h}|$. For $L \to \infty$, using the law of large numbers, (3.7) becomes

$$C_s(r) = \lim_{L\to\infty}\frac{1}{L}\sum_{i=1}^{L} C_1(\underline{h}\cdot\underline{u}_i) = E[C_1(\underline{h}\cdot\underline{u})] \tag{3.8}$$

Defining $f(\underline{u})$ as the probability density function of $\underline{u}$ we can write

$$E[C_1(\underline{h}\cdot\underline{u}))] = \int_c C_1(\underline{h}\cdot\underline{u}) f(\underline{u}) d\underline{u} \tag{3.9}$$

where c represents the unit circle or sphere and $d\underline{u}$ is defined as the differential length or area on c at the end of vector $\underline{u}$. In the case of a circle, in two dimensions, the probability density function $f(\underline{u})$ is given as

$$f(\underline{u}) = \frac{1}{2\pi} \tag{3.10}$$

In the case of a sphere in three dimensions $f(\underline{u})$ is given as:

$$f(\underline{u}) = \frac{1}{4\pi} \tag{3.11}$$

Combining equations (3.8), (3.9), (3.10) and (3.11) leads to the following equations relating unidimensional and multidimensional covariance functions. For the two dimensional field (n=2), the result is

$$C_s(r) = \frac{1}{2\pi} \int_{\text{unit circle}} C_1(\underline{h}\cdot\underline{u}) d\underline{u} \tag{3.12}$$

while for the three dimensional field (n=3) we have

$$C_s(r) = \frac{1}{4\pi} \int_{\text{unit circle}} C_1(\underline{h}\cdot\underline{u}) d\underline{u} \tag{3.13}$$

In the following, the cases of three and two dimensional fields are examined separately.

3.2.1 Three dimensional fields

Because of the second order stationarity and isotropy of the process, without loss of generality, we can define orthogonal (x,y,z) axes with origin at the point $\underline{x}_1$ and with the z axis in the direction of the vector $\underline{h} = x_2 - x_1$, as shown in Figure 3.4. The unit sphere where the vector $\underline{u}$ ends, is also shown. In spherical coordinates

$\underline{h}\cdot\underline{u} = r\cos\phi$, where $r = |\underline{h}|$, and

$d\underline{u} = 1^2 \sin\phi d\phi d\theta = \sin\phi d\phi d\theta$.

The integral (3.13) is then written as

$$C_s(r) = \frac{1}{4\pi} \iint_{\substack{\text{unit}\\ \text{sphere}}} C_1(r\cos\phi)\, \sin\phi d\phi d\theta$$

or

$$C_s(r) = \frac{1}{4\pi} \int_o^{2\pi} d\theta \int_o^{\pi} C_1(r\cos\phi)\, \sin\phi d\phi =$$

$$= \frac{1}{2} \int_o^{\pi} C_1(r\cos\phi)\, \sin\phi d\phi$$

Because of the symmetry of the unidimensional covariance function this equation becomes

$$C_s(r) = \int_o^{\pi/2} C_1(r\cos\phi)\, \sin\phi d\phi \qquad (3.14)$$

The projection of r along the line is

$\zeta = r\cos\phi \therefore d\zeta = -r\sin\phi d\phi$

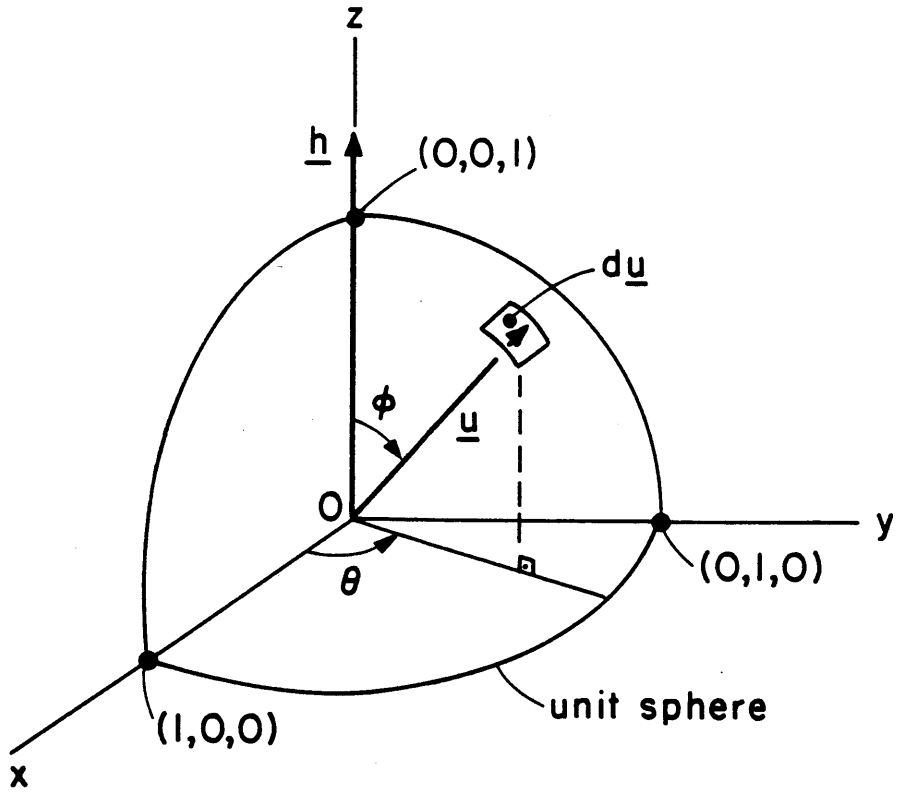

Figure 3.4 Definition sketch in the three dimensional case.

Substituting into (3.14) we get

$$C_s(r) = \int_r^o C_1(\zeta) \frac{-d\zeta}{r} = \frac{1}{r} \int_o^r C_1(\zeta) d\zeta$$

or

$$rC_s(r) = \int_o^r C_1(\zeta) d\zeta$$

Using Leibnitz' rule and differentiating, this becomes

$$\frac{d}{dr} (rC_s(r)) = C_1(r) \tag{3.15}$$

By changing notation the above equation is written as

$$C_1(\zeta) = \frac{d}{d\zeta} (\zeta C_s(\zeta)) \tag{3.16}$$

which relates the three dimensional covariance function to the unidimensional one.

In practice the three dimensional covariance is known and we want to preserve it during the simulation. So we set $C_s(\zeta) = C(\zeta)$ and get

$$C_1(\zeta) = \frac{d}{d\zeta} (\zeta C(\zeta)) \tag{3.17}$$

This equation gives the unidimensional covariance function $C_1(\zeta)$ as a function of the three dimensional $C(\zeta)$.

Some examples of unidimensional equivalents to typical three dimensional covariance functions are:

Exponential model

For a 3-D exponential covariance function of the form

$$C(r) = \sigma^2 e^{-br} \qquad 0 \leq r \leq \infty$$

the corresponding one dimensional covariance function is given by (3.17) as

$$C_1(\zeta) = \sigma^2 \frac{d}{d\zeta} (\zeta e^{-b\zeta}) = \sigma^2 (1-b\zeta) e^{-b\zeta} \qquad 0 \leq \zeta \leq \infty \qquad (3.18a)$$

Double exponential model

Expressed by the formula,

$$C(r) = \sigma^2 e^{-b^2 r^2} \qquad 0 \leq r \leq \infty$$

the corresponding unidimensional covariance function is given by:

$$C_1(\zeta) = \sigma^2 (1-2b^2\zeta^2) e^{-b^2\zeta^2} \qquad 0 \leq \zeta < \infty \qquad (3.18b)$$

Spherical model

Given by:

$$C(r) = \begin{cases} \sigma^2 [1 - \frac{3}{2}\frac{r}{a} + \frac{1}{2}\frac{r^3}{a^3}] & , \quad 0 \leq r \leq a \\ 0 & , \quad a \leq r \end{cases} .$$

the corresponding one dimensional covariance function is

$$C_1(\zeta) = \begin{cases} \sigma^2 [1 - \frac{3\zeta}{a} + \frac{2\zeta^3}{a^3}] & 0 \leq \zeta \leq a \\ 0 & a \leq \zeta \end{cases} \qquad (3.18c)$$

As the remainder of this chapter will demonstrate, it is not possible to find equivalent simple relationships for two dimensional fields.

3.2.2 Two dimensional fields

Define the origin of the orthogonal axes (x,y), in the plane of the field, with origin at point $\underline{x}_1$ and the y axis in the direction of the vector $\underline{h} = \underline{x}_2 - \underline{x}_1$ as shown in Figure 3.5. In polar coordinates we can write $\underline{h} \cdot \underline{u} = r \sin\theta$ and $d\underline{u} = d\theta$. Equation (3.12) then becomes

$$C_s(r) = \frac{1}{2\pi} \int_o^{2\pi} C_1(r \sin\theta)\, d\theta$$

Because the covariance function C_1 is an even function, the integral simplifies to:

$$C_s(r) = \frac{2}{\pi} \int_o^{\pi/2} C_1(r \sin\theta)\, d\theta \qquad (3.19)$$

We define

$$\zeta = r \sin\theta \qquad (3.20)$$

so that

$$d\zeta = r \cos\theta d\theta$$

Then since for $0 \leq \theta \leq \pi/2$:

$$\cos\theta = \sqrt{1-\sin^2\theta} = \sqrt{1 - \frac{\zeta^2}{r^2}} = \frac{1}{r}\sqrt{r^2-\zeta^2}$$

we get

$$d\theta = \frac{d\zeta}{\sqrt{r^2-\zeta^2}} \qquad (3.21)$$

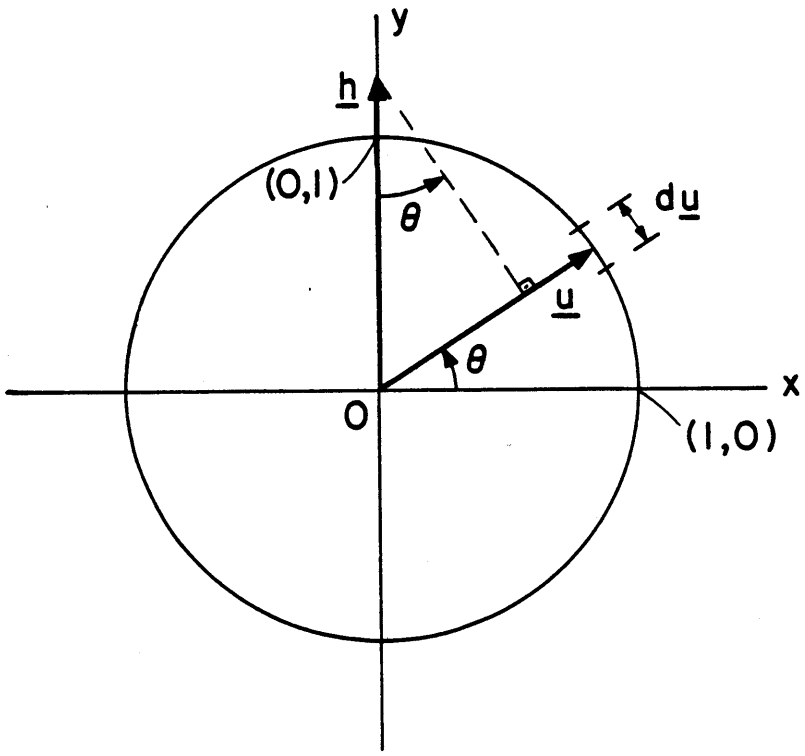

Figure 3.5 Definition sketch in the two dimensional case.

Substituting (3.20) and (3.21) into (3.19) leads to

$$C_s(r) = \frac{2}{\pi} \int_o^r C_1(\zeta) \frac{d\zeta}{\sqrt{r^2-\zeta^2}} \tag{3.22}$$

or

$$\int_o^r \frac{C_1(\zeta)}{\sqrt{r^2-\zeta^2}} d\zeta = \frac{\pi}{2} C_s(r) \tag{3.23}$$

In practice we know the two dimensional covariance function C(r) which we want to preserve. So we substitute $C_s(r) = C(r)$ and the above equation is written as

$$\int_o^r \frac{C_1(\zeta)}{\sqrt{r^2-\zeta^2}} d\zeta = \frac{\pi}{2} C(r) \tag{3.24}$$

This equation relates the two dimensional covariance function C(r) and the corresponding unidimensional one $C_1(\zeta)$ along the turning bands lines. It is an integral equation, in which we cannot directly express $C_1(\zeta)$ as a function of C(r), as we can in the three dimensional case. Nevertheless, particular solutions can be found in some cases, as shown in Section 3.4 for a few common two dimensional covariance models. In Section 3.3 an expression for the spectral density function of the one dimensional processes, as a function of the radial spectral density function of the two dimensional process, is derived. The line process then can be generated using a spectral method (such as Rice,1954 or Shinozuka and Jan, 1972). This result makes the generation of the line process easy and we don't need to actually solve (3.24) for $C_1(\zeta)$ as we do in the case of other unidimensional

generation procedures. In either case, the unidimensional process is generated discretely along the turning bands lines, although this is not an a priori requirement for the spectral method unidimensional gnerator.

3.2.3 Discussion

Equations (3.8), (3.12), and (3.13) are obtained in the limit as the number of lines goes to infinity. The lines are assumed to be randomly oriented, as taken form a uniform distribution on the unit circle or sphere. It can be easily shown that these TBM equations are also obtained with the less costly option of spacing the lines evenly on the unit circle or sphere with prescribed directions. More importantly, although the first approach preserves the statistics of th field over the ensemble, a large error is introduced in the spacial statistics of each generated realization. This process is not ergodic unless the number of lines is very large. in the second approach (utilizing evenly spaced lines) the genrated process is ergodic, even for a limited number of lines, as long as the unidimensional process used in the turning bands is ergodic.

The relative errors of the second, even spacing, approach as a function of the number of lines is discussed in

Section 3.6. A similar discussion for the first approach, of random spacing, is given in Mantoglou and Wilson (1981). The second, even spacing, approach is preferred because the simulated covariance function converges to the theoretical one much faster, and the generated process is ergodic. It is the approach used here after. In three dimensions exprience has shown that 15 lines, joining the mid-points of the opposite edges of a regular icosahedron, are adequate (Journel and Huijbregts, 1978). For two dimensional fiedls in hydrologic applications, 4-16 lines should be sufficient, depending on the accuracy desired (see Section 3.3 and 3.6).

We note that if C(r) is a proper two or three dimensional covariance function, then the funciton $C_1(\ )$ given by Equation (3.17) or (3.24) is a positive definite function in one dimension and can be used as a unidimensional covariance funciton.

3.3 Two dimensional fields: generation of the unidimensional process using a spectral method

In this section we derive, for the first time, a simple expression for the one dimensional spectral density function $S_1(\omega)$ as a function of the radial spectral density function $f(\omega)$ of the two dimensional process. Then using this expression the I-D spectral

density function $S_1(\omega)$ is calculated for some common two dimensional covariance models (Section 3.3.1). We use the above derived 1-D expressions and a spectral method in order to generate the one dimensional line processes (Section 3.3.2). Finally we discuss questions as to the accuracy of the method, as a function of the different parameters and approximations involved, and give some examples comparing the imposed theoretical statistics and those obtained from the model using a finite number of simulations.

3.3.1 Spectral representation of the unidimensional process

It was shown in Section 2.2.3 that a two dimensional isotropic covariance function can be written as (Eq. 2.30)

$$C(r) = \sigma^2 \int_o^\infty J_o(\omega r) f(\omega) d\omega \tag{3.25}$$

where:

- $C(r)$ is the two dimensional covariance function,
- $f(\omega)$ is the radial spectral density function of the two dimensional process,
- σ^2 is the variance of the process, and
- J_o is a Bessel function of order 0.

Applying a Hankel transform to this equation gives (Eq. 2.31):

$$f(\omega) = \frac{\omega}{\sigma^2} \int_o^\infty C(r) J_o(\omega r) r dr \tag{3.26}$$

The relationship between the two dimensional covariance function C(r) and the corresponding unidimensional covariance function $C_1(\zeta)$, along the turning bands lines, is given by (3.19) or (3.24). For $C_s(r) = C(r)$ equation (3.19) is written as

$$C(r) = \frac{2}{\pi} \int_o^{\pi/2} C_1(r \sin \theta)\, d\theta \tag{3.27}$$

Let $S_1(\omega)$ be the spectral density function of the line process corresponding to the covariance function $C_1(\zeta)$. Using (2.17) we can write

$$C_1(\zeta) = 2 \int_o^{\infty} \cos(\omega\zeta)\, S_1(\omega)\, d\omega \tag{3.28}$$

For $\zeta = r \sin \theta$ this becomes

$$C_1(r \sin \theta) = 2 \int_o^{\infty} \cos(\omega r \sin \theta)\, S_1(\omega)\, d\omega \tag{3.29}$$

Substituting (3.29) into (3.27) gives

$$C(r) = \frac{2}{\pi} \int_o^{\pi/2} \{2 \int_o^{\infty} \cos(\omega r \sin \theta)\, S_1(\omega)\, d\omega\}\, d\theta$$

Changing the order of integration this becomes

$$C(r) = \frac{4}{\pi} \int_o^{\infty} S_1(\omega)\, \{\int_o^{\pi/2} \cos(\omega\, r \sin \theta)\, d\theta\}\, d\omega \tag{3.30}$$

From Gradshteyn-Ryzhik (p. 952, 1965) we get, for the integral inside the brackets,

$$\int_o^{\pi/2} \cos(\omega r \sin \theta)\, d\theta = \frac{\pi}{2} J_o(\omega r) \tag{3.31}$$

Substituting (3.31) into (3.30) leaves

$$C(r) = \frac{4}{\pi} \int_o^\infty S_1(\omega) \frac{\pi}{2} J_o(\omega r)\, d\omega$$

or

$$C(r) = 2\int_o^\infty J_o(\omega r)\, S_1(\omega)\, d\omega \tag{3.32}$$

Applying a Hankel transform to this equation leads to

$$S_1(\omega) = \frac{1}{2}\, \omega \int_o^\infty C(r)\, J_o(\omega r)\, r\, dr \tag{3.33}$$

Comparing equations (3.33) and (3.26) we obtain:

$$S_1(\omega) = \frac{\sigma^2}{2}\, f(\omega) \tag{3.34}$$

This means that the spectral density function of the unidimensional process along the turning bands lines is given by one-half of the radial spectral density function of the two dimensional process multiplied by the variance!

We can use (3.34) to derive the spectral density function of the unidimensional process for various two dimensional covariance functions. For example:

Exponential Type Given: $C(r) = \sigma^2 e^{-br} \qquad r \geq 0$

Then using (2.32) and (3.34) we get:

$$S_1(\omega) = \frac{\sigma^2}{2}\, \frac{\omega}{b^2[1 + \omega^2/b^2]^{3/2}} \tag{3.35}$$

Bessel type Given: $C(r) = \sigma^2 br K_1(br) \quad r \geq 0$

Then using (2.33)and (3.34) we get:

$$S_1(\omega) = \sigma^2 \frac{\omega}{b^2[1 + \omega^2/b^2]^2} \tag{3.36}$$

Double exponential Given: $C(r) = \sigma^2 \exp\left[-b^2 r^2\right] \quad r \geq 0$

Then using (2.34)and (3.34) we get:

$$S_1(\omega) = \frac{\sigma^2}{4b^2} \exp\left[-\frac{\omega^2}{4b^2}\right] \tag{3.37}$$

3.3.2 Generation of the line process

After obtaining the spectral density function of the unidimensional process we can easily generate the process along the turning bands lines using any spectral method. Here we use the classical method proposed by S.O. Rice (1954) and modified by Shinozuka and Jan (1972). For unidimensional processes it is proven in the above references that this method is superior to the corresponding method of Mejia and Rodriguez-Iturbe (1974) in terms of accuracy and cost. A brief review of this method was given in Chapter 2. In particular, please note that this method is ergodic; thus, this resulting multidimensional field is ergodic.

If the unidimensional covariance function $C_1(\zeta)$ and the corresponding spectral density function, obtained in Section 3.3.1, is $S_1(\omega)$, then the unidimensional process can be generated by

$$z_i(\zeta) = 2 \sum_{k=1}^{M} [S_1(\omega_k)\Delta\omega]^{1/2} \cos(\omega_k'\zeta + \phi_k) \qquad (3.38)$$

where: ϕ_k = independent random angles uniformly distributed between 0 and 2π

$\omega_k = (k-1/2)\Delta\omega \qquad k=1,\ldots M$

$\omega_k' = \omega_k + \delta\omega \qquad k=1,\ldots M$

where it has been assumed that the spectral density function $S_1(\omega)$ is insignificant outside the region $[-\Omega, +\Omega]$. The discretization frequency $\Delta\omega$ is defined as: $\Delta\omega = \frac{\Omega}{M}$, where M is the number of harmonics used. The frequency $\delta\omega$ is a small random frequency added in order to avoid periodicities and is uniformly distributed between $-\frac{\Delta\omega'}{2}$ and $+\frac{\Delta\omega'}{2}$, where $\Delta\omega'$ is a small frequency, $\Delta\omega' << \Delta\omega$. (3.38) is obtained from (2.51) if we recall the symmetry of the spectral density function $S_1(\omega)$. It can be proven (Shinozuka and Jan, 1972) that the process given by (3.38) has zero mean and covariance function $C_1(\zeta)$, as $M\to\infty$, $\Omega\to\infty$ and $\Delta\omega\to 0$. In practical applications we have $M<\infty$, $\Omega<\infty$ and $\Delta\omega>0$, so that a small error is introduced. It is also noted that this process is Gaussian.

In the turning bands method, (3.38) is used to generate values at discrete points. These points are chosen to be the middle points of the segments defined by the bands along each line. The same value is assigned to the entire segment or band as shown in Figure 3.6.

We note that using the above described spectral method we could generate directly values on the turning bands lines at the projections

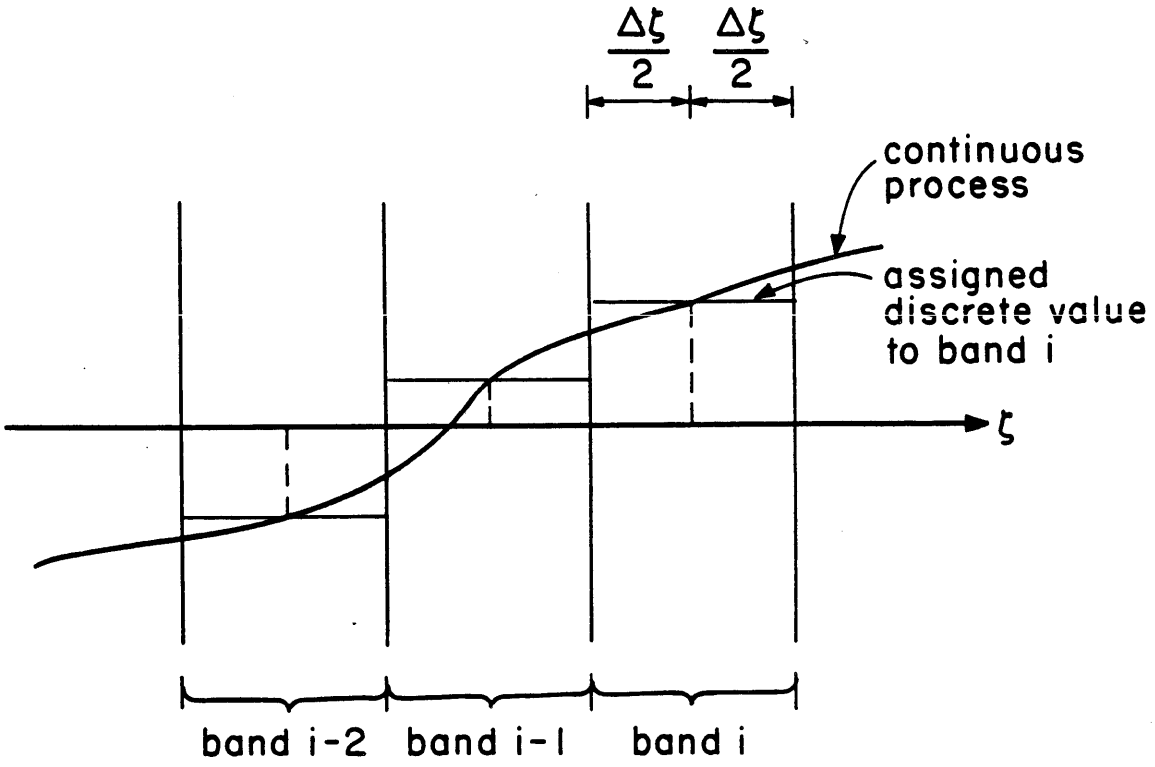

Figure 3.6 Continuous and discrete process on a turning bands line.

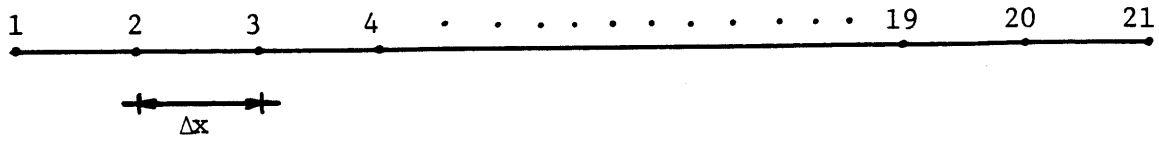

Figure 3.7 Points of the field where values are generated.

of the points of the field. This approach would eliminate the error introduced by the generation of the line process discretely in "bands". However, the cost increases rapidly since the number of points generated along the lines is equal to the number of points of the field. Although we tested this approach, it was abandoned because of its high cost.

3.3.3 Examples and Discussion

A series of examples illustrating the simulation of random fields using the turning bands methods (TBM) with the undimensional spectral process is given in this section. The statistics of the random field to be simulated (i.e., mean, variance, covariance) are assumed to be known.

A sample realization

Figure 3.8 is a contur map of a realization of an isotropic, stationary random field generated with the TBM. The random field has zero mean, unit variance $\sigma^2 = 1$, and a covariance function of the exponential type with scale parameter b = 1. The dimensions of the simulated area in the figure are: Xmax = 1.2 and Ymax = 0.96. Simulations take place at the discrete points of the grid shown. The number of columns in the grid is: NX = 100 and the number of rows NY = 80, giving a total of N = 8000 simulated points. These points were interpolated using a linear function in the contouring program (Kafritsas, 1980). The number of lines used in the turning bands model was L = 16 and the discretization along the lines was $\Delta\zeta = 0.012$. The number of harmonics in the generation of the unidimensional process was set equal to M = 100 and the maximum frequency $\Omega = 40$.

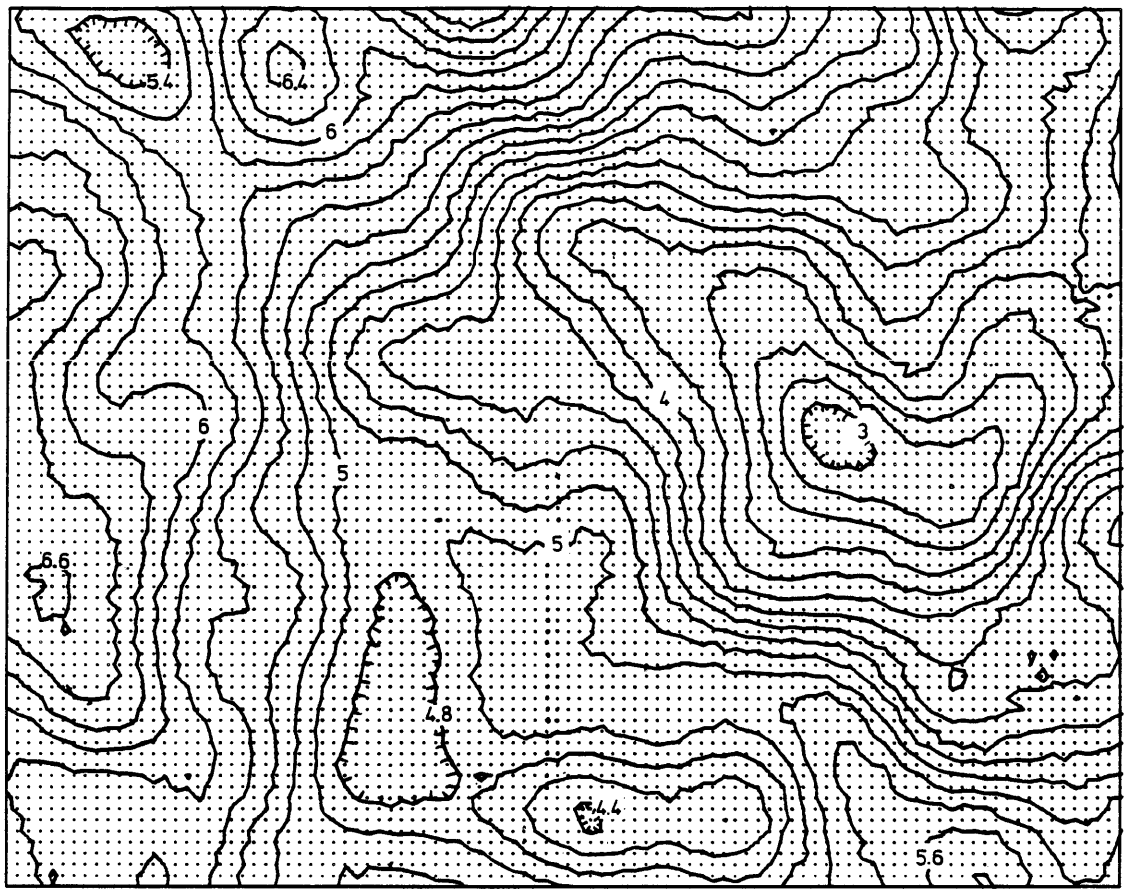

Figure 3.8 An example realization of a stationary random field generated with the TBM.

How well does a single realization like this or a sequence of many realizations generated with the TBM, preserve the statistics of the underlying random field? Some further examples will help demonstate, but first let us look at error sources.

Simulation error

There are three major sources of error in the use of simulation. The first is due to estimation of the statistics of the underlying random field from a limited data set. We are ignoring this error here, although it is undoubtably important. The second error concerns the simulation method. Model error is introduced due to the discretizations or approximations used in the TBM such as the finite number of lines, the discretization along lines, the discretization of the spectrum of the line process, and the finite number of harmonics used in the generation of the unidimensional process. These errors and their convergence as a function of these different model parameters is described in Section 3.6 of this report. The final source of error is the estimation error introduced by the use of a finite number of simulations. As the number of realizations increases, this estimation error tends to zero.

Ensemble statistics of a finite sample of realizations

An experiment was performed to illustrate the covergence of the ensemble statistics, toward the theoretical values is the number of simulations increase. In this experiment values of realizations of a two dimensional field with a zero mean (m=0), unit variance (σ^2=1), and exponential covariance were generated at a series of N = 11 points lying along a straight ling in two dimensional space each point separated from the other by a dis-

tance $\Delta x = 0.20/b$. The number of lines in the TBM method was L = 16, with $\Delta\zeta = 0.075/b$ discretization of the line process. The number of harmonics used was M = 75 with spectrum discretization $\Delta\omega = 0.40b$ ($\Omega = 30b$). Two thousand simulations were performed with the statistics calculated after every one hundred simulations. These statistics were found for the number of simulations NS = 100, 200, 300...2000; the results for several of these are given in Table 3.1. Comparison of these values to the theoretical statistics also shown in Table, demonstrates that the ensemble statistics approach the theoretical values as NS increases. Figure 3.9 presents this information graphically for the mean (m=0) and covariance, at NS = 100, 500, and 1500 realizations. The differences between the simulated ad theoretical values is mainly due to estimation error, which tends to zero with large NS, and model error.

In order to obtain some idea of the magnitude of the estimation errors, we note that the standard deviations of the estimated means $\bar{z}_{NS}$ from NS independent simulations is given by

$$\sigma_{\bar{z}_{NS}} = \frac{\sigma}{\sqrt{NS}} \tag{3.39}$$

In our case $\sigma = 1$ and we get for different number of simulating NS:

$$\sigma_{\bar{z}_{100}} = 0.10 \tag{3.40}$$

$$\sigma_{\bar{z}_{500}} = 0.045 \tag{3.41}$$

$$\sigma_{\bar{z}_{1500}} = 0.026 \tag{3.42}$$

STATISTICAL PROPERTIES		SIMULATED VALUES FOR NS SIMULATIONS						THEORETICAL VALUES
		NS = 100	200	500	1000	1500	2000	
MEAN		-0.099204	0.0936193	0.019788	-0.012051	-0.001087	-0.011165	0.00
STANDARD DEVIATION		0.928536	0.982405	0.982405	0.979543	0.975490	0.987686	1.00
VARIANCE		0.862179	0.876458	0.965120	0.959505	0.951581	0.975524	1.00
Covariance Between First Point and Point i	C(1)	0.652918	0.700064	0.806222	0.829815	0.824170	0.849715	0.818731
	C(2)	0.586860	0.591288	0.684934	0.716814	0.697518	0.727950	0.670320
	C(3)	0.455875	0.490171	0.553011	0.572730	0.561206	0.592301	0.548812
	C(4)	0.402377	0.401577	0.449401	0.463462	0.442771	0.472535	0.449329
	C(5)	0.361473	0.329773	0.388515	0.397108	0.379382	0.418981	0.367879
	C(6)	0.253728	0.287987	0.328116	0.322939	0.300225	0.321414	0.301194
	C(7)	0.113112	0.200176	0.246632	0.253247	0.247608	0.265874	0.246597
	C(8)	0.055712	0.142944	0.183683	0.199640	0.205055	0.221617	0.201897
	C(9)	0.019040	0.110630	0.095955	0.135741	0.141510	0.154022	0.165299
	C(10)	0.046938	0.103012	0.065695	0.107287	0.115567	0.127946	0.135335

TABLE 3.1

Simulated and Theoretical Statistics
for Different Numbers of Simulation

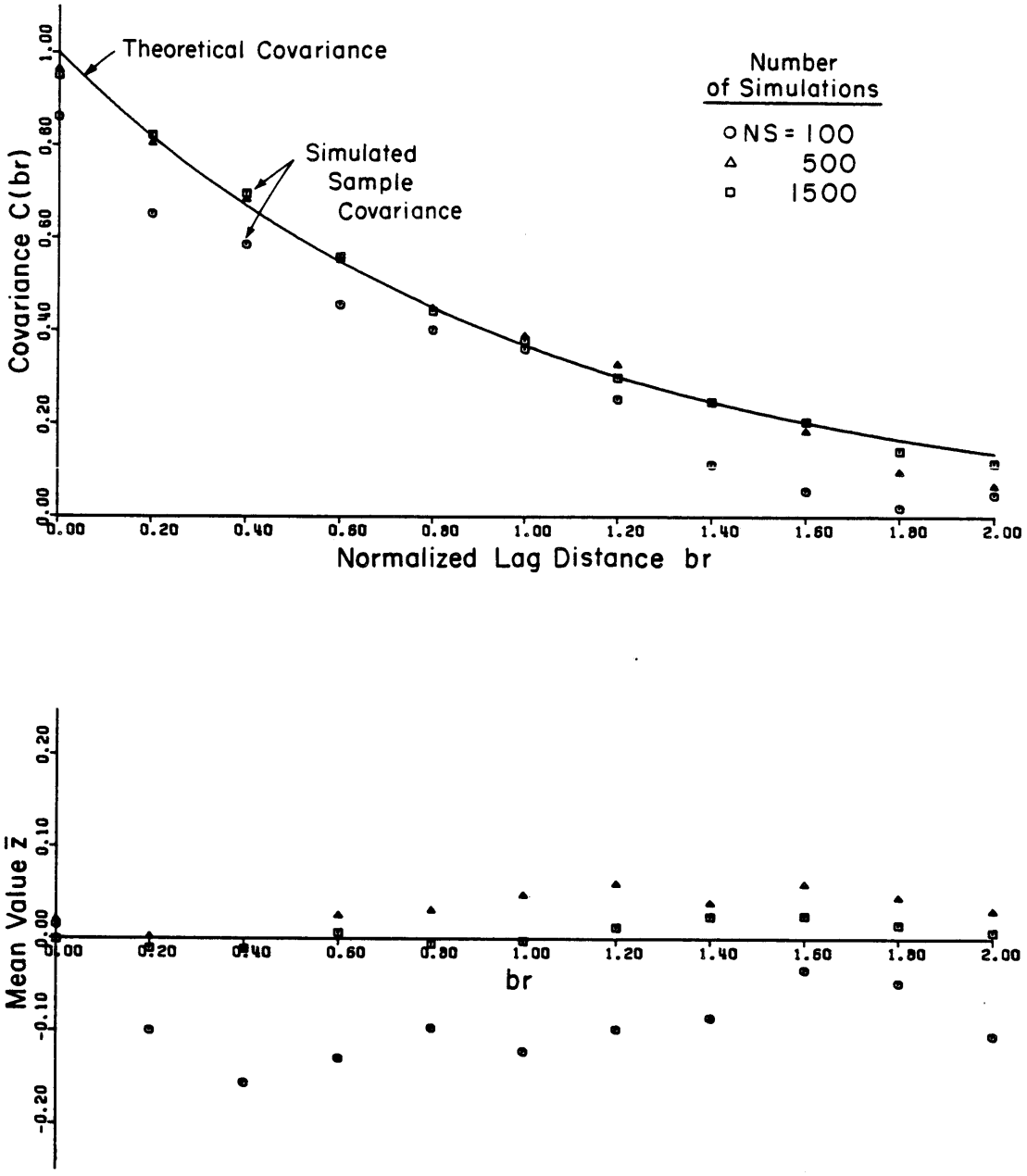

Figure 3.9 Simulated and theoretical means and covariance functions for different number of simulations.

These standard deriations may be used to define confidence limits in Figure 3.9. They demonstrate that the observable deviation in each case is mainly due to estimation error.

This experiment demonstrates that the TBM preserves well the ensemble statistics (mean and covariance) of the process. However, the experiment also reveals a problem: a large number of simulations are needed to reduce the estimation error to the degree at which the generated exponential covariance can be discriminated from, say, a Bessel type covariance. This indicates that if the number of data realizations from which the statistics of the underlying random field were estimated is small (less than a few hundred) then the type of covariance function to be fitted is not important. A Bessel or exponential model will fit equaly well (Mantoglou and Wilson, 1982). Moreover, in cases were the theoretical covariance function is assumed to be known exactly, a large number of realization should be performed in order to preserve it fairly well. This point is of great concern to those attempting Monte Carlo simulation of groundwater flow and mass tranport.

Additional examples of generation for the same field but with different values of the TBM parameters and with a limited number of simulations are presented in Figure 3.10, 3.11, and 3.12. In all these simulations, the values of the TBM, parameters were: $L = 16$, $\Delta\zeta = 0.12/b$, $M = 80$, $\Omega = 40b$. Figure 3.10 shows a result for NS = 100 simulations while figures 3.11 and 3.12 are the results of NS = 200 simulations having a different seed number. Though in those simulations the parameters of the simulation model used and the number of realizations are the same, the statistics

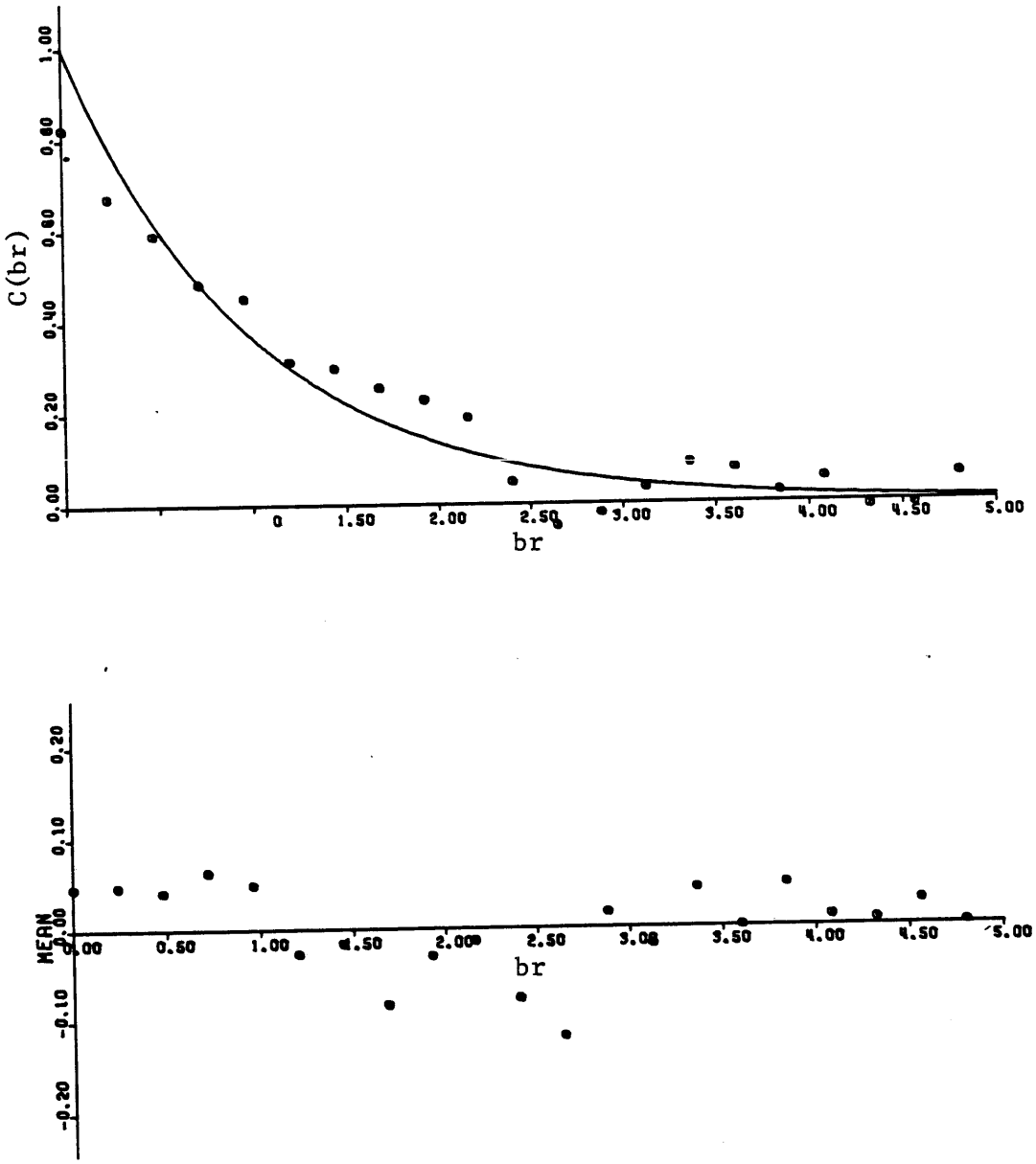

Figure 3.10 Theoretical and sample covariances and means, NS = 100, L = 16, $\Delta\zeta$ = 0.12, M = 80, Ω = 40

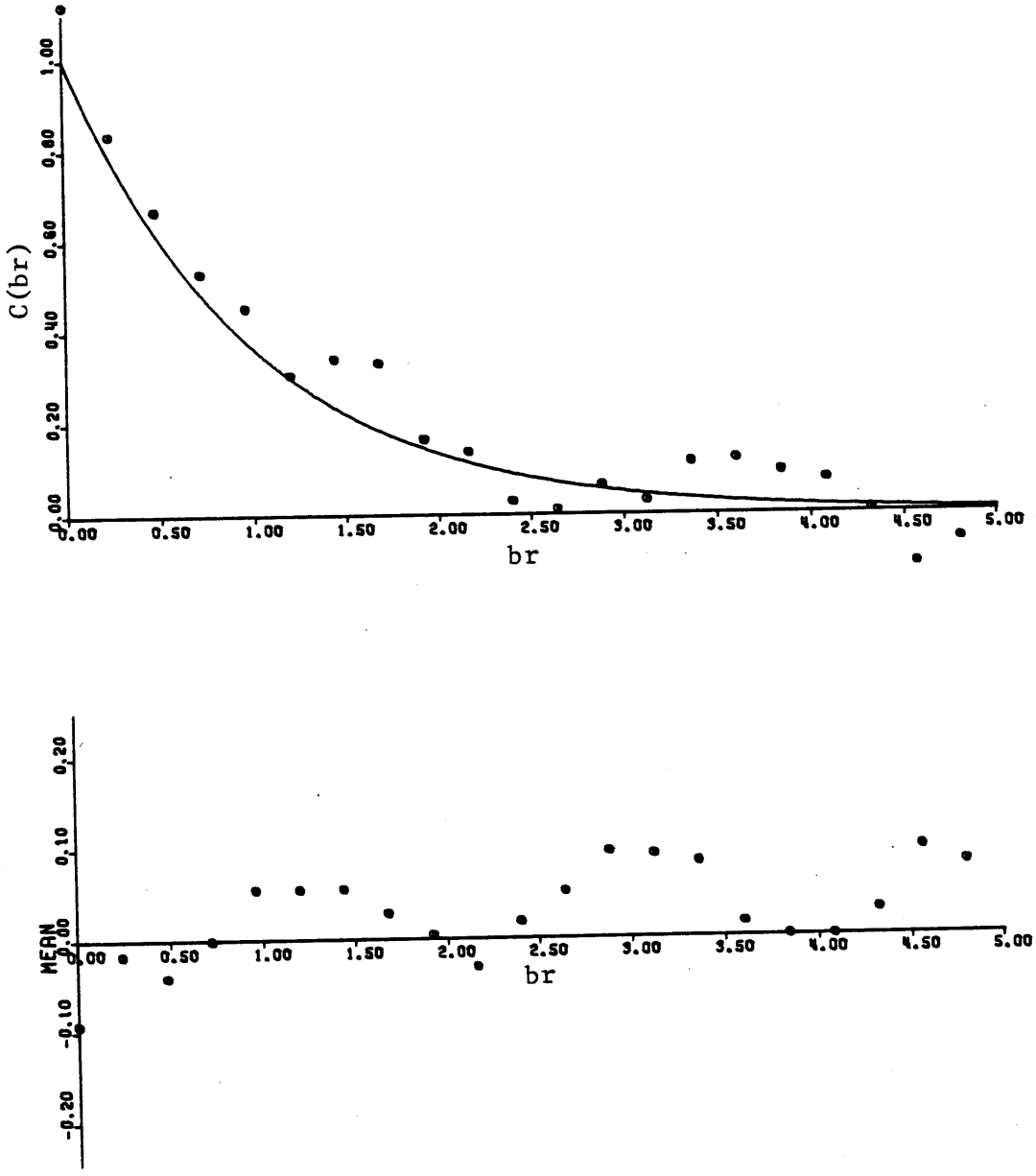

Figure 3.11 Theoretical and sample covariances and means, NS = 200, L = 16, $\Delta\zeta$ = 0.12, M = 80, Ω = 40

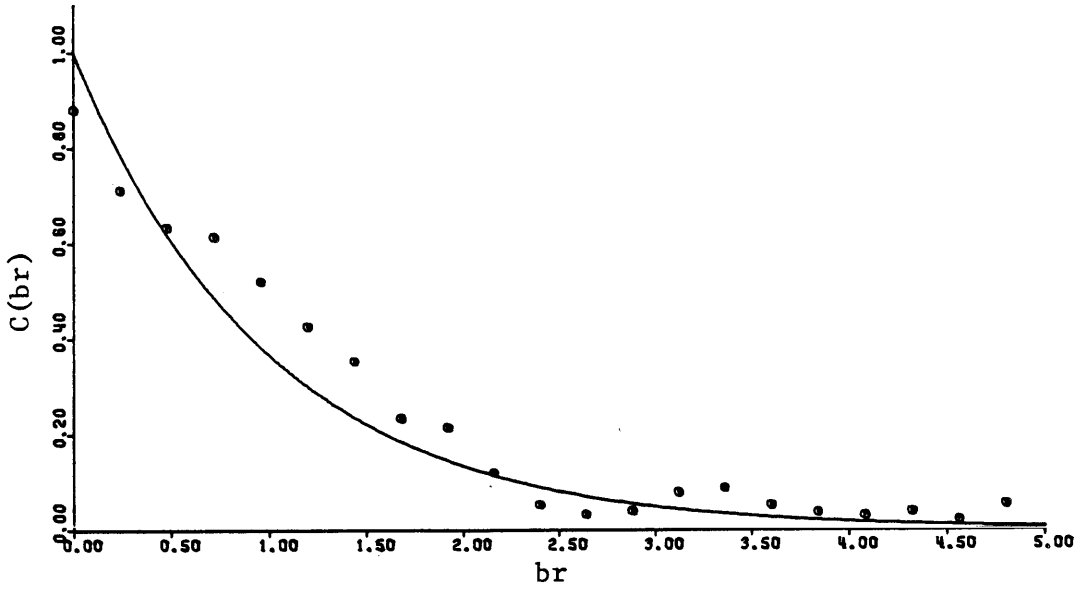

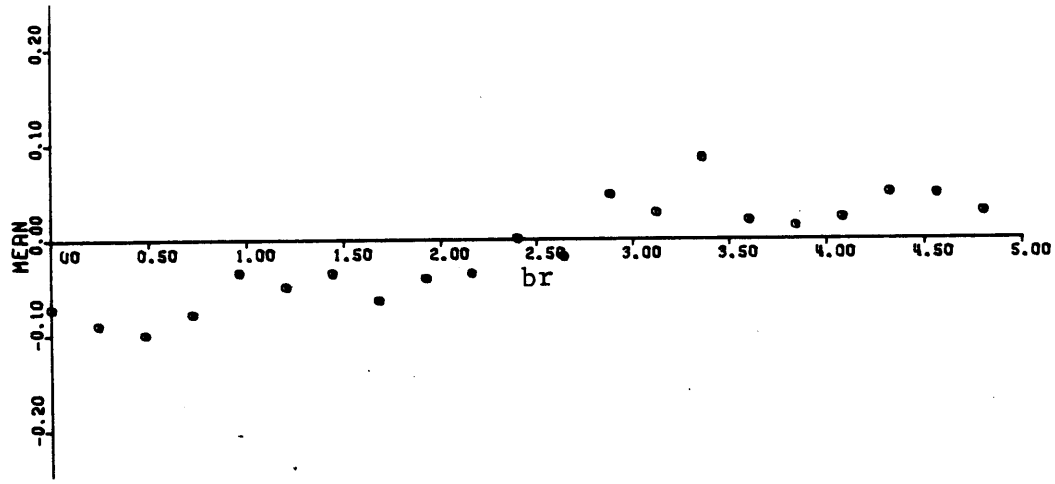

Figure 3.12 Theoretical and sample covariances and means, NS = 200, L = 16, $\Delta\zeta$ = 0.12, M = 80, Ω = 40

of the simulations are different becasue a different seed number is used. This result further illustrates the error introduced in the estimation of statistics from a finite ensemble sample.

Spatial statistics of one realization

The process generated by the TBM is ergodic (see Section 3.2.3). An example will demonstrate this. Consider a square area with dimensions Xmax = Ymax = 9.0/b. The field was simulated at N = 8100 points in a 90 x 90 grid (NX = NY = 90). The underlying process has zero mean, unit variance ($\sigma^2 = 1$) and exponential covariance. The TBM parameters were L = 16, $\Delta\zeta = 0.09/b$, M = 100, and $\Delta\omega = 0.40b$ ($\Omega = 40b$). Only are realization was generated, and the statistics of this realization as obtained by spatial averaging are shown in Table 3.2.

	MEAN	VARIANCE (STD. DEV.)	C(1)	C(2)	C(3)	C(4)	C(5)
SPACIAL STATISTICS FROM ONE REALIZATION	-0.0059	1.021 (1.010)	0.862	0.704	0.569	0.458	0.366
THEORETICAL STATISTICS	0.0	1.00	0.813	0.670	0.549	0.449	0.368
			C(6)	C(7)	C(8)	C(9)	C(10)
			0.282	0.214	0.173	0.139	0.111
			0.301	0.247	0.202	0.165	0.135

TABLE 3.2 Spacial statistics of a single realization.
(L = 16, $\Delta\zeta = 0.09/b$, M = 100, $\Omega = 40b$; N = 8100)

The theoretical and simulated statistics are very close. It should be noted that there is an estimation error due to the finite dimensions of the field and the finite number of points generated. This spacial estimation error tends to zero as the dimendions of the field, and the number of simulated points increase. The remaining error is the turning bands model error.

We also note that because of the areal correlation, the estimated spacial statistics from finite areas will have consistently smaller variance than the theoretical ones. This is easily seen when the dimension of the area being simulated is small compared to the correlation length. For example, the field of Figure 3.8 with maximum distance $Xmax = 1.2/b \cong b^{-1}$ has a sample variance $s^2 = 0.747$, while the theoretical variance is $\sigma^2 = 1$. From Table 3.2 we see that the variance of the realizations taken over a much larger area, with $Xmax = 9.0/b >> b^{-1}$, is $s^2 = 1.021 \cong \sigma^2 = 1$. This shows that the theoretical covariance is approached as the relative dimensions of the field are increased.

3.4 Derivation of the unidimensional covariance functions: generation along the turning bands lines using a moving average process

In this section we analytically calculate unidimensional covariance functions that correspond to common two dimensional covariance functions, by solving the integral equation (3.24). After obtaining these unidimensional covariance functions any method based on the generation of a line process directly from the covariance function can be used: for example, an autoregressive (AR) type process or a matrix inversion method. If the unidimensional covariance function can be written as a convolution product of a function f(u) and its transpose f(-u) then a moving average (MA) process can be used. To easily generate the line process as a MA process, a slight modification of the original covariance is proposed. First, however, we need a brief review of the moving average process (Journel and Huijbregts, 1978).

3.4.1 Unidimensional moving average process

In Figure 3.13 let the line D represent a turning bands line on which we want to generate the unidimensional process at discrete points (midpoints of the bands). The process has specified covariance $C_1(\zeta)$. Let the discretization length be $\Delta\zeta$. Generate another discrete process T on a line parallel to D, as a realization of a random process with a uniform one dimensional distribution function having zero mean, unit variance and with no correlation. Let the discretization length of this process be α. Choose α such that $\Delta\zeta/\alpha = \mu$, where

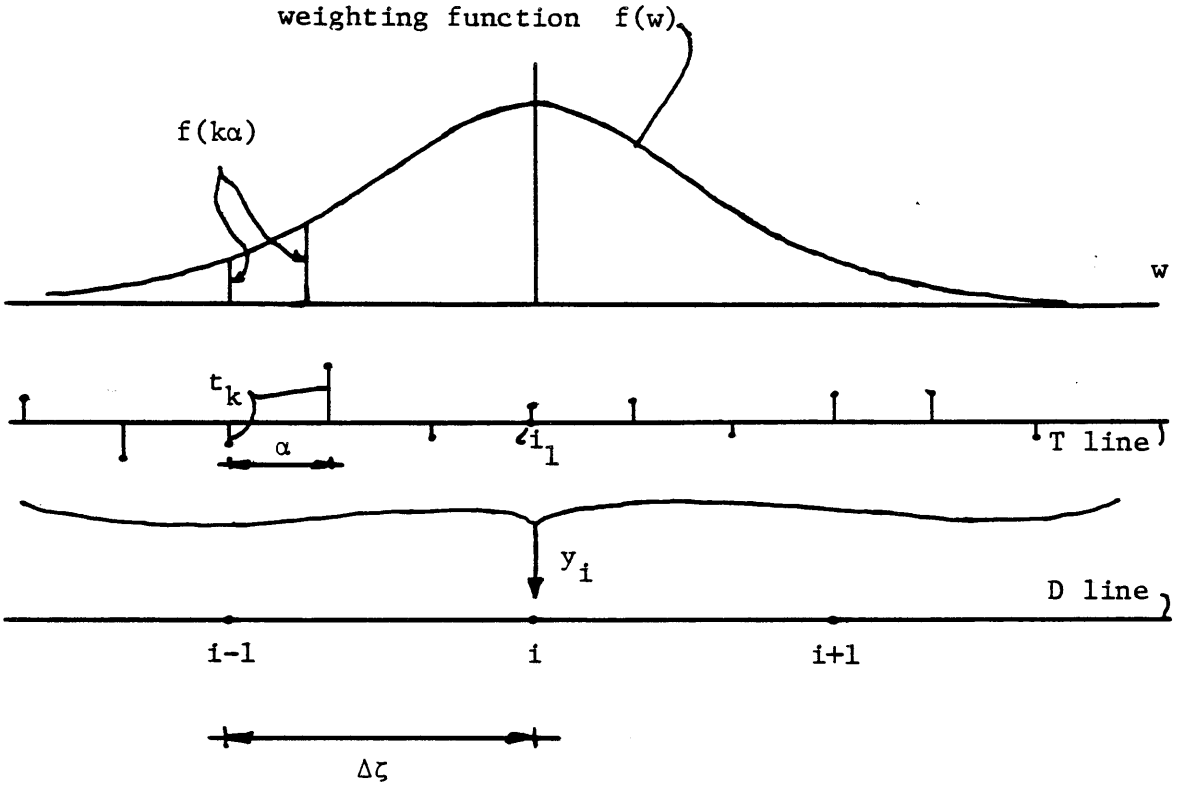

Figure 3.13 Schematic representation of the MA process.

μ is an integer, so that each of the discrete points on line D corresponds to one point on line T, as illustrated in Figure 3.13. Let the point i on line D correspond to point i_1 on line T. Define a MA process on line D given by

$$y_i = \sum_{k=-\infty}^{\infty} f(k\alpha)\ t_{i_1+k} \tag{3.43}$$

where the t_{i_1+k} are realizations of the random variable T and $f(k\alpha)$ is a weighting function. The question is: "what should the weighting function $f(k\alpha)$ be in order that y_i has the specified unidimensional covariance function $C_1(\zeta)$"?

Take two points i and $i+\zeta$ on line D. The discrete covariance C_1^d of the line process y_i is defined as:

$$C_1^d(\zeta) = E[y_i y_{i+\zeta}] =$$

$$= E\{ \sum_{k=-\infty}^{+\infty} t_{i_1+k}\ f(k\alpha) \sum_{k'=-\infty}^{+\infty} t_{\zeta_1+k'}\ f(k'\alpha)\}$$

where $\zeta_1 = (i_1 + \mu\zeta)$. Define $\ell = (\mu\zeta + k')$ and the above equation is written as:

$$C_1^d(\zeta) = E\ \{ \sum_{k=-\infty}^{+\infty} \sum_{\ell=-\infty}^{+\infty} t_{i_1+k}\ t_{i_1+\ell}\ f(k\alpha)\ f(\ell-\mu\zeta)\alpha\} \tag{3.44}$$

Because the process T is uncorrelated and has unit variance this sum becomes:

$$C_1^d(\zeta) = \sum_{k=-\infty}^{+\infty} f(k\alpha)\ f(k\alpha-\mu\zeta\alpha) \qquad (3.45)$$

As $\alpha \to 0$ the sum is replaced by the integral

$$C_1(\zeta) = \int_{-\infty}^{+\infty} f(w) f(w-\zeta) dw$$

If we define

$$\tilde{f}(w) = f(-w)$$

then the integral is re-written as

$$C_1(\zeta) = \int_{-\infty}^{+\infty} f(w)\ \tilde{f}(\zeta-w) dw \qquad (3.46)$$

This means that if the unidimensional covariance function $C_1(\zeta)$ can be written as a convolution product of a function f by its transpose $\tilde{f}$, then we can generate the underlying process as a moving average process. A technique for the calculation of the function $f(w)$ in the general case of $C_1(\zeta)$ is proposed in Mantoglou and Wilson (1982)

The discrete approximation given by (3.45) of the covariance function (3.46) involves some error which increases as the discretization length, α, increases. This error can be calculated (Journel and Huijbregts, 1978) and corrected. In practice, for common $f(w)$ functions, a multiplicative correction is enough to ensure the equality of the variances: $C_1^d(0) = C_1(0)$. Also, as will be shown later, the function f for some common models has the property that $f(w) \to 0$ as $w \to \infty$. So instead of using an infinite number of elements in the summation (3.43) we use only a finite number, k_{max}.

3.4.2 Generation of the line process as a MA process for some three dimensional models

In this section we derive the weighting function f(w) for some three dimensional covariance models.

Exponential model

For the three dimensional covariance function C(r) given by:

$$C(r) = \sigma^2 e^{-br} \qquad 0 \leq r < \infty$$

The corresponding one dimensional covariance function is given by (3.18a)

$$C_1(\zeta) = \sigma^2 \frac{d}{d\zeta} (\zeta e^{-b\zeta}) = \sigma^2(1-b\zeta)e^{-b\zeta} \qquad 0 \leq \zeta < \infty \qquad (3.47)$$

This one dimensional covariance function $C_1(\zeta)$ is the well-known "hole function," and has been used extensively to model one dimensional processes. It is shown in Figure 3.14. This covariance function can be expressed as a convolution product of the type given by (3.46). The weighting function f(w) is found to be (Journel and Huijbregts, 1978).

$$f(w) = \begin{cases} 2\sigma\sqrt{b}\ (1-bw)e^{-bw} & w \geq 0 \\ 0 & w < 0 \end{cases} \qquad (3.48)$$

which approaches zero asymptotically as $w \to \infty$, and has the same shape as the hole function. In practice the function f(w) is significantly non-zero only in the interval $[0, 4/b]$. If the discretization interval on line T is α, the number of the summation elements in (3.43) is given by:

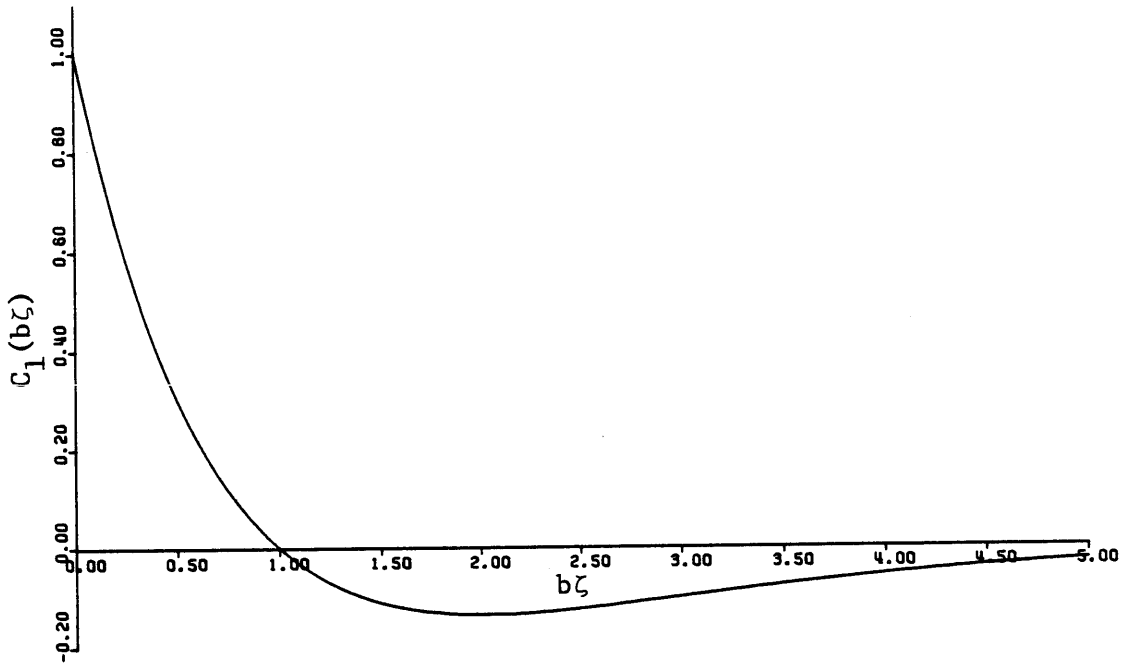

Figure 3.14 The "hole type" covariance function.

$$k_{max} = \frac{4/b}{\alpha} + 1 = \frac{4}{b\alpha} + 1$$

The density of the discrete approximation should be large, which means that $(b\alpha)$ should be small, in order to reproduce the asymptotic tendency of the covariance $C_1(\zeta)$ towards zero. If we choose $b\alpha \leq 0.125$ then we get $k_{max} \geq 161$.

Double exponential model

For

$$C(r) = \sigma^2 e^{-b^2 r^2} \qquad r \geq 0$$

we get from (3.18b):

$$C_1(\zeta) = \sigma^2(1 - 2b^2\zeta^2)e^{-b^2\zeta^2} \qquad \zeta \geq 0 \tag{3.49}$$

This covariance function is expressed as a convolution product $C_1(\zeta) = f * \tilde{f}$ (Journel and Huijbregts, 1978) where f given by:

$$f(w) = \frac{16\sigma^2 b^3}{\sqrt{\pi}} we^{-2b^2 w^2} \qquad -\infty \leq w < +\infty \tag{3.50}$$

In practice this function is significant in the interval $[-2/b, 2/b]$.

Spherical model

For completeness we note that the one dimensional covariance function $C_1(\zeta)$ corresponding to the spherical type model is given by (3.18c):

$$C_1(\zeta) = \begin{cases} \sigma^2\left[1 - \frac{3\zeta}{a} + \frac{2\zeta^3}{a^3}\right], & 0 \leq \zeta \leq a \\ 0 & a \leq \zeta \end{cases} \tag{3.51}$$

and the weighting function f(w) is given by:

$$f(w) = \begin{cases} \sigma\sqrt{12/a^3}\ w\ , & -\frac{a}{2} \leq w \leq \frac{a}{2} \\ 0\ , & \text{otherwise} \end{cases} \tag{3.52}$$

3.4.3 Derivation of the unidimensional covariance functions for some two dimensional models: generation of the unidimensional process as a MA process

In Section 3.3.1 we derived a formula which relates the spectral density function of the unidimensional process in the turning bands lines to the radial spectral density function of the two dimensional isotropic process. Based on that formula we calculated the unidimensional spectral density function for some common two dimensional covariance models. Here we are going to use those equations to derive expressions for one dimensional covariance functions. Then we'll modify the original covariance functions, so that we can generate the corresponding one dimensional processes as moving average process. Furthermore, we are going to derive some new two dimensional models such that the corresponding one dimensional processes are simple and easy to simulate by moving averages. The procedure is illustrated through examples.

Exponential covariance in two dimensions

First assume that the two dimensional model has covariance of exponential type given by

$$C(r) = \sigma^2 e^{-br} \tag{3.53}$$

Then, as was shown in Section 3.3.1, the corresponding one dimensional process has a spectral density function given by

$$S_1(\omega) = \frac{\sigma^2}{2} \frac{\omega}{b^2[1 + \frac{\omega^2}{b^2}]^{3/2}} \tag{3.54}$$

The covariance function corresponding to the above spectral density function is given by

$$C_1(\zeta) = 2\int_o^\infty \cos(\omega\zeta)\ S_1(\omega)\ d\omega =$$

$$= \frac{\sigma^2}{b^2} \int_o^\infty \cos(\omega\zeta) \frac{\omega}{[1 + \omega^2/b^2]^{3/2}} d\omega \tag{3.55}$$

In Appendix A this integral is calculated, leading to:

$$C_1(\zeta) = \sigma^2\{1 - \frac{\pi}{2} b\zeta[I_o(b\zeta)-L_o(b\zeta)]\} \tag{3.56}$$

where I_o is a Bessel function of order zero, and L_o is a modified Struve function of order zero (Abramowitz and Stegun, 1964). It was not possible to calculate the weigting function f(w) of equation 3.46 analyticaly in that case. However, the technique proposed by Mantoglou and Wilson (1982) based on a numerical integration can be applied for the calculation of the function f(w). The unidimensional process can be simulated as a MA process then. Another approach will be presented latter.

In Figure 3.15 the exponential covariance function of the two dimensional process is shown, as well as the corresponding one dimensional covariance function given by (3.56). It is assumed that $\sigma^2 = 1$.

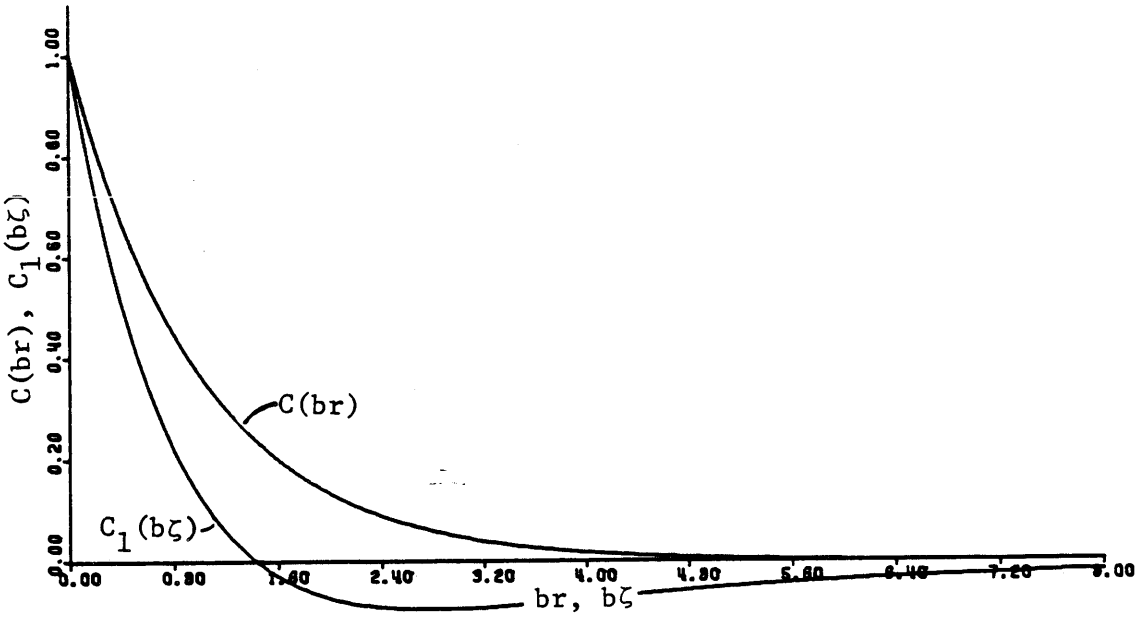

Figure 3.15. Two dimensional exponential type covariance function C(br) and the corresponding unidimensional covariance function $C_1(b\zeta)$.

Bessel type two dimensional covariance

If the two dimensional covariance function is of Bessel type, then the corresponding one dimensional process has a spectral density function given by (3.36)

$$S_1(\omega) = \sigma^2 \frac{\omega}{b^2[1 + \omega^2/b^2]^2} \tag{3.57}$$

The covariance function is given by

$$C_1(\zeta) = \frac{2\sigma^2}{b^2} \int_0^\infty \cos(\omega\zeta) \frac{\omega}{[1 + \omega^2/b^2]^2} d\omega \tag{3.58}$$

This integral is calculated in Appendix A, resulting in:

$$C_1(\zeta) = \sigma^2\{1 - \frac{b\zeta}{2} [e^{-b\zeta}Ei(b\zeta) - e^{b\zeta}Ei(-b\zeta)]\} \tag{3.59}$$

where Ei is the exponential integral function. It was not possible again to calculate f(w) analyticaly and a numerical integration should be performed (Mantoglou and Wilson 1982).

Figure 3.16 plots the unidimensional covariance function given by (3.59) and the corresponding two dimensional covariance function given by a Bessel function as

(3.60)

$$C(r) = \sigma^2 br K_1 (br) \tag{3.60}$$

where it is assumed that $\sigma^2 = 1$.

Comparison with the one dimensional "hole function"

If we compare Figures 3.15 and 3.16 to Figure 3.14, we see that the shape of the one dimensional covariance functions obtained above for the exponential and Bessel type models are similar to the shape of the hole covariance function given by

$$C_h(\zeta) = \sigma^2(1-a\zeta)e^{-a\zeta}$$

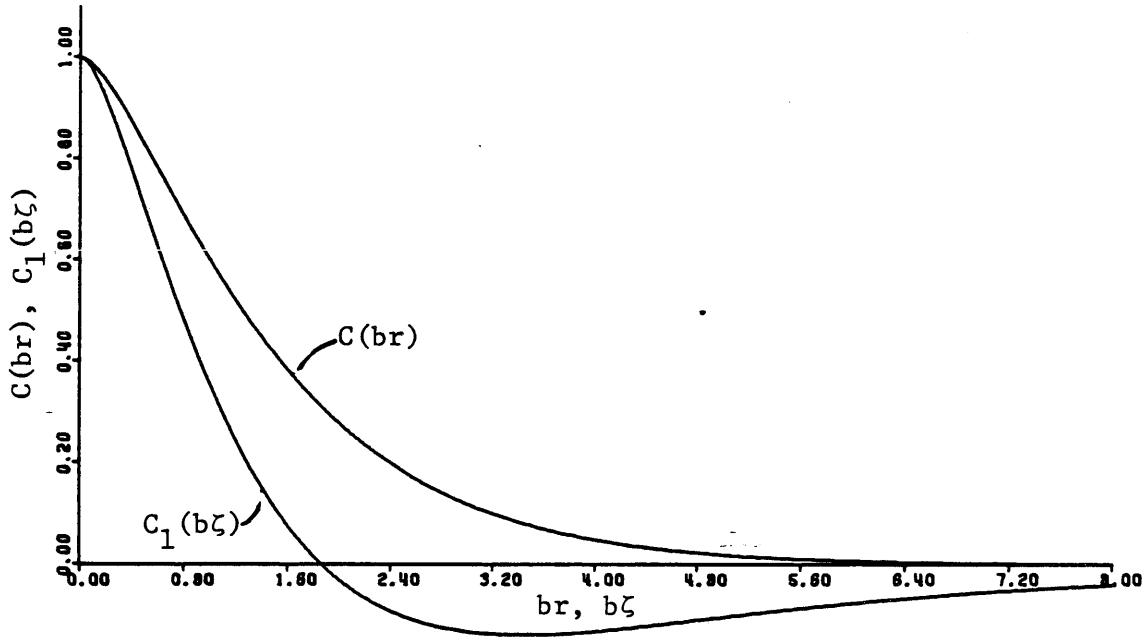

Figure 3.16. Two dimensional Bessel type covariance function C(br) and the corresponding unidimensional covariance function $C_1(b\zeta)$

The hole covariance function has been used extensively to model one dimensional processes, as noted in Section 3.4.2. It also has the important property that it can be written as a convolution product of a function with its transpose, which makes possible generation along the lines using the MA process. These properties lead to a comparison of the covariances given by (3.56) and (3.59) with the hole type covariance function given by (3.47) or (3.61). The result is given in Figure 3.17a), revealing that the shape of all these covariance functions is similar.

The next step is to find the two dimensional covariance function corresponding to the hole type unidimensional covariance function, and compare it to the exponential and Bessel type models. The derivation primarily concerns the calculation of the integral in (3.24), and is given in Appendix B. It is found there that the two dimensional covariance function corresponding to the hole type unidimensional covariance function is given by

$$C(r) = \sigma^2\{I_o(ar)-L_o(ar) + ar[I_1(ar)-L_1(ar) - \frac{2}{\pi}]\} \qquad (3.61)$$

where I_1 and L_1 are Bessel and Struve functions of order 1 and are defined in Appendix B.

We next compare the two dimensional covariance function given by (3.61) to the exponential and Bessel type models. The result is shown in Figure 3.17b. The comparison reveals that the covariance function given by (3.61) is similar to the exponential and Bessel type models. Because it has been found that many two dimensional processes follow

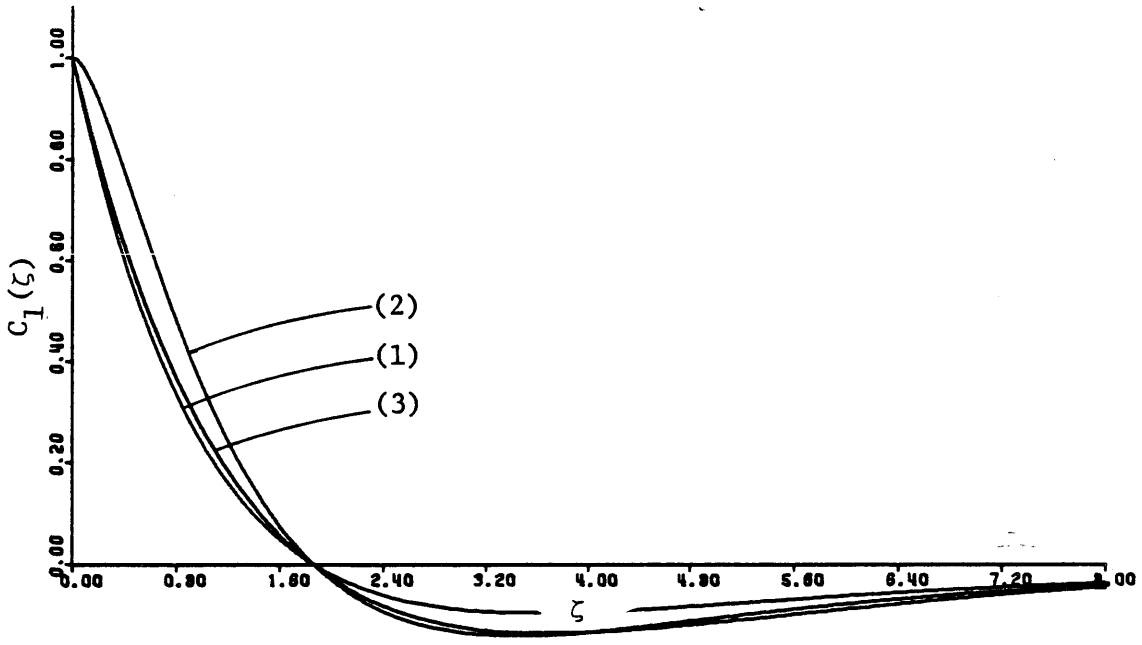

Figure 3.17a. Comparison of the unidimensional covariance functions, corresponding to the exponential type (curve 1) and Bessel type (curve 2) two dimensional covariances, to the hole function (curve 3).

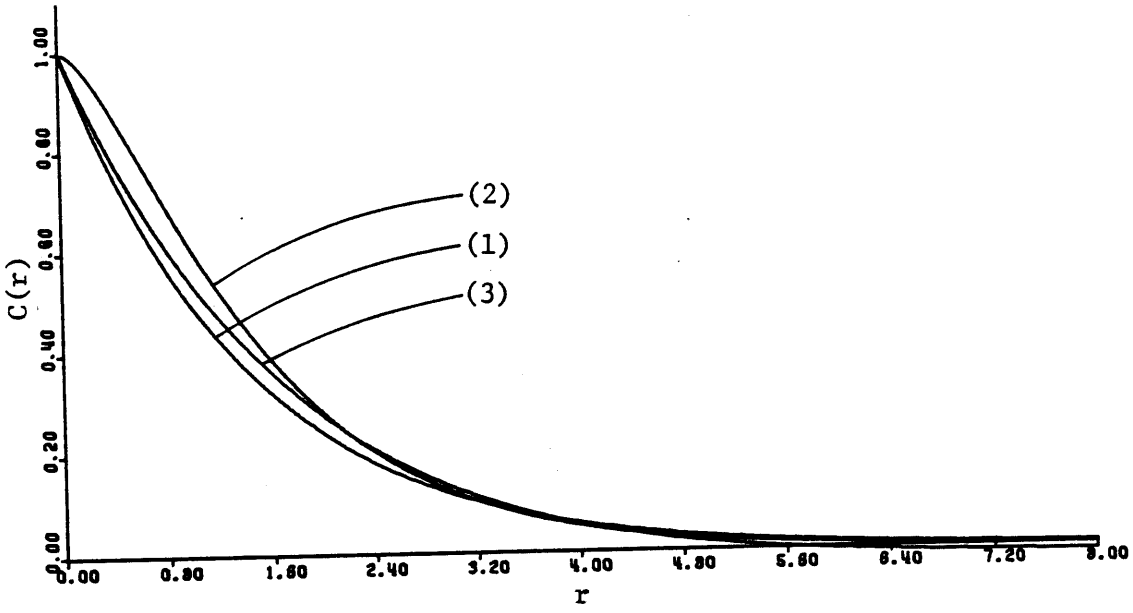

Figure 3.17b. Comparison of the exponential (curve 1) and Bessel (curve 2) models to the two dimensional covariance function corresponding to the hole function (curve 3).

covariance functions close to exponential or Bessel type, we can infer that the covariance function given by (3.61) will also fit two dimensional processes. This is especially evident when one considers the estimation error in the covariance function.

The above discussion leads to the conclusion that we can fit a model of the type in (3.61) to the two dimensional covariance function. The corresponding unidimensional process then will have a hole type covariance function. Then we can use a MA process to generate the unidimensional process. The benefit of this procedure is reduction in cost by generating the line process as MA process, instead of using the spectral method, which in general should be more expensive.

We note here that Chiles (1974) has proposed a much more complicated 2D covariance function such that the corresponding unidimensional function can be written in the form of Equation (3.46) where the function f(w) is of polynomial type.

Simulation using the unidimensional MA process and the hole function

In order to test the proposed method we re-examined the example presented in Section 3.3.3 and in Figure 3.10 - 3.12. Here we assumed that the two dimensional covariance function is given by (3.61) with $a = 1$ and $\sigma^2 = 1$. The band width was specified as $\Delta\zeta = 0.12$. The length α of discretization of the uniform process T (Figure 3.13) was chosen to be $\alpha = 0.024$. The number of the summation elements was set to $k_{max} = 168$ and the range of the function $f(w)$ was $w_{max} = 4$. The number of lines was set to 16. We performed two runs with the number

of simulations set to 100 and 200 respectively. The results of the comparison between the theoretical covariance and those obtained from the sample statistics are shown in Figures 3.18-3.19.

3.5 Generation along turning band lines using an autogressive (AR) process

For the sake of completeness we derive in Appendix B the two dimensional covariance function corresponding to one dimensional covariance function of exponential type, that is

$$C_1(\zeta) = \sigma^2 e^{-a\zeta} \tag{3.62}$$

The corresponding two dimensional covariance function is given by

$$C(r) = \sigma^2 [I_o(ar) - L_o(ar)] \tag{3.63}$$

In this case the unidimensional process is generated very easily as a simple bidirectional autoregressive (AR) process of order 1, and is much cheaper to implement than all the other processes we discussed before. However, the simulated two dimensional covariance function has a long tail, and is of relatively little interest in hydrology. Consequently we will present no further analysis of this approach.

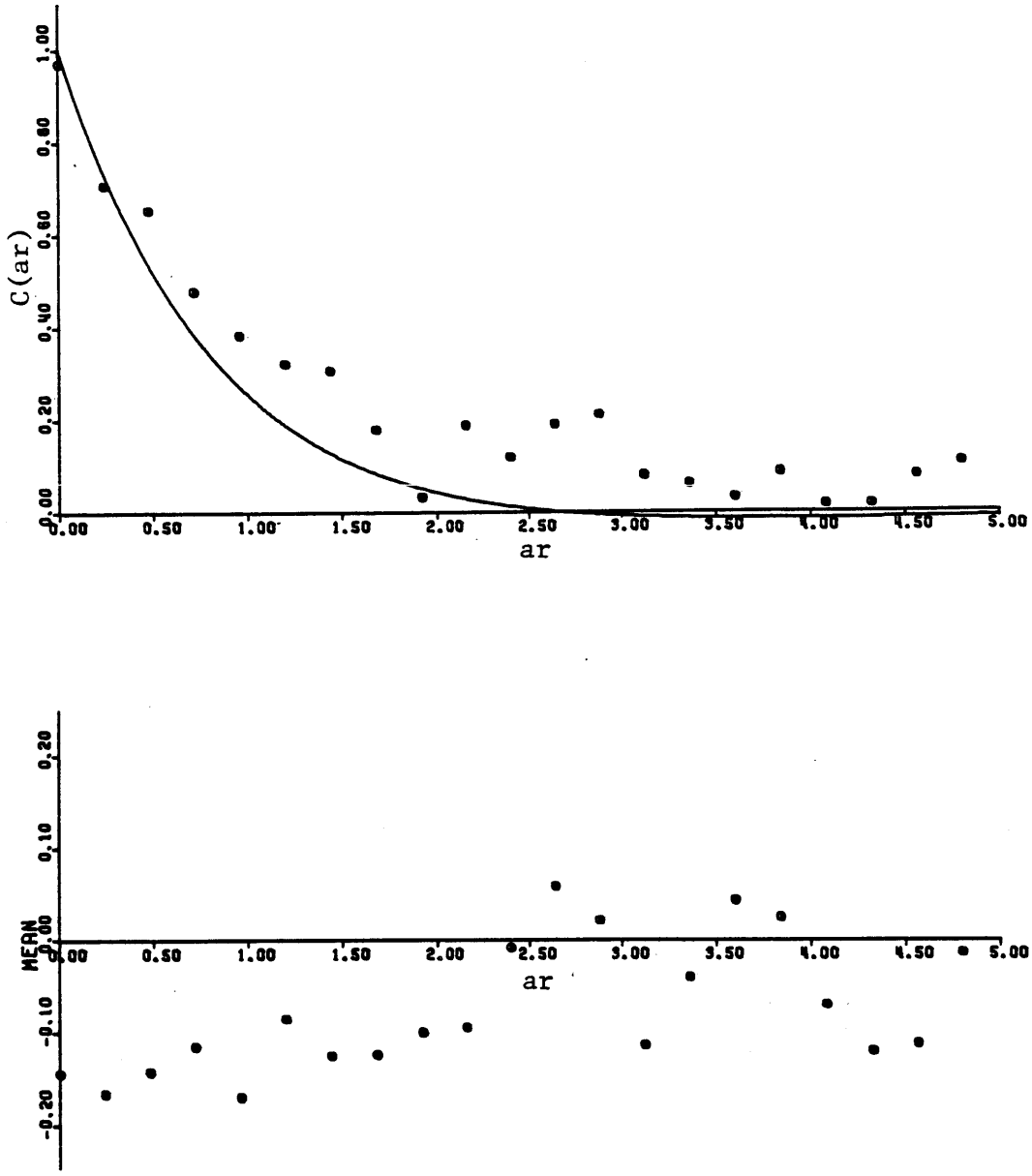

Figure 3.18. Theoretical and sample covariances and means. NS = 100, L = 16, $\Delta\zeta = 0.12$, $\alpha = 0.024$

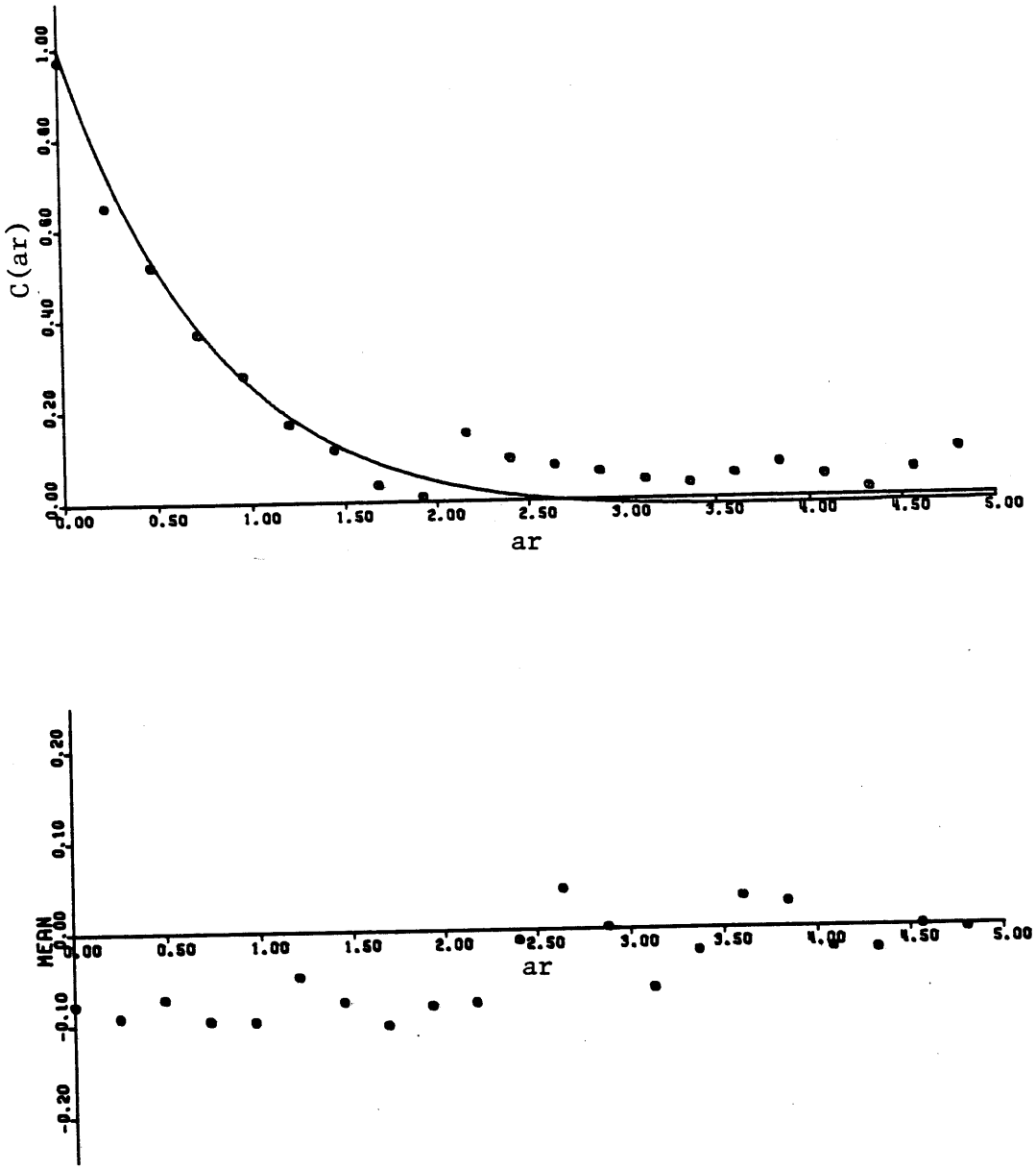

Figure 3.19. Theoretical and sample covariances and means. NS = 200, L = 16, $\Delta\zeta$ = 0.12, α = 0.024.

3.6 Accuracy of the turning bands method

As stated previously the turning bands method (TBM) exactly preserves the mean of the process, but some error is introduced in the covariance function due to the finite number of lines (L), the discretization along the lines ($\Delta\zeta$) and the discretization of the spectrum of the line process (M, Ω).

There is a tradeoff between accuracy and cost. A more accurate model will be more expensive. In practical hydrologic applications, the imposed (theoretical) statistics are very often obtained from a limited set of data points in the field and a limited number of realizations (very often only one). So it is expected that the errors in the estimation of the covariance function, etc., are quite significant and the true covariance function is different from the one we fit with a model. Consequently, in the simulation of the process, we may not always be justified in using a very exact (and thus more expensive) generation model, by increasing the number of lines, etc. How well should we preserve the model covariance function, when it does not represent exactly the reality? It would be wiser to choose the parameters of the model such that there is consistency between these input data estimation errors and the simulation model errors.

As will be shown later in this section, the errors due to discretization along the lines and discretization of the spectrum are not important for adequately small discretization length ($\Delta\zeta$), and a large number of harmonics (M). The main source of error then is due to the finite number of lines.

In Mantoglou and Wilson (1981) the convergence properties of the TBM model covariance function to the theoretical one are derived for the case

when the lines are randomly distributed over the unit circle. It is proven there that the standard deviation of the error in the covariance function is given by

$$\sigma_\varepsilon(r) = \frac{A(r)}{\sqrt{L}}$$

when A(r) a function of the distance r. This equation shows that for randomly spaced lines the TBM model covariance function converges to the theoretical one very slowly ($1/\sqrt{L}$), as the number of lines increases. As will be shown in the next subsection when the lines are evenly spaced, the TMB covariance function tends is the theoretical one very fast (as $1/\sqrt{L}$).

In this section we will first derive an equation giving the rate of convergence of the turning bands model covariance function to the theorectical one, as a function of the number of lines (L). Then we will provide examples which illustrate the errors between the theoretical and the model covariance functions for different numbers of lines and discretization lengths along the lines. Finally, we will compare the theoretical one dimensional covariance functions to those obtained from a finite number of harmonics. The discussion and the associated graphs are useful in the selection of model parameters.

3.6.1 Convergence of the TBM with the number of lines

The convergence of the TBM covariance function to the true covariance function, can be calculated as follows. Define the true covariance fucntion C(r) as (3.19)

$$C(r) = \frac{2}{\pi}\int_0^{\pi/2} C_1(r\sin\theta)\, d\theta \qquad (3.64)$$

or, because $C_1(\ )$ is symmetric

$$C(r) = \frac{1}{\pi}\int_o^{\pi} C_1(r\ \sin\theta)\ d\theta \tag{3.65}$$

For finite L, (3.7) with $\underline{h}\cdot\underline{u}_i = r\ \sin\theta_i$ gives the TBM simulated covariance function:

$$C_s(r) = \frac{1}{L}\sum_{i=1}^{L} C_1(r\ \sin\theta_i) \tag{3.66}$$

which converges to C(r) as $L\to\infty$.

An error in the covariance function is introduced due to finite number of lines and can be defined by:

$$\varepsilon = C_s(r)-C(r)$$

$$= \frac{1}{L}\sum_{i=1}^{L} C_1(r\ \sin\theta_i) - \frac{1}{\pi}\int_o^{\pi} C_1(r\ \sin\theta)\ d\theta \tag{3.67}$$

As described in Section 3.2.3 the lines are evenly spaced along the unit circle. Let's assume that L is an even number. Also, for the moment, assume that the points at distance r, where the covariance function is calculated, lie on one of the turning bands lines. Let i and i + 1 be two adjacent TBM lines. The angle formed between these two lines is $\Delta\theta = \pi/L$. By replacing:

$$g(\theta) = C_1(r\ \sin\theta) \tag{3.68}$$

We get from (3.65)

$$C(r) = \frac{1}{\pi}\int_o^{\pi} g(\theta)\ d\theta = \frac{1}{\pi}\sum_{i=1}^{L}\int_{\theta_i}^{\theta_i+\Delta\theta} g(\theta)\ d\theta = \frac{1}{\pi}\sum_{i=1}^{L} I_i \tag{3.69}$$

where $\theta_1 = 0$, $\theta_i = (i-1)\,\Delta\theta$ and:

$$I_i = \int_{\theta_i}^{\theta_i+\Delta\theta} g(\theta)\, d\theta \tag{3.70}$$

The function $g(\theta)$ is expanded in a Taylor series with center at θ_i:

$$g(\theta) = g(\theta_i) + (\theta-\theta_i)g'(\theta_i) + \frac{(\theta-\theta_i)^2}{2!}\, g''(\theta_i) + O[(\theta-\theta_i)^3] \tag{3.71}$$

where the prime indicates derivative. Defining $\phi = \theta-\theta_i$ the integral in (3.70) can be evaluated term by term:

$$I_i = \int_o^{\Delta\theta} \{g(\theta_i) + \phi g'(\theta_i) + \frac{\phi^2}{2}\, g''(\theta_i) + O[\phi^3]\}\ d\phi$$

$$= g(\theta_i)\Delta\theta + g'(\theta_i)\,\frac{\Delta\theta^2}{2} + g''(\theta_i)\,\frac{\Delta\theta^3}{6} + O[\Delta\theta^4]] \tag{3.72}$$

Equation (3.65) is evaluated from (3.68), (3.69) and (3.72), where terms of $O[\Delta\theta^4]$ and higher are neglected:

$$C(r) \overset{\sim}{=} \frac{1}{\pi}\,\{\sum_{i=1}^{L} C_1(r\,\sin\theta_i)\,\Delta\theta + \frac{1}{2}\sum_{i=1}^{L}[C_1(r\,\sin\theta_i)]'\Delta\theta^2$$

$$+ \frac{1}{6}\sum_{i=1}^{L}[C_1(r\,\sin\theta_i)]''\,\Delta\theta^3\} \tag{3.73}$$

Since $\Delta\theta = \pi/L$ the first term of this series cancels out the first term of the right-hand side of the error term (3.67), leaving

$$\varepsilon \overset{\sim}{=} -\frac{1}{2L}\sum_{i=1}^{L}[C_1(r\,\sin\theta_i)]'\,\Delta\theta - \frac{\pi}{6L^2}\sum_{i=1}^{L}[C_1(r\,\sin\theta_i)]''\,\Delta\theta \tag{3.74}$$

Redefining the function $g(\theta_i) = [C_1(r \sin\theta_i)]'$, the first term of this error estimate can be approximated using the integral series approximation (3.69) and the Taylor series expansion (3.72):

$$\int_o^\pi [C_1(r \sin\theta)]' \, d\theta \overset{\sim}{=} \sum_{i=1}^{L} [C_1(r \sin\theta_i)]' \, \Delta\theta$$

$$+ \frac{1}{2} \sum_{i=1}^{L} [C_1(r \sin\theta)]'' \, \Delta\theta^2 \qquad (3.75)$$

where higher order terms have been neglected. Since

$$\int_o^\pi [C_1(r \sin\theta)]' \, d\theta = C_1(r \sin\theta)\Big|_o^\pi = 0 \qquad (3.76)$$

(3.75) can be rearranged to give

$$\sum_{i=1}^{L} [C_1(r \sin\theta_i)]' \, \Delta\theta \overset{\sim}{=} - \frac{\pi}{2L} \sum_{i=1}^{L} [C_1(r \sin\theta_i)]'' \, \Delta\theta \qquad (3.77)$$

Substituting into (3.74) we get:

$$\varepsilon \overset{\sim}{=} \frac{\pi}{12L^2} \sum_{i=1}^{L} [C_1(r \sin\theta_i)]'' \, \Delta\theta \qquad (3.78)$$

The summation can be approximated as

$$\sum_{i=1}^{L} [C_1(r \sin\theta_i)]'' \, \Delta\theta \overset{\sim}{=} \int_o^\pi [C_1(r \sin\theta)]'' \, d\theta = I_1 \qquad (3.79)$$

where

$$I_1 = [C_1(r \sin\theta)]' \Big|_{\theta=0}^{\pi} = \frac{dC_1(r \sin\theta)}{d\theta} \Big|_{\theta=0}^{\pi}$$

Defining $\zeta = r \sin\theta$, the derivative becomes

$$\frac{dC_1(r \sin\theta)}{d\theta} = \frac{dC_1(\zeta)}{d\zeta}\frac{d\zeta}{d\theta} = (r \cos\theta)\frac{dC_1(\zeta)}{d\zeta}$$

or

$$I_1 = (r \cos\theta)\frac{dC_1(\zeta)}{d\zeta}\Bigg|_{\theta=0,\zeta=0}^{\theta=\pi,\zeta=0} = -2r\frac{dC_1(\zeta)}{d\zeta}\Bigg|_{\zeta=0}$$

The derivative, evaluated at $\zeta = 0$, is the slope of the unidimensional covariance function at the origin, where $C_1(\zeta) = C_1(0) = \sigma^2$ is the variance of the unidimensional process equal to the variance of the corresponding two dimensional process. Define constant K

$$K = -\frac{1}{\sigma^2 b}\frac{C_1(\zeta)}{d\zeta}\Bigg|_{\zeta=0} \tag{3.80}$$

where σ is the standard deviation of the two dimensional process, and b^{-1} is the correlation length, then the error is given by (3.78) with substitutions (3.79) and (3.80) is:

$$\varepsilon = \frac{\pi\sigma^2 Kbr}{6L^2} \tag{3.81}$$

This estimation for the error has been derived with the assumptions that the number of lines is even and the points where the covariance is calculated lie on one of the turning bands lines. If these points lie on the bisector between two adjacent lines the error is given by:

$$\varepsilon = \frac{-\pi\sigma^2 Kbr}{12L^2} \tag{3.82}$$

For any other direction of the line connecting the points the error will lie within these bounds:

$$\frac{-\pi\sigma^2 Kbr}{12L^2} \leq \varepsilon \leq \frac{\pi\sigma^2 Kbr}{6L^2} \tag{3.83}$$

For uniformly distributed angle of the line connecting the simulated points, the expected covariance error lies halfway between the bounds of (3.81) and (3.82);

$$E[\varepsilon] = \frac{\pi\sigma^2 Kbr}{24L^2} \tag{3.84a}$$

and the standard deviation of the error is

$$\sigma_\varepsilon' = \frac{3\pi\sigma^2 Kbr}{12^{3/2} L_2} = 0.227 \frac{\sigma^2 Kbr}{L^2} \tag{3.84b}$$

The square root of the moment of the error about the theoretical covariance is given by:

$$\sigma_\varepsilon = \frac{7\pi\sigma^2 Kbr}{36L^2} = 0.231 \frac{\sigma^2 Kbr}{L^2} \tag{3.84c}$$

The coefficient K depends on the type of the covariance function. If, for example, $C_1(\ )$ is a hole function (2.9), then K can be calculated from (3.80) to be $K=2/\sigma^2 b$. For a two dimensional exponential covariance function (2.10), the corresponding one dimensional covariance function (3.56) yields $K = 1.6/\sigma^2 b$.

The error estimates show that the simulated covariance asymptotically converges to the true covariance as $1/L^2$. They also indicate

that the error increases linearly with distance r, at least for small r. For large r the higher order terms neglected in (3.81) are important and the error has a finite limit as $r \to \infty$. For a fixed number of lines L this error can be easily shown to be:

$$\lim_{r\to\infty} \varepsilon = \begin{cases} \sigma^2/L & ; \text{ for points on a TBM line} \\ 0 & ; \text{ for points on bisector between two lines} \end{cases}$$

so that the error is always between

$$0 \leq \varepsilon \leq \frac{\sigma^2}{L} \quad \text{as } r\to\infty \tag{3.85}$$

For small distances r compared to the correlation length, equation (3.81) gives the maximum error. If the accepted error is known in a particular problem, we can find the minimum number of lines necessary to meet this criterion, using for r the largest distance between the simulated points of the field. In the case of an exponential two dimensional covariance function (2.10) for example, we have

$$\sigma^2_{bK} = \left[\frac{-dC_1(\zeta)}{d\zeta}\bigg|_{\zeta=0}\right] \simeq 1.6 \tag{3.86}$$

so that from (3.81) the error is

$$\varepsilon \simeq 0.84\, \frac{\sigma^2_{br}}{L^2} \tag{3.87}$$

If the maximum distance of the field is $r_{max} = 2/b$ (two correlation

lengths), and for L = 8, this error estimate becomes $|\varepsilon| \leq 0.026\sigma^2$ or 2.6% of the point variance.

3.6.2 Examples of covariance convergence with number of lines

In order to find the error in the covariance function we can use (3.66) directly for the calculation of $C_s(r)$, where $C_1(r)$ is the unidimensional covariance function calculated in Section 3.4. For this example, we took a covariance function of the exponential type (2.10) and variance $\sigma^2 = 1$. The points of distance r where the covariance function is calculated were selected to lie on one of the turning bands lines or on the bisector between two lines, in order to obtain the limits of the error. Figures 3.20 - 3.22 show the theoretical covariance function and the bands within which the simulated covariance function lie, for different numbers of lines. In those figures the top curves give the simulated covariance when the points lie on one of the turning bands lines and the bottom curves give the simulated covariance function when the points lie on the bisector between two lines. We see from these curves that the simulated covariance approaches the theoretical covariance very rapidly as L increases. These figures provide a useful guideline in the selection of the number of lines for a particular problem.

The process generated by the proposed TBM is ergodic, even for a finite number of lines, as long as the line process is itself ergodic (the process generated by Rice's (1954) and Shinozuka and Jan's (1972) methods are ergodic). Thus the Figures 3.20 - 3.22 represent ensemble

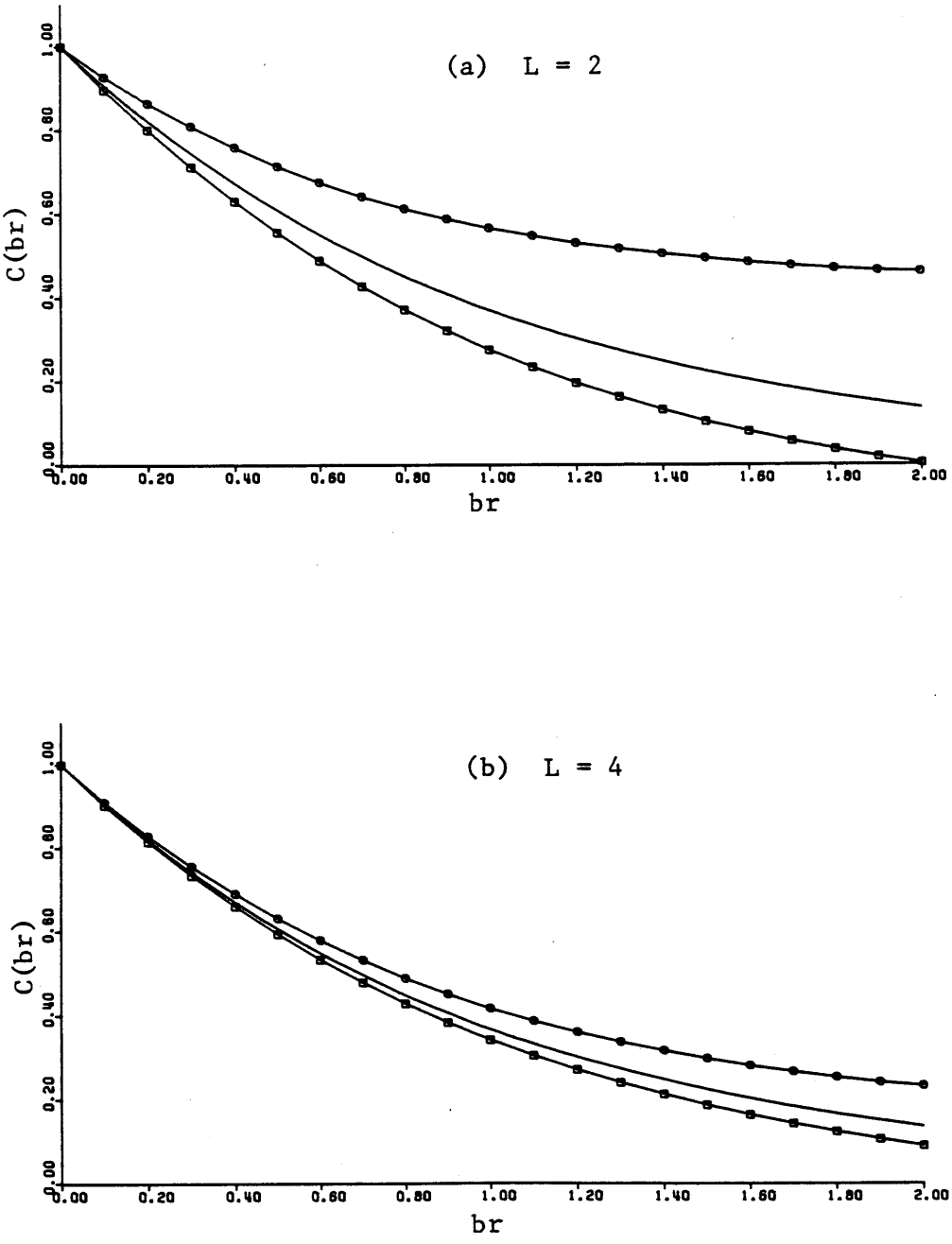

Figure 3.20 Limits of error in the covariance function due to finite number of lines.

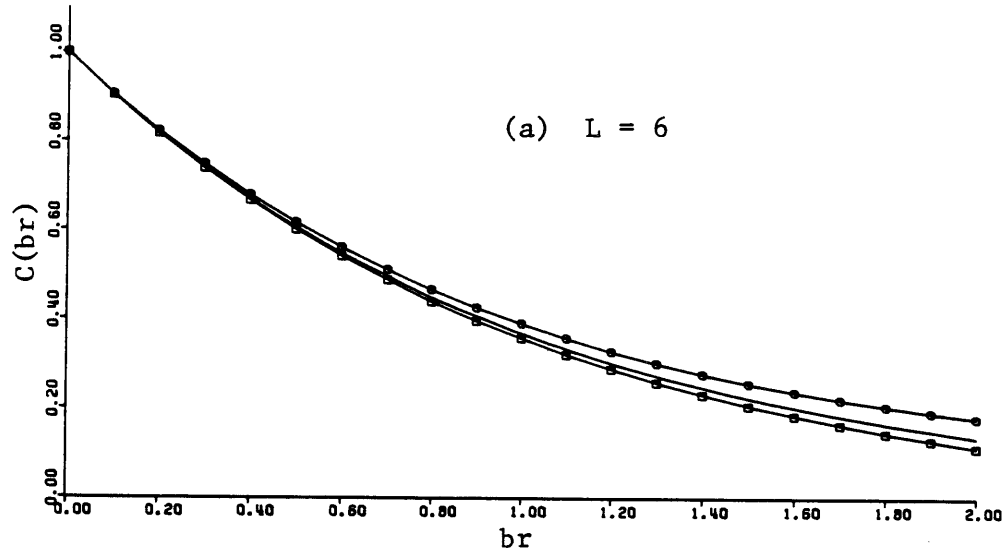

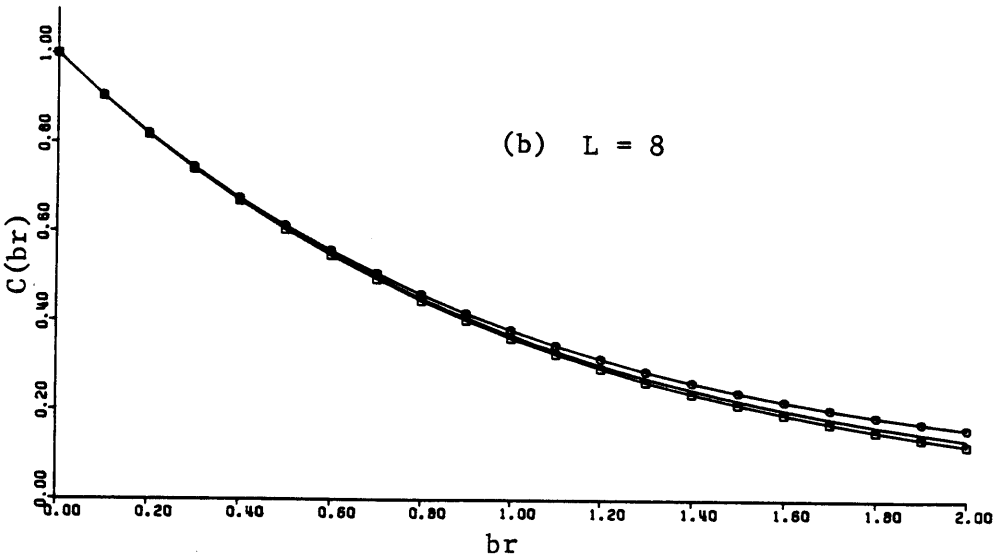

Figure 3.21 Limits of error in the covariance function due to finite number of lines.

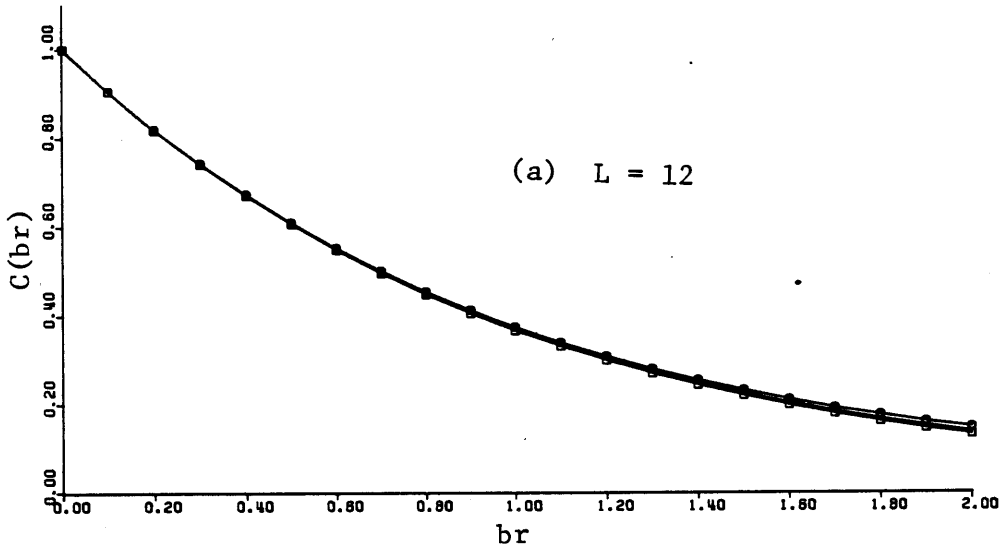

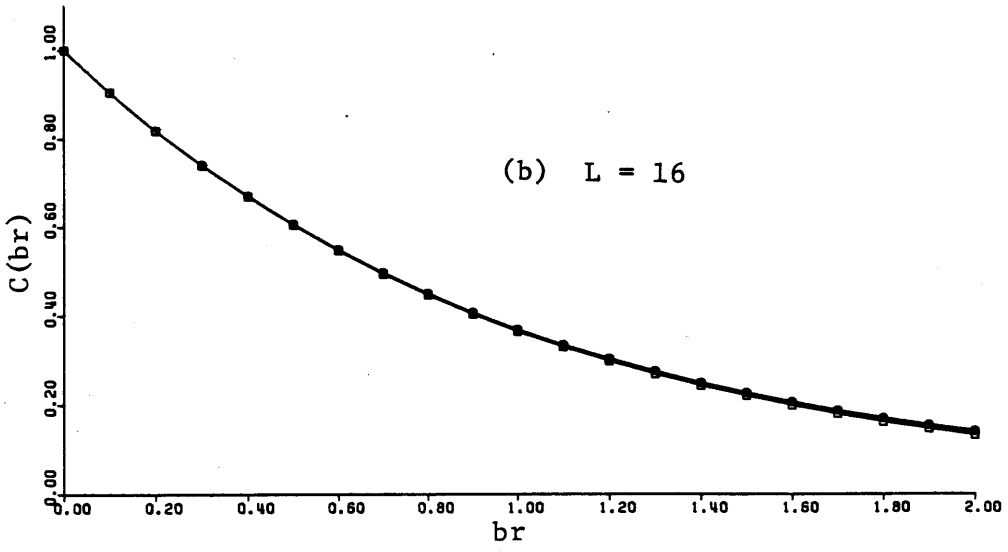

Figure 3.22 Limits of error in the covariance function due to finite number of lines.

as well as space averages. In this procedure the turning bands lines have been evenly spaced on the unit circle, the angle θ_1 of the first line specified ($\theta_1 = 0$). Suppose instead that the angle of the first line for each realization, was uniformly distributed between 0 and π/L. Then the resulting process would preserve the covariance over the ensemble better, but it would no longer be ergodic. That is, space and ensemble covariances would be the same only for large L. In another approach the lines could be randomly uniformly distributed over the unit circle. We then obtain a process which over the ensemble of realizations exactly preserves the theoretical covariance, but has a large error in the spatial average. This error decreases very slowly is L increases, so once again we have a process which is ergodic only for very large L. Thus it seems that the approach with evenly spaced lines on the unit circle and with prespecified line angles, is preferred (see also discussion in Section 3.2.3).

3.6.3 Effect of discretization along the lines

Another potentially important source of error is the discretization along the lines. In order to test how the discretization length $\Delta\zeta$ affects the accuracy of the model we use equation (3.66) where now the argument in the function $C_1(\ )$ is:

$$s_i = ||r \sin\theta_i/\Delta\zeta||\cdot\Delta\zeta \tag{3.88}$$

where $||\xi||$ represents the greatest integer such that: $||\xi|| \leq \xi$. If the number of lines in our example is L = 16, then the error due to

finite number of lines should be very small, as we've already seen in Figure 3.22. So we can assume that any additional error in the experiment is due to discretization. Once again an unit exponential covariance function was used. The points where the simulated covariance function was calculated lie on one of the turning bands lines. The origin of the turning bands lines was taken at mid point between two simulated points, as shown in Figure 3.23.

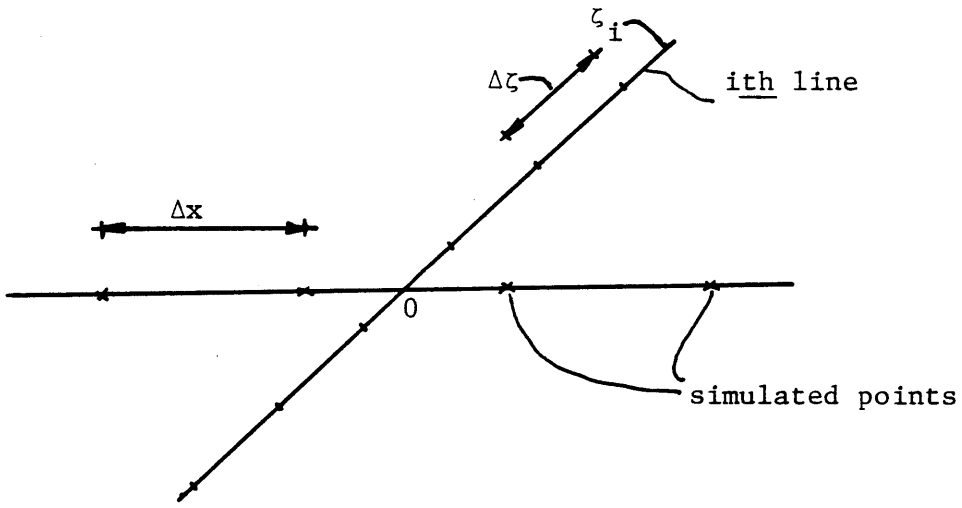

Figure 3.23 Origin of the turning bands lines in respect to the simulated points.

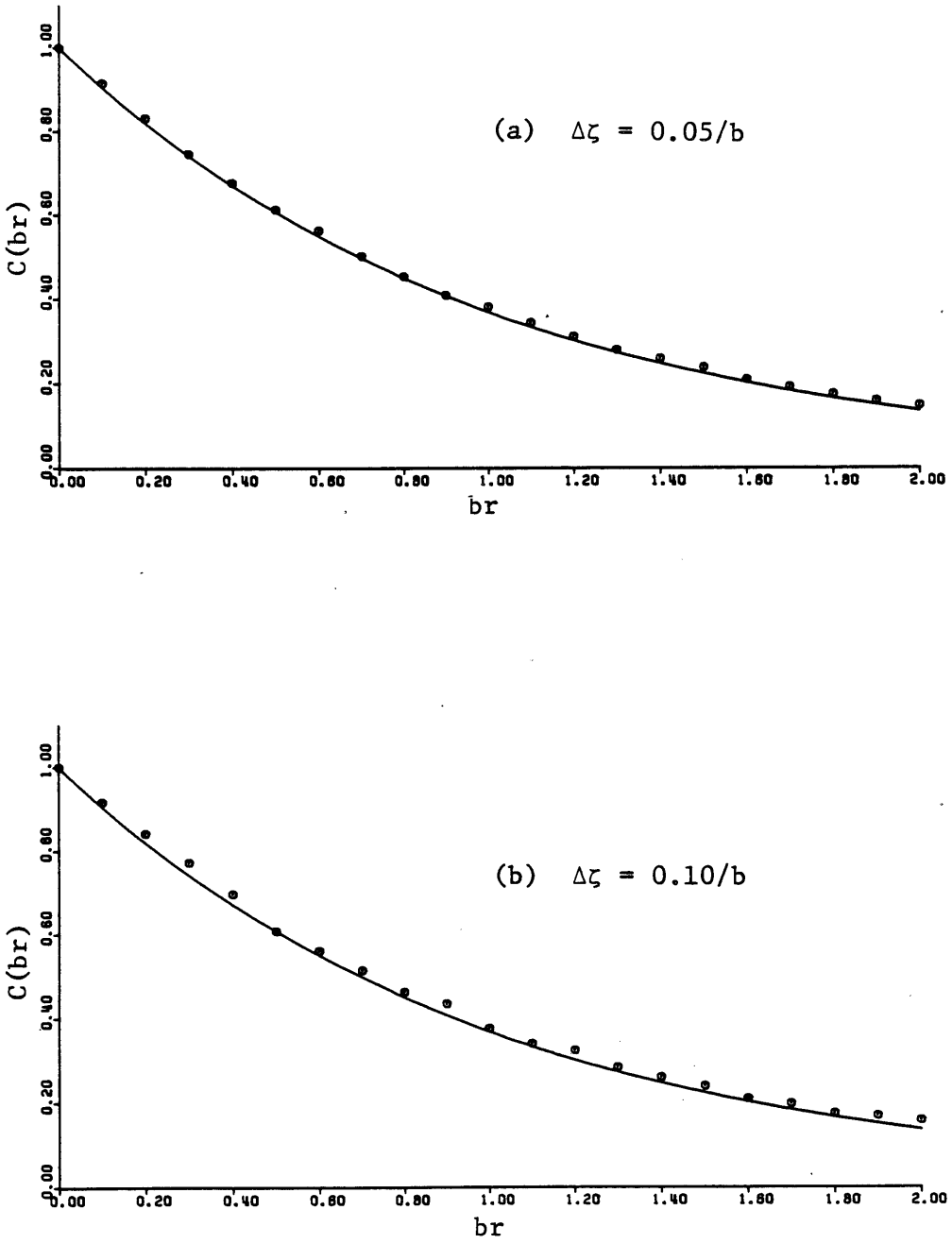

Figure 3.24 Error in the covariance function due to discretization along the turning bands lines.

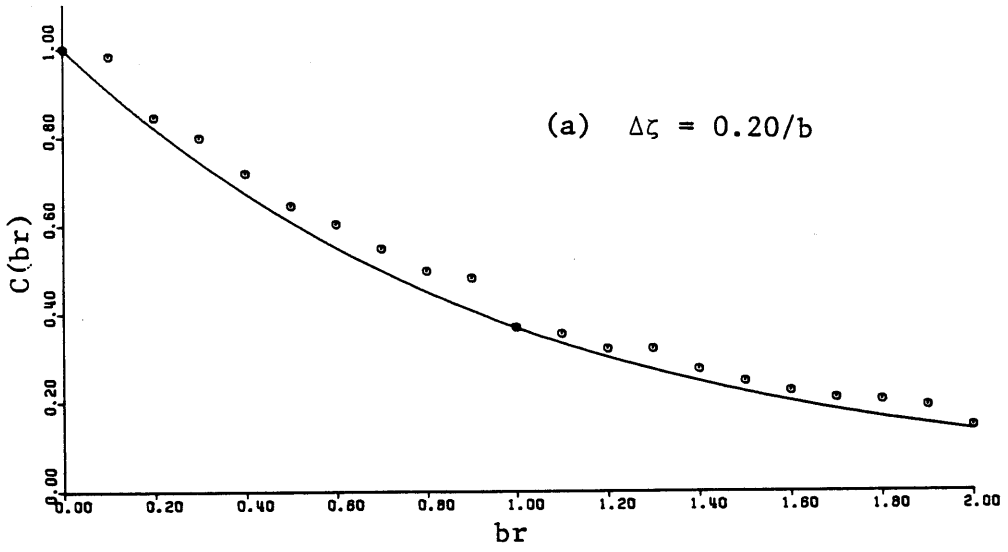

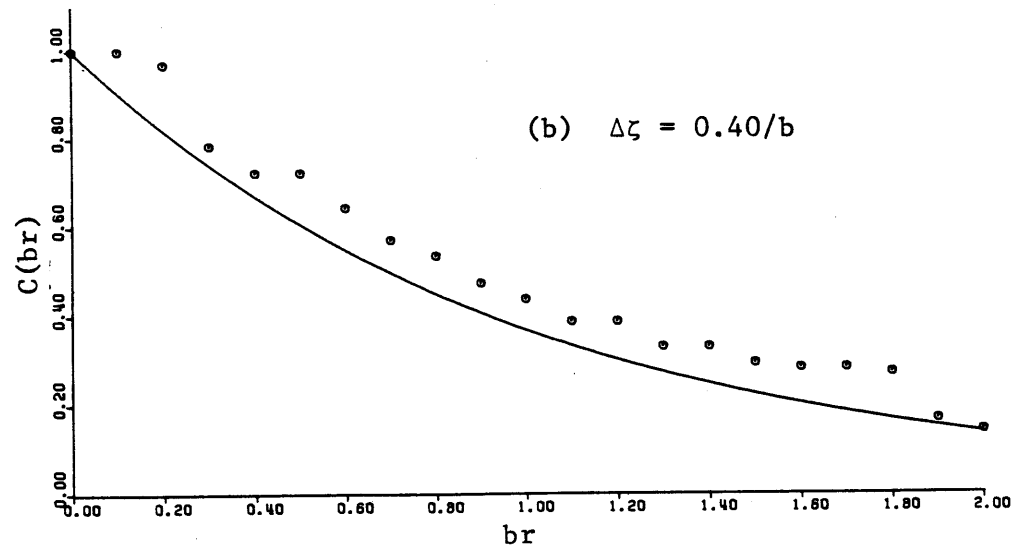

Figure 3.25 Error in the covariance function due to discretization along the turning bands lines.

Figures 3.24 and 3.25 present a comparison of the theoretical covariance and the one obtained by the simulation model for discretization lengths from $\Delta\zeta = 0.05/b$ to $0.40/b$ ($1/b$ represents the correlation length). The distance between two adjacent simulated points was $\Delta x = 0.10/b$, thus $\Delta\zeta/\Delta x$ varied from 0.5 to 4. From the figures we see that for $\Delta\zeta = 0.05/b$ or $0.1/b$ we have very good accuracy; for $\Delta\zeta = 0.20/b$ the accuracy is adequate, while for $\Delta\zeta = 0.40/b$ the accuracy is significantly reduced. We can use these figures as guidelines for selecting $\Delta\zeta$ to provide the level of desired accuracy.

In practical applications when we generate a rectangular grid of grid spacing $\Delta x, \Delta y$ for example, it is wise to take $\Delta\zeta < \min(\Delta x, \Delta y)$ so we avoid problems such as where to take the origin of the turning bands lines.

3.6.4 Effect of spectral method line generation process approximations

The accuracy of the turning bands method finally depends on the accuracy of the method used in the generation of the line process. We examine here the spectral method proposed in Section 3.3.2. The accuracy of this method depends on the maximum frequency at which the spectrum is truncated (Ω), and the number of harmonics (M). The model covariance function is given by:

$$C_1(\zeta) = 2 \frac{\Omega}{M} \sum_{k=1}^{N} S_1(\omega_k)\cos(\omega_k\zeta) \tag{3.89}$$

where $\omega_k = (k-1/2)\Omega/M$. Again take the case of two dimensional exponen-

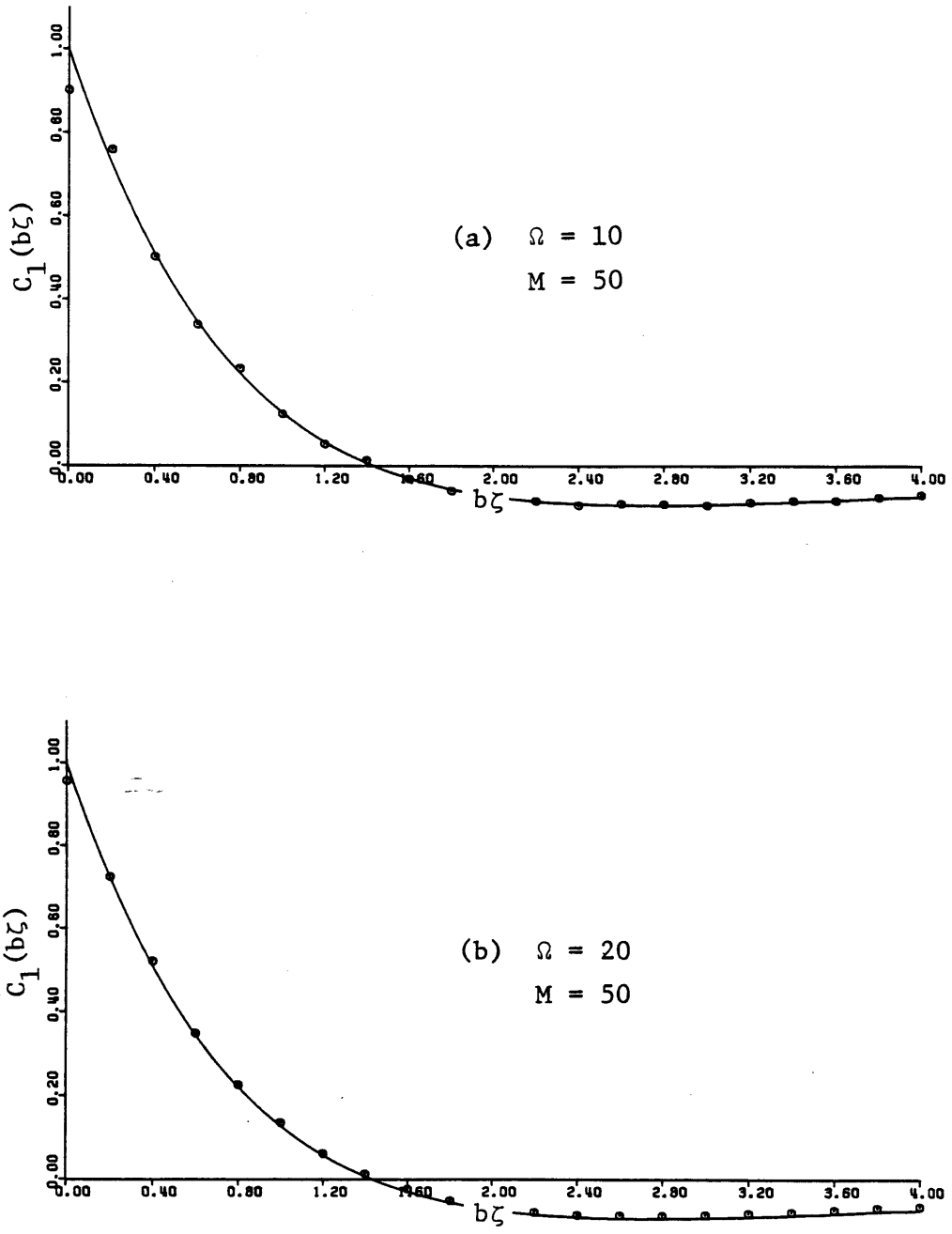

Figure 3.26 Error in the unidimensional covariance function due to spectral method approximations.

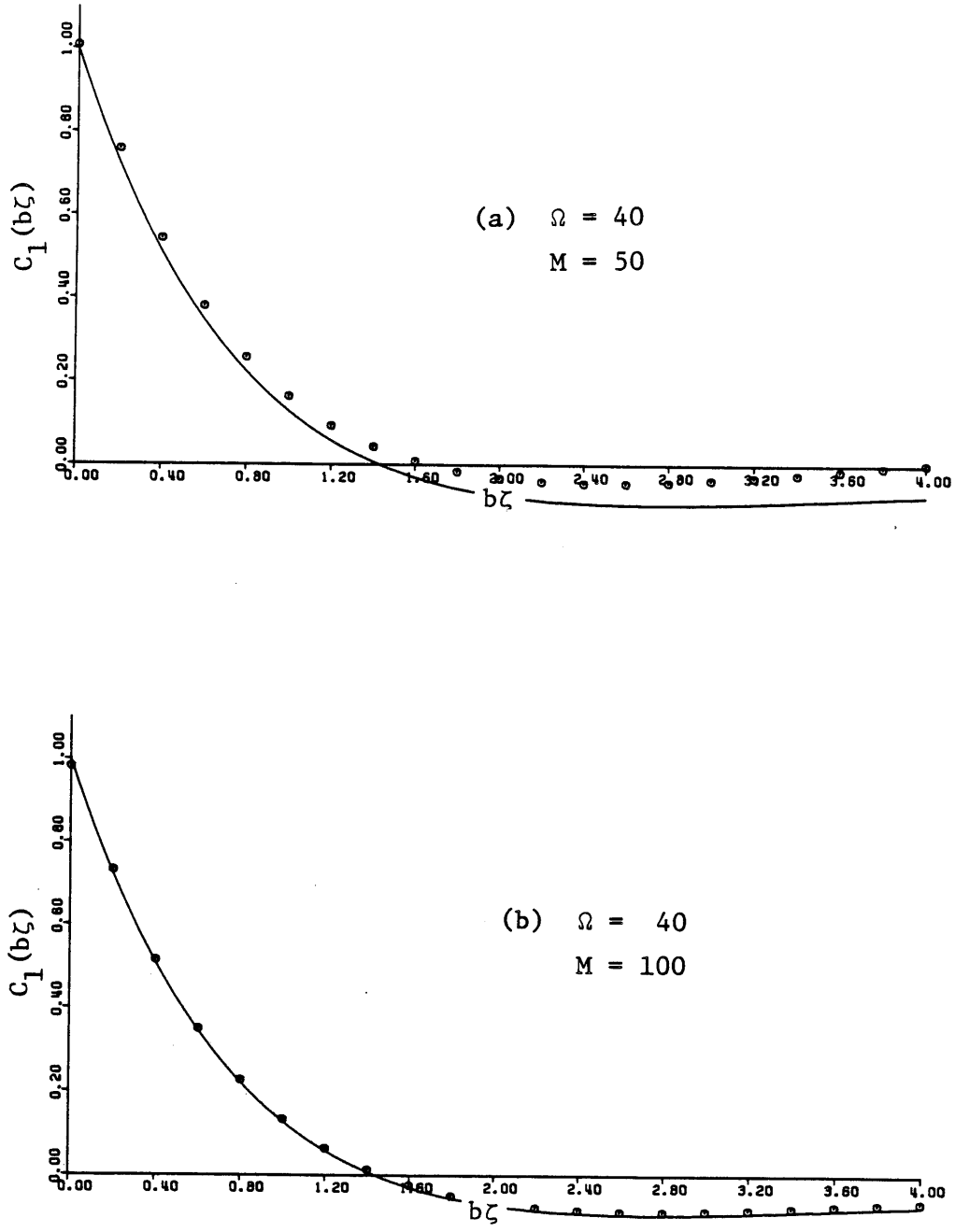

Figure 3.27 Error in the unidimensional covariance function spectral method approximations.

tial type covariance function. The corresponding unidimensional covariance function $C_1(\ )$ is given by (3.56).

Figures 3.26 - 3.27 compare the theoretical unidimensional covariance function (solid curves) to the covariance function given by the spectral model. In Figures 3.26a, 3.26b and 3.27a the number of harmonics is kept constant equal to M = 50 while the maximum frequency Ω increases from Ω = 10b to Ω = 40b. For small Ω's (small $\Delta\omega = \Omega/M$) we have very good accuracy for large distances, but we have some error for small distances (especially for the variance). Figures 3.27a and 3.27b compare the cases with constant Ω = 40b and M varying from 50 to 100. While the accuracy in Figure 3.27a (M = 50) is not very good at large distances, the accuracy shown in Figure 3.27b (M = 100) improves rapidly. The last case shown in Figure 3.27b (Ω = 40b, M = 100) preserves both the variance and the correlation at large distances very well. Those curves provide useful guidelines for choosing the maximum frequency (Ω) and the number of harmonics (M).

3.6.5 Summary

We have examined all the sources of error introduced in the turning bands method. These are: the number of lines (L), the discretization along the lines ($\Delta\zeta$), the maximum cutoff frequency of the spectrum (Ω) and the number of harmonics used (M). For the case of exponential covariance functions, for example, and L = 8, $\Delta\zeta$ = 010/b, Ω = 40b, M = 100 and r = 2/b, the maximum error in the covariance function is less than 3% of the square root of the variance (σ^2) or:

$$\varepsilon < 0.03\sigma^2 \qquad (3.90)$$

The cost of the turning bands method is practically proportional to the number of lines (L) and the number of harmonics (M) used in the generation of the line process and inversely proportional to the discretization length ($\Delta\zeta$). Or:

$$\text{cost} \propto \frac{L \cdot M}{\Delta\zeta} \tag{3.91}$$

In the next section we compare the turning bands method with other simulation methods in terms of accuracy and cost.

3.7 Comparison of the turning bands method to other simulation methods in terms of accuracy and cost

In this section we will compare the turning bands method with other methods used in the generation of two dimensional random fields, in terms of accuracy and cost. The well-known methods based on the generation of the field using the spectrum, presented in Section 2.5. are examined.

3.7.1 Error and convergence

In the turning bands method (TBM), with the lines evenly spaced on the unit circle, there is some error in the covariance function which tends to zero very rapidly (as $1/L^2$) as the number of lines increases, but the process generated by this approach is ergodic for a finite number of lines.

The method proposed by Mejia and Rodriguez-Iturbe (1974) has certain problems. For a finite number of harmonics (N) this method gives no error in the estimation of the covariance function as an

ensemble average, but the error in the spatial average estimation of the covariance function is large. Thus, this process is not ergodic unless $N \to \infty$. The square root of the variance of the covariance function estimated as a space average is given by Mejia and Rodriguez-Iturbe (1974) as:

$$\sigma_\varepsilon = \sqrt{\mathrm{Var}[C(r)]} = \sqrt{\frac{\sigma^2 C(2r) - 2C^2(r) + \sigma^4}{2N}} \tag{3.92}$$

This equation shows that the covariance function slowly tends to the theoretical one as $1/\sqrt{N}$.

Let's now compare the two methods in terms of an example. Let's take the two dimensional covariance function to be of exponential type, with a maximum distance in the field of 2/b, with L = 8 lines, with discretization along the lines of $\Delta\zeta = 0.10/b$, a maximum frequency of $\Omega = 40b$ and M = 100 harmonics used for the generation of the line process using the spectral method. For these values of the parameters L, $\Delta\zeta$, Ω and M, only the error due to the finite number of lines is significant. From (3.87) or Figure 3.21 we find the maximum error to be: $\varepsilon \tilde{=} 0.026\sigma^2$. As a criterion of equivalent accuracy of TBM to the method of Mejia and Rdoriguez-Iturbe (1974) we have chosen to equate the maximum TBM error ε to the standard deviation of the method of Mejia and Rodriguez-Iturbe. Let's now calculate N such that $\sigma_\varepsilon = \varepsilon$. From (3.92) for r = 2/b we get:

$$\sigma_\varepsilon = 0.7034\sigma^2/\sqrt{N} = \varepsilon$$

Thus N = 723 harmonics, a significant number.

If for the criterion of equivalent accuracy we had instead decided to equate the moments of the errors around the theoretical covariance, we have for the TBM error standard deviation (3.84c), $\sigma_{\varepsilon,TBM} = 0.01\sigma^2$ and for $\sigma_{\varepsilon,MR} = \sigma_{\varepsilon,TBM}$ we would require $N = 4900$! This example illustrates the slow convergence of the method of Mejia and Rodriguez-Iturbe.

The method of Shinozuka and Jan (1972) has the advantage over the method of Mejia and Rodriguez-Iturbe (1974) in that it is strictly ergodic and converges rapidly as the number of harmonics increases, but the cost of the method increases rapidly, too. Taking into account that for the one dimensional process we use a number of harmonics $M = 100$, for the same levels of accuracy in the generation of the two dimensional process, we should approximately (depending on the shape of the spectral density function) use a number of $N = N_1 \times N_2 = (100)^2$ harmonics. Using the symmetry properties of the two dimensional spectral density function in the isotropic case this number is reduced to: $N = \frac{1}{2} \times (\frac{100}{2})^2 = 1250$ harmonics. A more comprehensive calculation of the errors is necessary though for a thorough comparison.

3.7.2 Cost

The cost (c_T) of the turning bands method is essentially proportional to the number of lines (L), to the number of harmonics used in the generation of the line process (M), to the main diagonal (or largest distance) across the simulated field (R_{xy}), and the number of simulations performed NS, while it is inversely proportional to the

discretization length along the lines ($\Delta\zeta$). We can write this relationship as:

$$c_T \propto (NS)\ (L)\ (M)\ (R_{xy})/\Delta\zeta \tag{3.95}$$

For a given accuracy (constant L, M, $\Delta\zeta$) the cost of the method is proportional to the distance (R_{xy}) across the field. This means that increasing the size of the area, but keeping it similar in shape to the original one and keeping the discretization distances of the generated points constant, the cost of the TBM increases as the square root of the number of generated points n.

$$c_T \propto \sqrt{n} \tag{3.96}$$

Note also that (3.95) implies that the cost is shape dependent. The TBM is most efficient for square shapes.

The cost of the methods of Mejia and Rodriguez-Iturbe (1974) and Shinozuka and Jan (1972), are proportional to the number of harmonics (N), to the number of simulations performed (NS) and to the number of points generated (n) or:

$$c_{M,S} \propto (NS)\ (N)\ (n) \tag{3.97}$$

This shows that the cost of those methods is proportional to the number of points generated,

$$c_{M,S} \propto n \tag{3.98}$$

while in the turning bands method the cost is only proportional to the

square root of the number of generated points (3.96)! This property makes the turning bands method much cheaper than the other methods, particularly when we generate a large number of points of the field.

We present here an example comparing the relative cost (measured in CPU time on a IBM 370/168 CMS system) of the different methods. For the same number of harmonics (but better accuracy) the method of Shinozuka and Jan has approximately the same cost as the method of Mejia and Rodriguez-Iturbe. We have chosen to test the cost for the methods of Mejia and Rodriguez-Iturbe and Shinozuka and Jan with N = 200 harmonics, versus a turning bands model with spectral line process and L = 8, M = 100, Ω = 40b and $\Delta\omega$ = 0.40b, and $\Delta\zeta$ = 0.025/b the maximum distance R_{xy} is 2/b. Following the discussion in Section 3.7.1 the accuracy at the turning bands model with these parameters is much better than the other models.

This example employs the two dimensional gridded field of Figure 3.28. The generated values of the field at each grid point could be used, for example, in a contour plot program, or in a conditional simulation or as input to some physcial model. The number of rows NX and columns NY in the grid are identical, with a total of n = NX·NY grid points. The grid spacing is $\Delta x = \Delta y = 0.025/b$. The field has a zero mean with a unit variance ($\sigma^2 = 1$) exponential covariance function (2.10) with unit correlation length (b = 1).[2] In the experiment the grid spacing was kept constant while the grid domain and the number of simulated points was increased. For each size grid we generated one realization of the field at the n points using both the method of

2 The run cost is independent of these parameters for both the spectral method and TBM, thus this information is superfluous.

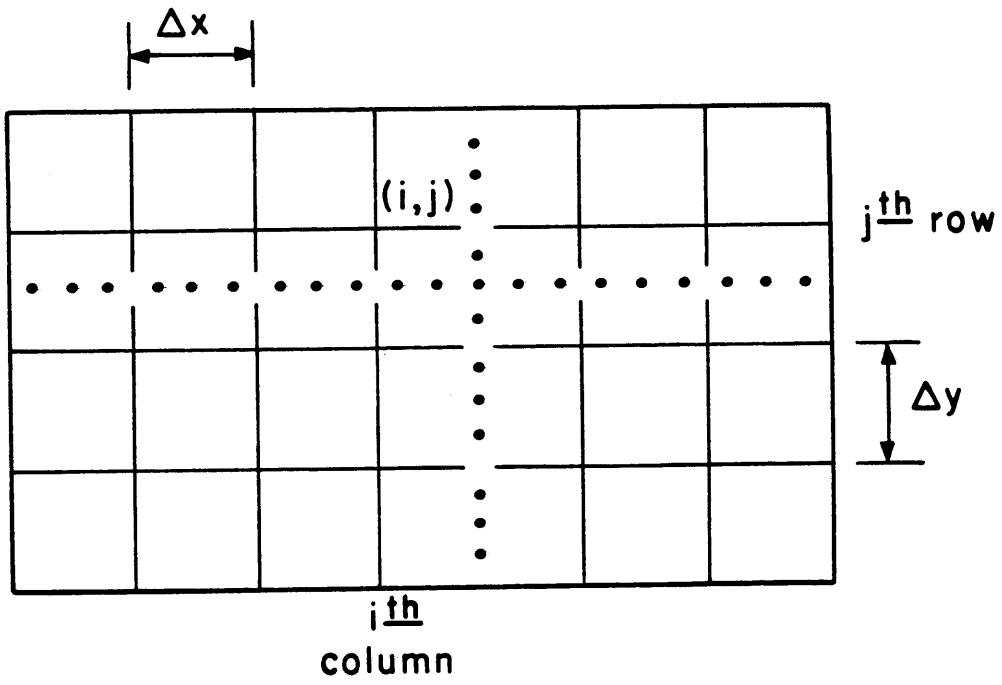

Figure 3.28 Grid of generated field for cost comparison.

Mejia and Rodriguez (1974) and the TBM with spectral line process, observing the CPU time. Figure 3.29 is a plot of CPU cost as a function of the number of points.

The figure clearly demonstrates that the TBM with spectral line process is superior in terms of cost to the method of Mejia and Rodriguez-Iturbe (1974), or by inference Shinozuka and Jan (1972). The cost of their model increases according to $c_T \propto n$, as expected from (3.98), while the TBM increases at $c_T \propto n^{1/2}$, as in (3.96). For $n = 400$ points in a 20 x 20 grid, their cost is 12 times higher. For $n = 2500$ points, in a 50 x 50 grid, their cost is 32 times higher!

The TBM was also run using the moving average (MA) unidimensional line process of Section 3.4.3. In this case we assumed that the two dimensional covariance function was given by (3.61) with parameter $a = 1$ and unit variance, $\sigma^2 = 1$.[3] The MA process was generated using $k_{max} = 161$, and the experiment repeated. These results are also plotted on Figure 3.29. This method is about 20% less expensive for the parameters chosen than using TBM with the spectral generation of the line process. Nevertheless, the spectral line method has the advantages of handling any properly posed covariance function as well as anisotropic fields (see Chapter 4). The MA line process is more restrictive in its admissible covariance functions and can handle anisotropy only via coordinate transformation (also, see Chapter 4).

---

[3] The cost is independent of these parameters.

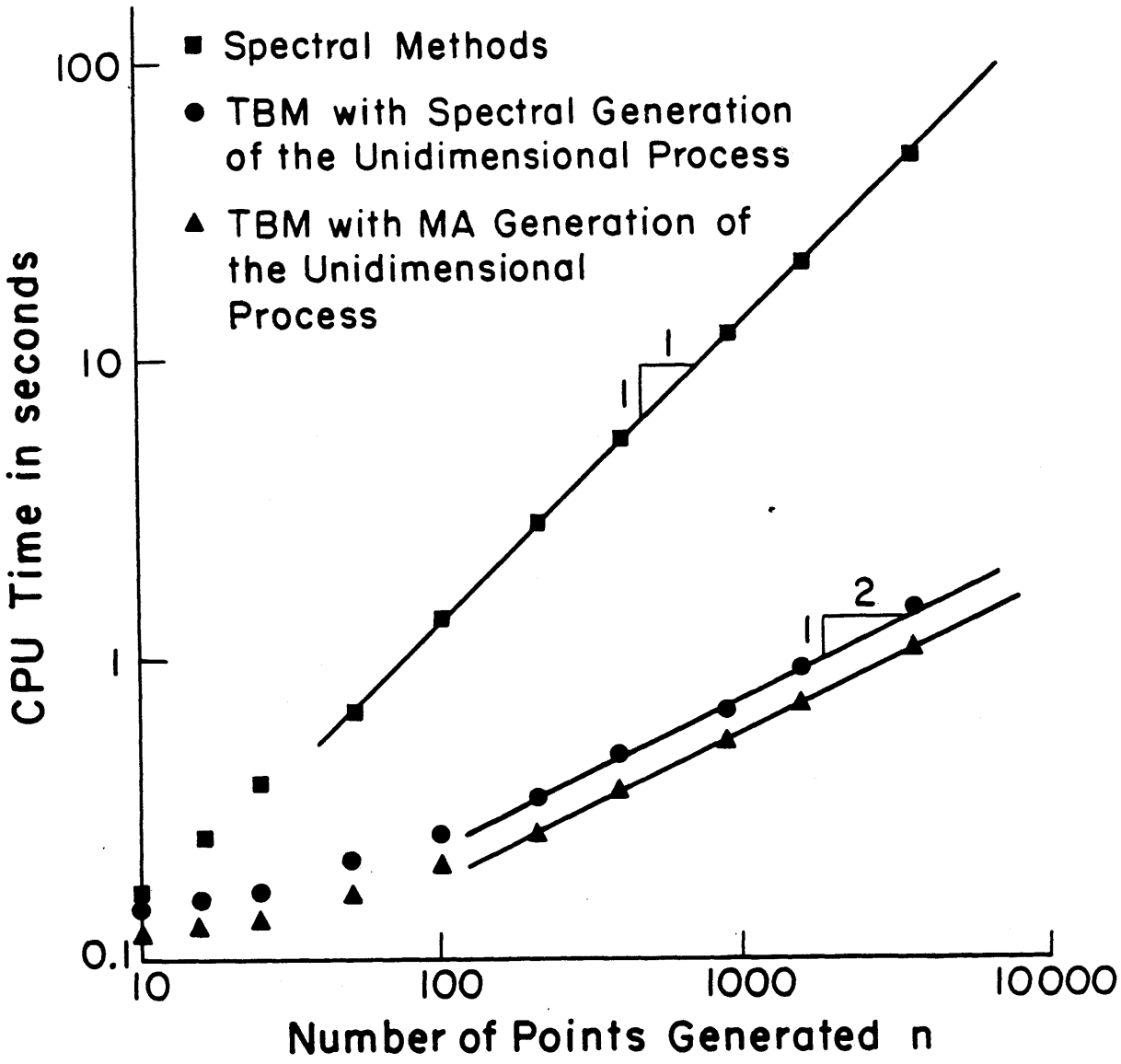

Figure 3.29 Comparison of the TBM to the spectral methods in terms cost.

3.8 Summary and conclusions

In this chapter we have presented the turning bands method (TBM) for generating realizations of multi-dimensional random fields, with particular reference to the two-dimensional case. We introduced an equation relating the spectral density function of the unidimensional line process to the radial spectral density function of the two dimensional process. The line process can now be generated using a spectral method, so that the TBM can be used to simulate any well posed covariance function. The method was demonstrated through a series of examples.

We also developed a moving average line process generator. By deriving the one-dimensional equivalents to various two dimensional covariance functions, we noted that they resemble the "hole" type covariance function. In turn, the two dimensional equivalent to the one dimensional "hole" function resembles common two dimensional covariance models. Thus we found that the "hole" function can be used for the moving average line generation.

We investigated the accuracy of the turning bands method. The process is ergodic, while the covariance quickly converges with $1/L^2$, where L is the number of lines, as demonstrated both theoretically and by example. We also developed guidelines for choosing model parameters in order to strictly limit model error. With judicious parameter selection, the TBM simulation method is both inexpensive and accurate.

We compared the turning bands method with two dimensional spectral generation models. The TBM is considerably less expensive than the 2-D spectral methods for the same levels of accuracy, with a cost proportional to the square root of the number of points simulated, while the other methods have a cost linearly proportional to the number of points. This relative cost was amply demonstrated through a case study grid generation.

CHAPTER 4

SIMULATION OF TWO DIMENSIONAL STATIONARY ANISOTROPIC RANDOM FIELDS

4.1 Introduction

Throughout Chapter 3 we assumed that the field is isotropic, and based the proposed simulation method on that assumption. However, there are situations for which we have to simulate anisotropic random fields. In these cases the covariance function between two points of the field depends on the angle orientation of a line connecting the points, relative to the coordinate system. In some cases a transformation of the coordinate system can lead to an isotropic field in the transformed system. Then we can use spectral methods or the isotropic turning bands method to simulate the transformed isotropic field, applying the inverse transformation to the results to get back to the original anisotropic field (Journel and Huijbregts, 1978). In other situations the transformation does not work, and we must use other methods for the direct simulation of the anisotropic field. As an example of this type of anisotropic field we mention here the field of areal averages which is treated in Chapter 5.

In this chapter we are going to extend, for the first time, the turning bands method (TBM) to the direct simulation of two dimensional anisotropic random fields. This method is applied for an anisotropic two dimensional covariance function of exponential type. In Chapter 5 we present an example of the application of this method to the areal average process.

4.2 Mathematical development

The derivation of equations for this situation is similar to the isotropic case. We again generate randomly distributed lines in the plane with the origin at (0,0). On those lines independent unidimensional processes are generated having zero mean. Here, in contrast to the isotropic case, we allow the unidimensional covariance functions to depend on the direction of the lines and write them as $C_{1,i}(\zeta)$, where the subscript i indicates the direction of the line along which the unidimensional realization is generated. At each point in the plane the corresponding values of the unidimensional processes are assigned, as in the isotropic case. For L independent realizations along each of L turning bands lines, the simulated value of the field at point N is

$$z_s(\underline{x}_N) = \frac{1}{\sqrt{L}} \sum_{i=1}^{L} z_i(\underline{x}_N \cdot \underline{u}_i) \qquad (4.1)$$

where $\underline{x}_N$ is the vector distance of the point N, $\underline{u}_i$ is the unit vector along line i, and $z_i(\underline{x}_N \cdot \underline{u}_i)$ is the corresponding value of the unidimensional process along line i for point N.

The key question is "what is the appropriate unidimensional covariance function for each turning bands line, as a function of the direction of the lines?" Let's take two points of the field $\underline{x}_1$, $\underline{x}_2$ as shown in Figure 3.3. The covariance function between the simulated values at those points is given by:

$$C_s(\underline{x}_1,\underline{x}_2) = E\left[\left\{\frac{1}{\sqrt{L}} \sum_{i=1}^{L} z_i(\underline{x}_1\ \underline{u}_i)\right\} \left\{\frac{1}{\sqrt{L}} \sum_{j=1}^{L} z_j(\underline{x}_2\ \underline{u}_j)\right\}\right]$$

After the multiplications, and taking into account that the realizations along two different lines are independent, this becomes

$$C_s(\underline{x}_1,\underline{x}_2) = C_s(\underline{h}) = \frac{1}{L} \sum_{i=1}^{L} C_{1,i}(\underline{h}\cdot\underline{u}_i) \tag{4.2}$$

where $\underline{h} = \underline{x}_1 - \underline{x}_2$ and $C_{1,i}$ is the unidimensional covariance function along line i. Taking the limit $L\to\infty$ in (4.2), and applying the central limit theorem, we get:

$$C_s(\underline{h}) = E[C_{1,\underline{u}}(\underline{h}\cdot\underline{u})] \tag{4.3}$$

Because the probability density function of the unit vector is $f(\underline{u}) = 1/2\pi$ the expected value in the equation can be written as

$$C_s(\underline{h}) = \frac{1}{2\pi} \int_{\text{unit circle}} C_{1,\underline{u}}(\underline{h}\cdot\underline{u})\, d\underline{u} \tag{4.4}$$

This equation is similar to (3.12), with the difference that here the unidimensional covariance function depends on the direction $\underline{u}$ of the line, and is written as $C_{1,\underline{u}}$.

Let's define a system of axes x,y with origin (0,0)(Figure 4.1). at the end of vector $\underline{x}_1$. Note that the field given by (4.1) is wide sense stationary, so that this definition is not restrictive. Let ϕ and θ be the angles between the x axis and the vectors $\underline{h}$ and $\underline{u}$, respectively, as shown in Figure 4.1. In polar coordinates we have $\underline{h}\cdot\underline{u} = r\cos(\phi-\theta)$, where $r = |\underline{h}|$ and $d\underline{u} = d\theta$. Thus 4.4 becomes

$$C_s(\underline{h}) = \frac{1}{2\pi} \int_0^{2\pi} C_{1,\theta}[r\cos(\phi-\theta)]\, d\theta$$

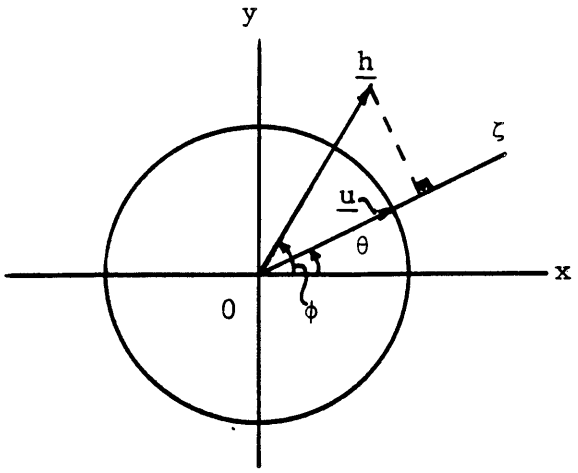

Figure 4.1 Definiiton sketch in the anisotropic case.

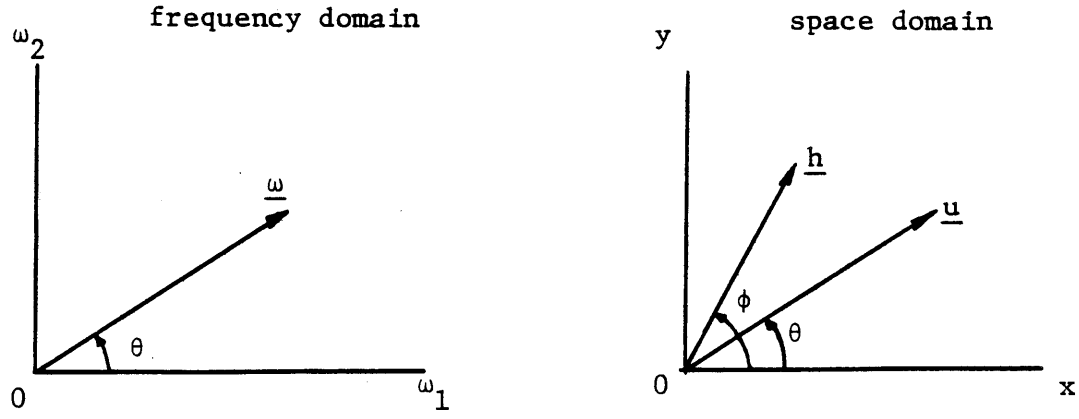

Figure 4.2 Frequency and space domains.

Because the covariance function is an even function, and because $C_{1,\pi+\theta}(\ ) = C_{1,\theta}(\ )$, the integral can be simplified:

$$C_s(\underline{h}) = \frac{1}{\pi}\int_o^{\pi} C_{1,\theta}[r\cos(\phi-\theta)]\,d\theta \qquad (4.5)$$

This equation corresponds to (3.19) in the isotropic case, but here the unidimensional covariance function is a function of the angle of the turning bands line.

Let $S_{1,\theta}(\omega)$ be the spectral density function of the unidimensional process, having covariance function $C_{1,\theta}(\zeta)$, corresponding to a turning bands line forming angle θ with the x axis. The covariance function on that line can be written as:

$$C_{1,\theta}(\zeta) = \int_{-\infty}^{+\infty} S_{1,\theta}(\omega)\, e^{i\omega\zeta}\, d\omega$$

or, for $\zeta = r\cos(\phi-\theta)$,

$$C_{1,\theta}[r\cos(\phi-\theta)] = \int_{-\infty}^{+\infty} S_{1,\theta}(\omega)\, e^{i\omega r\cos(\phi-\theta)}\, d\omega \qquad (4.6)$$

Substituting (4.6) into (4.5) we get:

$$C_s(\underline{h}) = \frac{1}{\pi}\int_o^{\pi}\int_{-\infty}^{+\infty} S_{1,\theta}(\omega)\, e^{i\omega r\cos(\phi-\theta)}\, d\omega d\theta \qquad (4.7)$$

In Figure 4.2 the axes ω_1, ω_2 of the frequency domain are shown, which are assumed to be parallel to the x,y axes. On this plane we define a vector $\underline{\omega}$ with length $|\underline{\omega}| = \omega$, forming angle θ with ω_1 axis.

The inner product of the vectors $\underline{\omega}$ and $\underline{h}$ is given by:

$$\underline{\omega}\cdot\underline{h} = \omega r \cos(\phi-\theta) \tag{4.8}$$

In polar coordinates

$$d\underline{\omega} = \omega d\omega d\theta \tag{4.9}$$

Looking at the limits of the integral (4.7) we see that ω ranges from $-\infty$ to $+\infty$ while θ ranges from 0 to π. This means that the vector $\underline{\omega}$ is moving over the entire R^2 plane. Substituting (4.8) and (4.9) into (4.7) gives

$$C_s(\underline{h}) = \frac{1}{\pi}\int_{R^2} S_{1,\theta}(\omega)\ e^{i\underline{\omega}\cdot\underline{h}}\ \frac{1}{\omega}\ d\underline{\omega}$$

or,

$$C_s(\underline{h}) = \int_{R^2} \left(\frac{S_{1,\theta}(\omega)}{\pi\omega}\right)\ e^{i\underline{\omega}\cdot\underline{h}}\ d\underline{\omega} \tag{4.10}$$

Taking the inverse Fourier transform of this equation we get:

$$\frac{S_{1,\theta}(\omega)}{\pi\omega} = \frac{1}{(2\pi)^2}\int_{R^2} C_s(\underline{h})\ e^{-i\underline{\omega}\cdot\underline{h}}\ d\underline{h} \tag{4.11}$$

In practice, the two dimensional covariance function $C(\underline{h})$ that we want to preserve is known. So we set $C_s(\underline{h}) = C(\underline{h})$, with the result

$$\frac{S_{1,\theta}(\omega)}{\pi\omega} = \frac{1}{(2\pi)^2}\int_{R^2} C(\underline{h})\ e^{-i\underline{\omega}\cdot\underline{h}}\ d\underline{h} \tag{4.12}$$

Comparing with (2.22) we see that the right-hand side of the above

equation is equal to the spectral density function $S(\underline{\omega})$ of the two dimensional process. Thus, we finally get:

$$S_{1,\theta}(\omega) = \pi\omega S(\underline{\omega}) \tag{4.13}$$

This equation relates the spectral density function $S_{1,\theta}(\omega)$ of the unidimensional process to the spectral density function $S(\underline{\omega})$ of the two dimensional process. The vector $\underline{\omega}$ can be written as $\underline{\omega} = (\omega_1, \omega_2) = (\omega \cos\theta, \omega \sin\theta)$ and (4.13) becomes

$$S_{1,\theta}(\omega) = \pi\omega S(\omega \cos\theta, \omega \sin\theta) \tag{4.14}$$

If we find the spectral density function of the two dimensional process, then we can also find the spectral density function of the unidimensional process along the turning bands lines. As in the isotropic case, the line process is generated using a spectral method.

We note here that the above result has been established with the assumption that the direction vectors of lines are uniformly distributed on the unit circle. That means that the lines should be equally spaced around the circle, as they were in the isotropic case. In general more lines should be used than in the isotropic case in order to describe the differences in each direction due to anisotropy.

4.3 Example

In order to test the proposed method a simple example was examined. The two dimensional anisotropic covariance function was assumed to be of the exponential type given by:

$$C(\underline{h}) = C(x,y) = \sigma^2 \exp[-(h_1^2 x^2 + h_2^2 y^2)] \tag{4.15}$$

where x,y are the coordinates of the vector $\underline{h}$, and h_1, h_2 are parameters. Obviously when $h_1=h_2$ the covariance function given by (4.15) is isotropic.

We could have simulated the field having the above covariance by making a transformation in the axes, such that the field in the new axes was isotropic, then generated the isotropic field, and finally made an inverse transformation in the axes to get back to the original anisotropic field. Instead, we used the direct TBM for anisotropic fields, proposed above, in order to test the method. In the next chapter we apply this method to a more complex anisotropic field: the field of the areal averages.

In order to apply the turning bands method we first calculated the spectral density function of the two dimensional field. This is presented in Appendix C, with the result given by:

$$S(\omega_1,\omega_2) = \frac{\sigma^2}{2\pi} \frac{1}{h_1 h_2 \left(1 + \frac{\omega_1^2}{h_1^2} + \frac{\omega_2^2}{h_2^2}\right)^{3/2}} \tag{4.16}$$

Writing

$$\omega_1 = \omega \cos\theta \qquad \omega_2 = \omega \sin\theta$$

and using (4.14) this becomes:

$$S_{1,\theta}(\omega) = \pi\omega S(\omega\cos\theta,\ \omega\sin\theta) = \frac{\sigma^2}{2}\frac{\omega}{h_1 h_2\left[1+\omega^2\left(\frac{\cos^2\theta}{h_1^2}+\frac{\sin^2\theta}{h_2^2}\right)\right]^{3/2}} \tag{4.17}$$

Along each of the turning bands lines the above spectral density function was used for the generation of the unidimensional process, where θ was the angle of the turning bands line with the x axis. The unidimensional process was generated again, as in the isotropic case, with the method of Rice (1954) and Shinozuka and Jan (1972).

We generated points along both the x and y axes, as shown in Figure 4.3. The distance between the points along both axes was $\Delta X = \Delta Y = 0.24$. The parameters of the anisotropic covariance function were: $h_1 = 0.2$ $h_2 = 0.6$. The number of lines was 16 and the discretization along the lines was $\Delta\zeta = 0.12$. The discretization of the spectrum for the generation of the line processes varied, depending on the direction of the lines, but the number of harmonics was fixed at M = 50. The number of simulations was set to NS = 200.

Figure 4.4 plots the theoretical covariance functions along the x and y axes, compared to the sample covariance obtained from the 200 simulation at the discrete points of Figure 4.3. As we can see from this figure, the proposed method well preserves the theoretical covariance function. The errors observed are mainly due to sampling error (see Section 3.3.3), because of the finite sample (NS = 200). Another example application of this method is given in Section 5.3 in the next chapter.

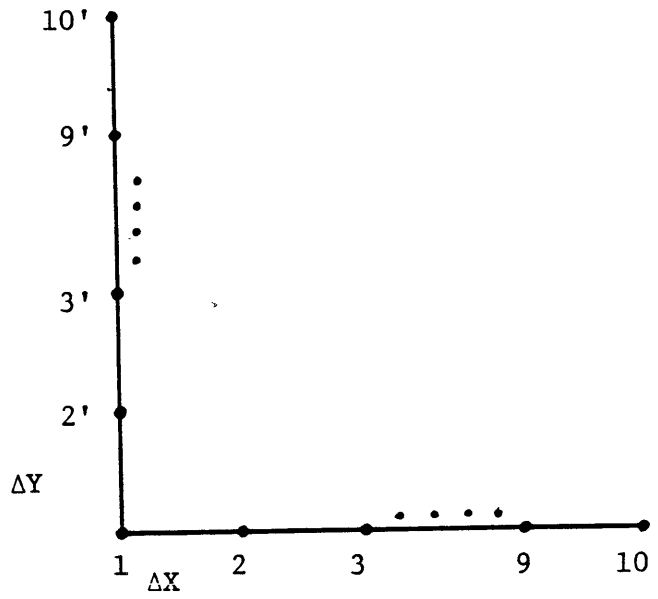

Figure 4.3 Simulated points of the anisotropic random field.

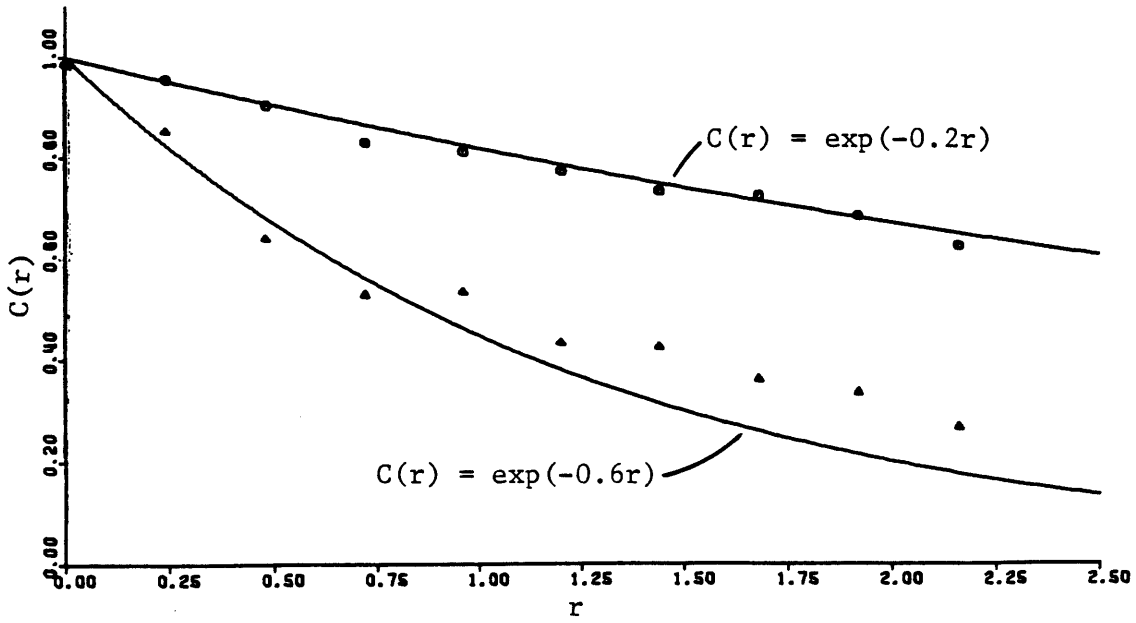

Figure 4.4. Theoretical and sample covariance functions. NS = 200, L = 16, $\Delta\zeta$ = 0.12, M = 50

CHAPTER 5

SIMULATION OF AREAL AVERAGE PROCESSES IN THE STATIONARY CASE

5.1 Introduction

There are situations in both hydrology and mining for which we are interested in the areal averages of the stationary point process. In surface hydrology, for example, we may wish to simulate average rainfall over a given area. In groundwater simulation models, aquifer properties are usually averaged over the areas defined by the cells or elements of a finite difference or finite element grid. In ore bodies we may want to simulate average ore grade under a given area.

Several methods have been proposed for the simulation of the process of areal averages. One very simple technique is based on the weighted average of point values generated at several locations within the area. Another method, proposed by Lenton and Rodriguez-Iturbe (1975), directly simulates the process of the areal averages. This method is similar to the one proposed by Mejia and Rodriguez-Iturbe (1974) for the generation of point processes. Wilson (1979) proposed a method which is based on the direct simulation of the field by decomposing the covariance matrix of the areal averages. All of these methods should be more expensive than the method proposed here, which is based on the direct simulation of the anisotropic field of areal averages using the analysis of the previous chapter.

In Section 5.2 we will derive some formulas for the covariance function and the spectrum of the areal average process. In Section 5.3 we will give some examples of generating the areal average process

directly based on the turning bands method for anisotropic processes, and in Section 5.4 we will review some of the simulation methods proposed for generation of areal average processes.

5.2 Correlation and spectrum of the process of areal averages[1]

Let $Z(\underline{x})$ represent the continuous, wide sense stationary point process of a two dimensional random field. Let A be some region of the field as shown in Figure 5.1, having in general any shape. We can then define a new process $Z_A(\underline{x})$ called the process of the areal averages given by:

$$Z_A(\underline{x}) = \frac{1}{A} \int_A Z(\underline{x}')d\underline{x}' \tag{5.1}$$

In this formula $\underline{x}$ represents the coordinate vector of a characteristic point within the region A. It is usually convenient to reference $\underline{x}$ to the centroid of A. The meaning of the process defined by (5.1) is that we allow the area A to translate without rotation on the x,y plane. For each position of the area (or the characteristic point $\underline{x}$ of the area) we define the new process given by (5.1) as the areal average process.

Because the integration in (5.1) takes place over the region A, which depends on $\underline{x}$, it is more consistent to write (5.1) as

$$Z_A(\underline{x}) = \frac{1}{A} \int_{A(\underline{x})} Z(\underline{x}')d\underline{x}' \tag{5.2}$$

where A represents the area and is not a function of $\underline{x}$, and $A(\underline{x})$

[1] A somewhat different representation of the properties of the field of the areal averages can be found in Mattern (1960) or Lenton and Rodriguez-Iturbe (1974).

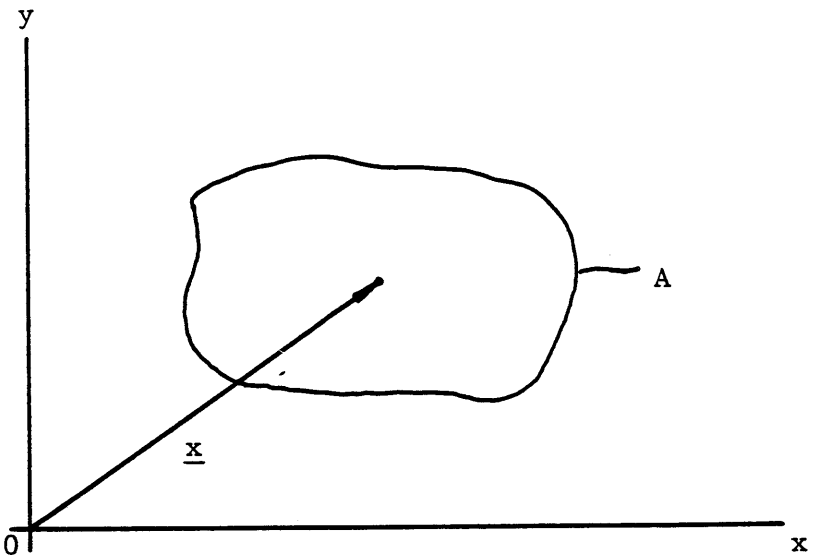

Figure 5.1 Region A and the characteristic vector $\underline{x}$.

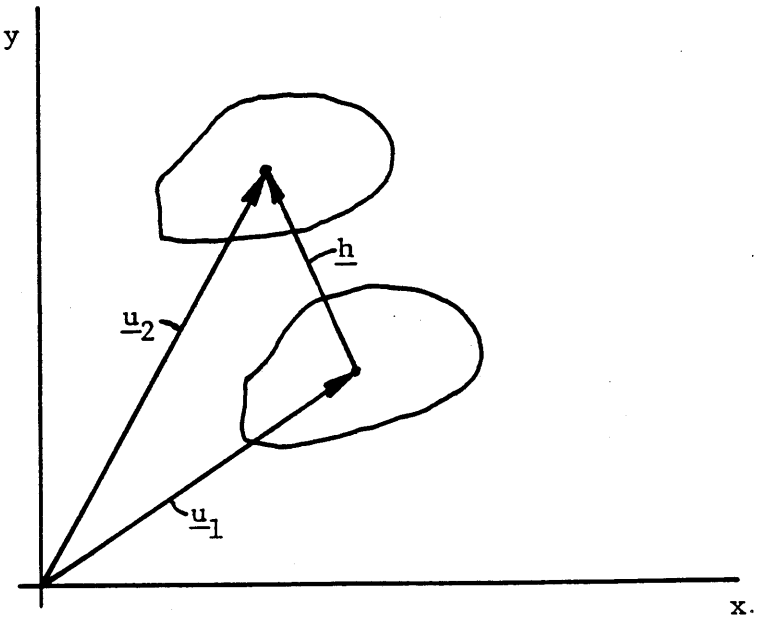

Figure 5.2 Definition of distance vector $\underline{h}$ between regions $A(\underline{u}_1)$ and $A(\underline{u}_2)$.

represents a particular region of area A and depends on the characteristic vector $\underline{x}$. The mean of this process is given by

$$E[Z_A(\underline{x})] = \frac{1}{A} E[\int_{A(\underline{x})} Z(\underline{x}')d\underline{x}'] = \frac{1}{A}\int_{A(\underline{x})} E[Z(\underline{x}')]d\underline{x}' = 0$$

where it is assumed that the point process has zero mean.

Covariance function variance reduction

Let's now analyze the covariance function of the process defined by (5.2). Let $\underline{u}_1$ and $\underline{u}_2$ be two points of the two dimensional field, and $\underline{h}$ be the vector distance between those points, or $\underline{h} = \underline{u}_2 - \underline{u}_1$ as shown in Figure (5.2). The areal average process for these two points is defined by:

$$Z_A(\underline{u}_1) = \frac{1}{A}\int_{A(\underline{u}_1)} Z(\underline{x}_1)d\underline{x}_1$$

$$Z_A(\underline{u}_2) = \frac{1}{A}\int_{A(\underline{u}_2)} Z(\underline{x}_2)d\underline{x}_2$$

The covariance function of the areal average process between points $\underline{u}_1$ and $\underline{u}_2$ will be given by:

$$C_A(\underline{u}_1,\underline{u}_2) = E[\frac{1}{A^2}\{\int_{A(\underline{u}_1)} Z(\underline{x}_1)d\underline{x}_1\}\cdot\{\int_{A(\underline{u}_2)} Z(\underline{x}_2)d\underline{x}_2\}] =$$

$$= \frac{1}{A^2}\int_{A(\underline{u}_1)}\int_{A(\underline{u}_2)} E[Z(\underline{x}_1)Z(\underline{x}_2)]d\underline{x}_1 dx_2 \qquad (5.3)$$

but:

$$E[Z(\underline{x}_1)Z(\underline{x}_2)] = C(\underline{x}_2,\underline{x}_1)$$

where $C(\underline{x}_2,\underline{x}_1)$ represents the covariance function of the point process, which is assumed to be wide sense stationary. Then we can write

$$C(\underline{x}_2,\underline{x}_1) = C(\underline{x}_2-\underline{x}_1) = C(\underline{v})$$

where $\underline{v} = \underline{x}_2-\underline{x}_1$. Equation (5.3) is now written as:

$$C_A(\underline{u}_1,\underline{u}_2) = \frac{1}{A^2}\int_{A(\underline{u}_1)}\int_{A(\underline{u}_2)} C(\underline{v})d\underline{x}_1 d\underline{x}_2 \tag{5.4}$$

From this we can infer that $C_A(\underline{u}_1,\underline{u}_2)$ is a function only of the vector $\underline{h} = \underline{u}_2-\underline{u}_1$, i.e., the process of areal averages is wide sense stationary. So we can write

$$C_A(\underline{h}) = \frac{1}{A^2}\int_{A(\underline{u}_1)}\int_{A(\underline{u}_2)} C(\underline{v})d\underline{x}_1 d\underline{x}_2 \tag{5.5}$$

We define now the probability density function of a vector $\underline{x}$ which is uniformly distributed on the region $A(\underline{u})$. This probability density function is given by

$$f_{\underline{u}}(\underline{x}) = \begin{cases} \frac{1}{A} & \text{if } \underline{x} \in A(\underline{u}) \\ 0 & \text{elsewhere} \end{cases}$$

and the integral (5.5) becomes

$$C_A(\underline{h}) = \int_{A(\underline{u}_1)}\int_{A(\underline{u}_2)} C(\underline{v}) f_{\underline{u}_1}(\underline{x}_1) f_{\underline{u}_2}(\underline{x}_2) d\underline{x}_1 d\underline{x}_2 \tag{5.6}$$

Because $f_{\underline{u}}(\underline{x}) = 0$ unless $\underline{x} \in A(\underline{u})$ we have

$$C_A(\underline{h}) = \int_{R^2} \int_{R^2} C(\underline{v}) f_{\underline{u}_1}(\underline{x}_1) f_{\underline{u}_2}(\underline{x}_2) d\underline{x}_1 d\underline{x}_2 \tag{5.7}$$

Based on (5.7) we can write $C_A(\underline{h})$ as an expected value given by:

$$C_A(\underline{h}) = E[C(\underline{v})] \tag{5.8}$$

where $\underline{v} = \underline{x}_2 - \underline{x}_1$ and $\underline{x}_1, \underline{x}_2$ are uniformly distributed in the regions $A(\underline{u}_1)$ and $A(\underline{u}_2)$, respectively.

This formula using the central limit theorem can be used to calculate the two dimensional covariance function of the areal average process via Monte Carlo simulation:

$$C_A(\underline{h}) = \frac{1}{N} \sum_{i=1}^{N} C(\underline{v}_i) \tag{5.9}$$

where N is a large number and $\underline{v}_i = \underline{x}_{2_i} - \underline{x}_{1_i}$ with $\underline{x}_{2_i}$, $\underline{x}_{1_i}$ uniformly and independently distributed over the regions $A(\underline{u}_2)$ and $A(\underline{u}_1)$, respectively. Some examples of calculation of the covariance function using equation (5.9) are given in Section 5.3.

Spectral representation

Let $S(\underline{\omega})$ be the spectral density function of the point process. Using (2.19) we can write

$$C(\underline{v}) = \int_{R^2} e^{i\underline{\omega}\underline{v}} S(\underline{\omega}) d\underline{\omega} \tag{5.10}$$

where $C(\underline{v})$ is the covariance function of the point process. Substituting into (5.7) gives

$$C_A(\underline{h}) = \int_{R^2}\int_{R^2} f_{\underline{u}_1}(\underline{x}_1) f_{\underline{u}_2}(\underline{x}_2) \left[\int_{R^2} e^{i\underline{\omega v}} S(\underline{\omega}) d\underline{\omega}\right] d\underline{x}_1 d\underline{x}_2$$

$$= \int_{R^2} S(\underline{\omega}) \left[\int_{R^2}\int_{R^2} e^{i\underline{\omega v}} f_{\underline{u}_1}(\underline{x}_1) f_{\underline{u}_2}(\underline{x}_2)\, d\underline{x}_1 d\underline{x}_2\right] d\underline{\omega} =$$

$$= \int_{R^2} S(\underline{\omega})\, a_{\underline{h}}(\underline{\omega}) d\underline{\omega} \tag{5.11}$$

where the function $a_{\underline{h}}(\underline{\omega})$ is given by

$$a_{\underline{h}}(\underline{\omega}) = \int_{R^2}\int_{R^2} e^{i\underline{\omega v}} f_{\underline{u}_1}(\underline{x}_1) f_{\underline{u}_2}(\underline{x}_2) d\underline{x}_1 d\underline{x}_2 \tag{5.12}$$

The subscript $\underline{h}$ denotes that the characteristic points in the two areas, where the above integral is taken, are at vector distance $\underline{h} = \underline{u}_2 - \underline{u}_1$.

Substituting $\underline{v} = \underline{x}_2 - \underline{x}_1$ into (5.12) results in

$$a_{\underline{h}}(\underline{\omega}) = \int_{R^2}\int_{R^2} e^{i\underline{\omega}(\underline{x}_2 - \underline{x}_1)} f_{\underline{u}_1}(\underline{x}_1) f_{\underline{u}_2}(\underline{x}_2) dx_1 dx_2 =$$

$$= \int_{R^2} e^{-i\underline{\omega x}_1} f_{\underline{u}_1}(\underline{x}_1) d\underline{x}_1 \int_{R^2} e^{i\underline{\omega x}_2} f_{\underline{u}_2}(\underline{x}_2) d\underline{x}_2 \tag{5.13}$$

We define the function $a_{\underline{u}}(\underline{\omega})$ as follows:

$$a_{\underline{u}}(\underline{\omega}) = \int_{R^2} e^{-i\underline{\omega}\underline{x}} f_{\underline{u}}(\underline{x})d\underline{x} \tag{5.14}$$

The complex conjugate of $a_{\underline{u}}(\underline{\omega})$ is:

$$a^*_{\underline{u}}(\underline{\omega}) = \int_{R^2} e^{i\underline{\omega}\underline{x}} f_{\underline{u}}(\underline{x})d\underline{x} \tag{5.15}$$

Thus (5.13) is written as:

$$a_{\underline{h}}(\underline{\omega}) = a_{\underline{u}_1}(\underline{\omega})\, a^*_{\underline{u}_2}(\underline{\omega}) \tag{5.16}$$

Let P be the characteristic point of the region, as shown in Figure 5.3. The vector $\underline{x}$ of a point in $A(\underline{u})$ can be written as:

$$\underline{x} = \underline{u} + \underline{w} \tag{5.17}$$

where $\underline{w}$ is a vector with origin at P, and end at the end of the vector $\underline{x}$. Let $f_o(\underline{w})$ be the probability density function of $\underline{w}$, then the probability density function of $\underline{x}$ is

$$f_{\underline{u}}(\underline{x}) = f_o(\underline{w}) \tag{5.18}$$

Differentiating gives $d\underline{x} = d\underline{w}$, so that (5.14) can be written as:

$$a_{\underline{u}}(\underline{\omega}) = \int_{R^2} e^{-i\underline{\omega}(\underline{u}+\underline{w})} f_o(\underline{w})d\underline{w} =$$

$$= e^{-i\underline{\omega}\underline{u}} \int_{R^2} e^{-i\underline{\omega}\underline{w}} f_o(\underline{w})d\underline{w} \tag{5.19}$$

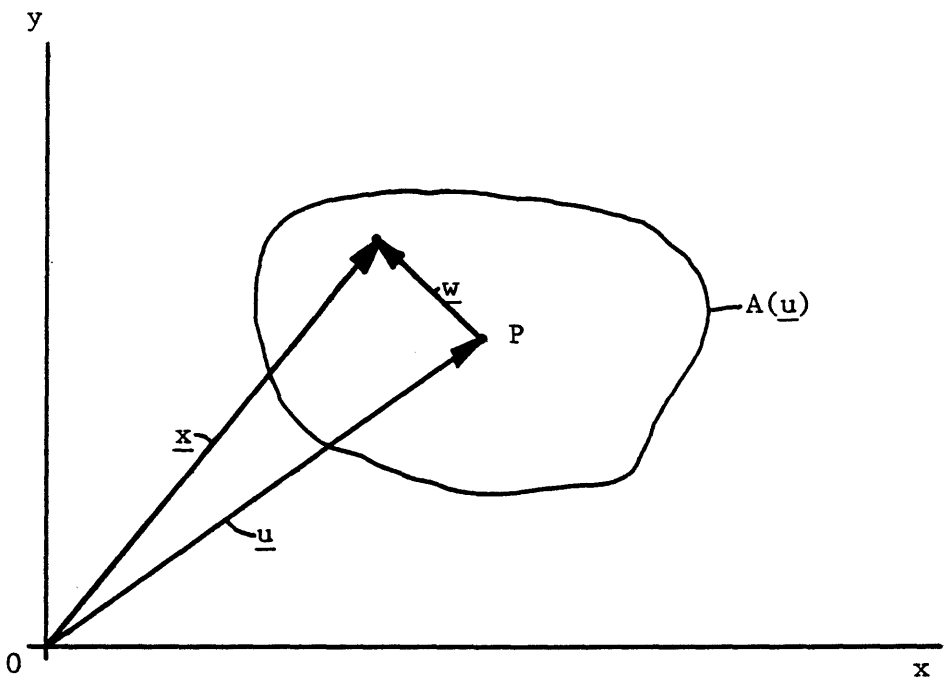

Figure 5.3 Change of coordinate system.

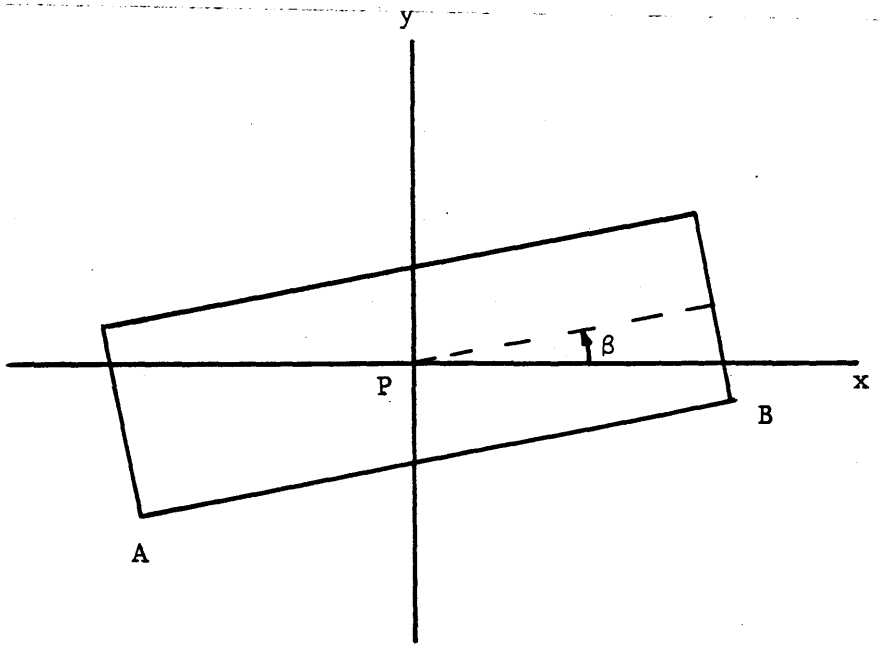

Figure 5.4 Example of definition of the angle of rotation β.

The integral in this equation is only a function of the vector $\underline{\omega}$ and the geometry of the region $A(\underline{u})$, and not of the relative position of $A(\underline{u})$ as defined by $\underline{u}$. Define geometric parameter $H(\underline{\omega})$,

$$H(\underline{\omega}) = \int_{R^2} e^{-i\underline{\omega}\underline{w}} f_o(\underline{w}) d\underline{w} \tag{5.20}$$

and (5.19) becomes:

$$a_{\underline{u}}(\underline{\omega}) = e^{-i\underline{\omega}\underline{u}} H(\underline{\omega}) \tag{5.21}$$

The complex conjugate of $a_{\underline{u}}(\underline{\omega})$ is

$$a^*_{\underline{u}}(\underline{\omega}) = [(e^{-i\underline{\omega}\underline{u}} H(\underline{\omega})]^* = e^{i\underline{\omega}\underline{u}} H^*(\underline{\omega}) \tag{5.22}$$

Substituting (5.21) and (5.22) into (5.16) gives

$$a_{\underline{h}}(\underline{\omega}) = e^{i\underline{\omega}\underline{h}} |H(\underline{\omega})|^2 \tag{5.23}$$

where $|H(\underline{\omega})|$ is the absolute value of $H(\underline{\omega})$.

The function $H(\underline{\omega})$ depends on both the geometry of the area, and the relative rotation of the area with respect to the x,y axes (angle β in Figure 5.4). We can calculate the function $H(\underline{\omega})$ for any rotation β, say, $\beta = 0$. The zero rotation of the area is defined arbitrarily, but is taken for convenience such that the integration of (5.20) is easiest. (For the example of the rectangle of Figure 5.4 it is convenient to define the zero rotation when AB is parallel to the x axis. In Appendix D we derive the relation between the function $H(\underline{\omega})$ for an area rotated at an angle β, and the function $H_o(\underline{\omega})$ corresponding to the zero rotation area:

$$H(\underline{\omega}) = e^{i\beta} H_o(\underline{\omega} e^{i\beta}) \tag{5.24}$$

or:

$$|H(\underline{\omega})|^2 = |H_o(\underline{\omega} e^{i\beta})|^2 \tag{5.25}$$

In Appendix E we derive characteristic functions $|H(\underline{\omega})|^2$ for some typical geometries (rectangles and triangles).

Substitute (5.23) into (5.11) to give the areal average covariance function:

$$C_A(\underline{h}) = \int_{R^2} e^{i\underline{\omega h}} [|H(\underline{\omega})|^2 S(\underline{\omega})] d\underline{\omega} \tag{5.26}$$

Taking the inverse Fourier transform of this equation we get:

$$|H(\underline{\omega})|^2 S(\underline{\omega}) = \frac{1}{(2\pi)^2} \int_{R^2} C_A(\underline{h}) e^{-i\underline{\omega h}} d\underline{h} \tag{5.27}$$

The right-hand side represents the spectral density function $S_A(\underline{\omega})$ of the areal average process, as given by (2.22), so that:

$$S_A(\underline{\omega}) = |H(\underline{\omega})|^2 S(\underline{\omega}) \tag{5.28}$$

If the point process is isotropic having radial spectral density function $f(\omega)$ we can write

$$S(\underline{\omega}) = S(\omega) = \frac{\sigma^2}{2\pi\omega} f(\omega)$$

where $\omega = |\underline{\omega}|$ and (5.28) becomes:

$$S_A(\underline{\omega}) = \frac{\sigma^2}{2\pi} \frac{f(\omega)}{\omega} |H(\underline{\omega})|^2 \qquad (5.29)$$

We note here that although the point process may be isotropic, the areal average process will not be isotropic, unless the area is a circle. This can be inferred from equations (5.20) and (5.29) easily.

After the spectral density function of the areal average process is obtained, we can use the turning bands method for the generation of anisotropic processes (see Chapter 4) in order to directly simulate the field of the areal averages. In the next section we give some examples of direct simulation of the areal average process using the turning bands method.

5.3 An example of calculation of the theoretical covariance and simulation of the areal average process

The theoretical covariance function of the areal average process can be calculated by numerical integration or by Monte Carlo simulation (Matern, 1960). The Monte Carlo simulation procedure via (5.9) is used here in the case of rectangular averaging regions. Then the Turning Bands Method (TBM) for generation of areal average processes described in the previous section is used to generate realizations of the averaged process for the same rectangular areas. The obtained covariance functions are compared to the theoretical ones.

Figure 5.5 shows the theoretical covariance functions for different sized square shapes (with side lengths $L_x = L_y$) when the line connecting the centroids of the squares is parallel to the sides of the

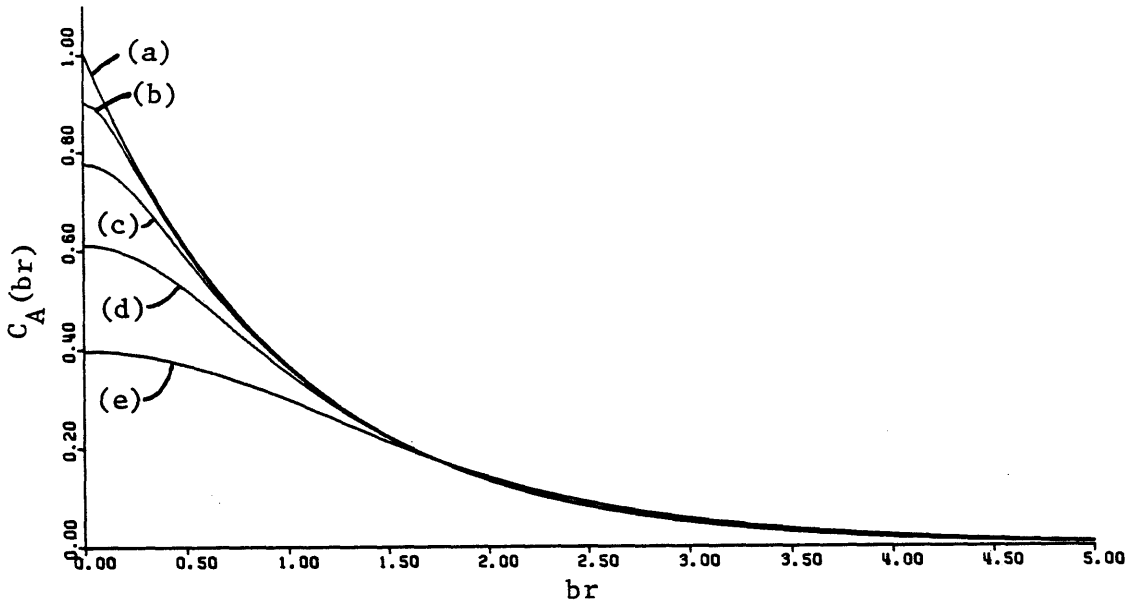

Figure 5.5 Theoretical covariance function of the areal average process: square areas ($L_x=L_y$).

(a) $b^2L_xL_y = 0$, (b) $b^2L_xL_y = 0.04$, (c) $b^2L_xL_y = 0.25$,

(d) $b^2L_xL_y = 1.0$, (e) $b^2L_xL_y = 4.0$

squares. The point covariance function in this example is of the exponential type (2.10). The symbol r represents the distance between the centroids of the regions, b is the parameter of the point covariance function, and br represents a normalized distance. This figure shows the point covariance function (top curve) and the covariance functions for normalized areas of sizes $b^2L_xL_y$ = 0.04, 0.25, 1.0, 4.0. When the shape changes to a rectangle with one side four times longer than the other ($L_x = 4L_y$) the covariance function of the areal average process is shown in Figures 5.6 and 5.7. In Figure 5.6 the axis is taken parallel to the long side, L_x, while in Figure 5.7 the axis is taken parallel to the short side, L_y. These figures show that the covariance function is different for each direction, and illustrate the anisotropy of the areal average process.

The figures also demonstrate the property that the areal averaged covariance function asymptotically approaches the point covariance function for large distances. In fact, for the square these distances are not very large when compared to the length of the sides of the averaging areas. For example, if two squares are adjacent to each other, such that $bL_x = bL_y = br$, then Figure 5.5 indicates a lag one covariance reduction of less than 5% for all lengths bL_x. In contrast the lag zero variance reduction along the ordinate is significant, especially for large $b \cdot L_x$. This property can be used to simplify the estimation of the theoretical areal average covariance function when needed (see, e.g., Section 5.4.2; Wilson, 1979; and Dettinger and Wilson, 1979), and greatly reduce its computational expense. However,

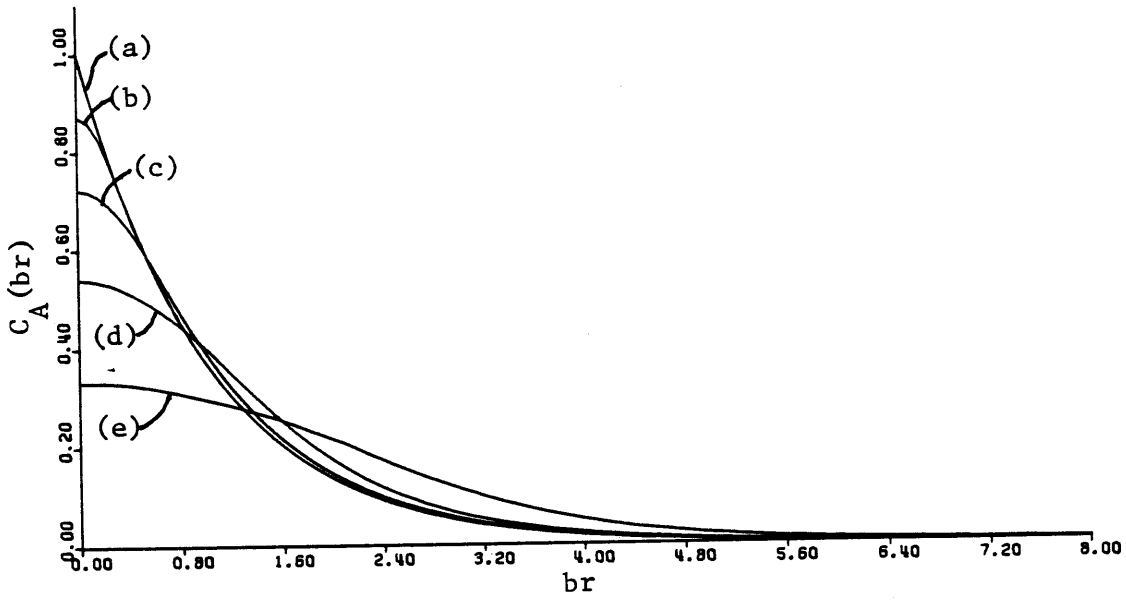

Figure 5.6 Theoretical covariance function of the areal average process: rectangular areas ($L_x=4L_y$). br parallel to L_x.

(a) $b^2L_xL_y = 0$, (b) $b^2L_xL_y = 0.04$, (c) $b^2L_xL_y = 0.25$,

(d) $b^2L_xL_y = 1.0$, (e) $b^2L_xL_y = 4.0$

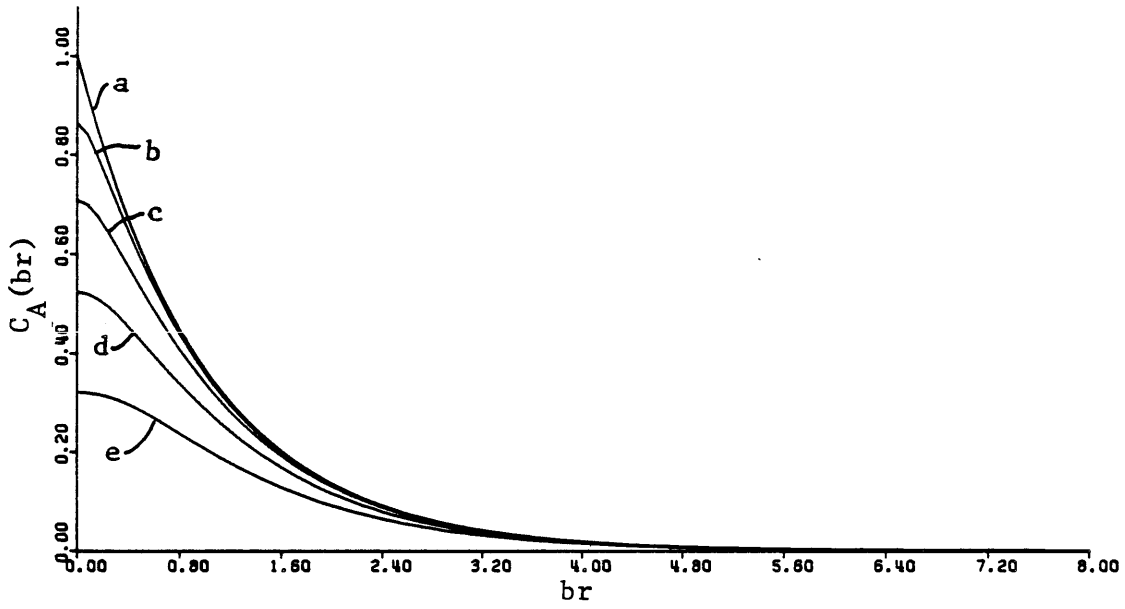

Figure 5.7 Theoretical covariance function of the areal average process: rentangular areas ($L_x = 4L_y$), br parallel to L_y.
(a) $b^2L_xL_y = 0$, (b) $b^2L_xL_y = 0.04$, (c) $b^2L_xL_y = 0.25$,
(d) $b^2L_xL_y = 1.0$, (e) $b^2L_xL_y = 4.0$

for rectangles, as one side becomes much longer than the other, this property converges much slower, as illustrated in Figures 5.6 and 5.7. When the rectangles are stacked "vertically" adjacent to each other (see Figure 5.7), such that $bL_y = br$, then the significant covariance reduction persists through 3 or 4 lags, not just one. Thus this property, although still useful for reducing computational effort, must be carefully considered for each areal pattern of shape, orientation and centroidal distance.

In order to apply the TBM to the direct generation of the areal average process we have chosen square areas ($L_x = L_y$), separated from each other by a normalized distance br between the centroids: br = 0, 0.2, 0.4, 0.6,...1.6, 1.8, 2.0. Experiments were performed for squares with normalized side length $bL_x = 0.5$ and $bL_x = 2.0$; that is, one-half and twice the correlation length of the point covariance function, which was of the exponential type with $\sigma^2 = 1$. Thus we simulated the theoretical curves of Figure 5.5 labeled $bL_x = 0.5$ and $bL_x = 2.0$.

In Appendices D and E we derive the function $|H(\underline{\omega})|^2$ for rectangular areas. The spectral density function of the unidimensional line process, on a TB line oriented at angle θ, for the areal average process is given by (4.13), (5.29) and (E.4).

$$S^{(1)}_{1,\theta}(\omega) = \sigma^2 \frac{8f(\omega)}{L_x^2 L_y^2 \omega^4 \cos^2\theta \sin^2\theta} \sin^2\left[\frac{L_x \omega \cos\theta}{2}\right] \sin^2\left[\frac{L_y \omega \sin\theta}{2}\right]$$

where $f(\omega)$ is the radial spectral density function of the point process

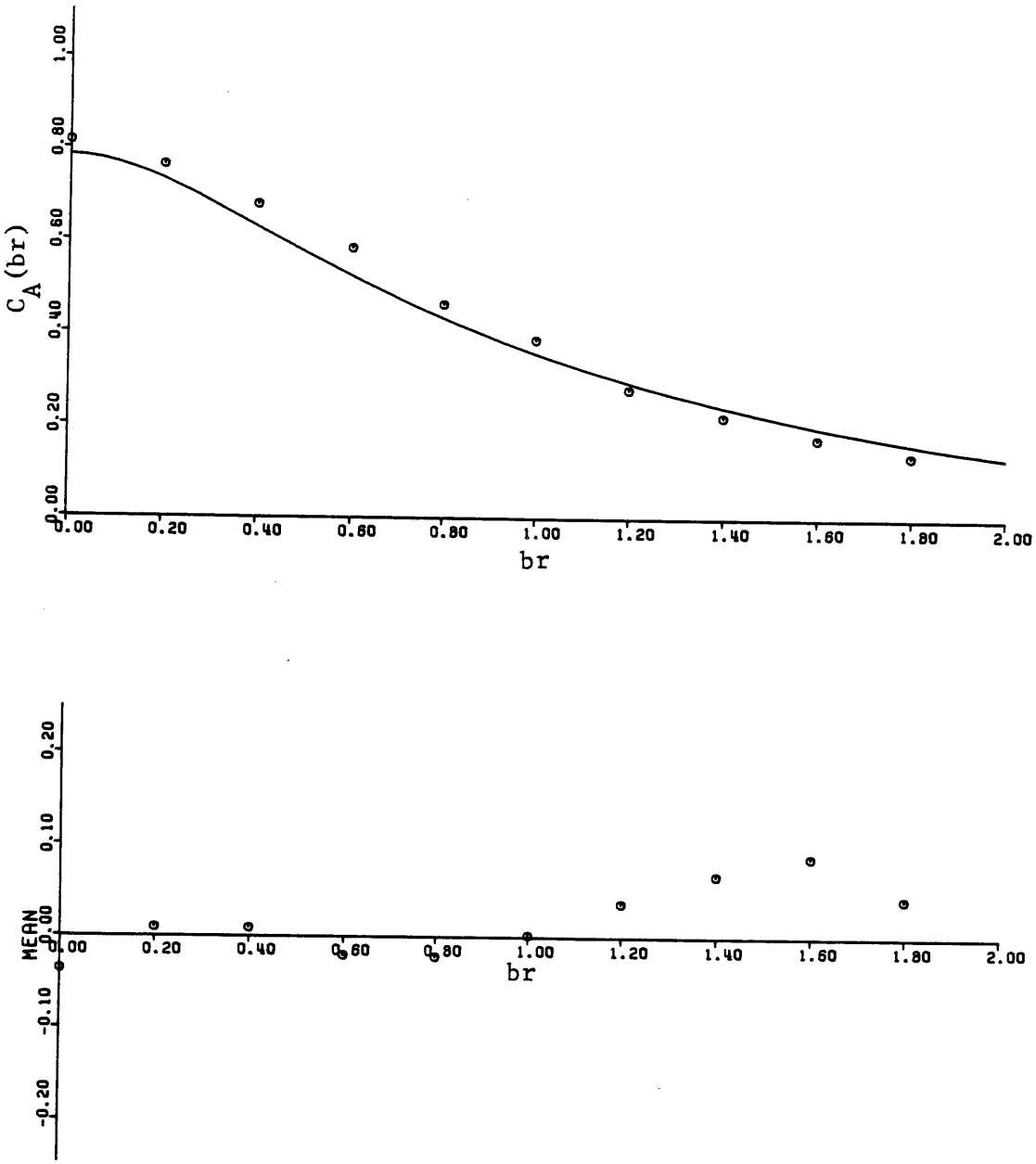

Figure 5.8 Theoretical and sample covariance function and mean of the areal average process: $b^2 L_x L_y = 0.25$.

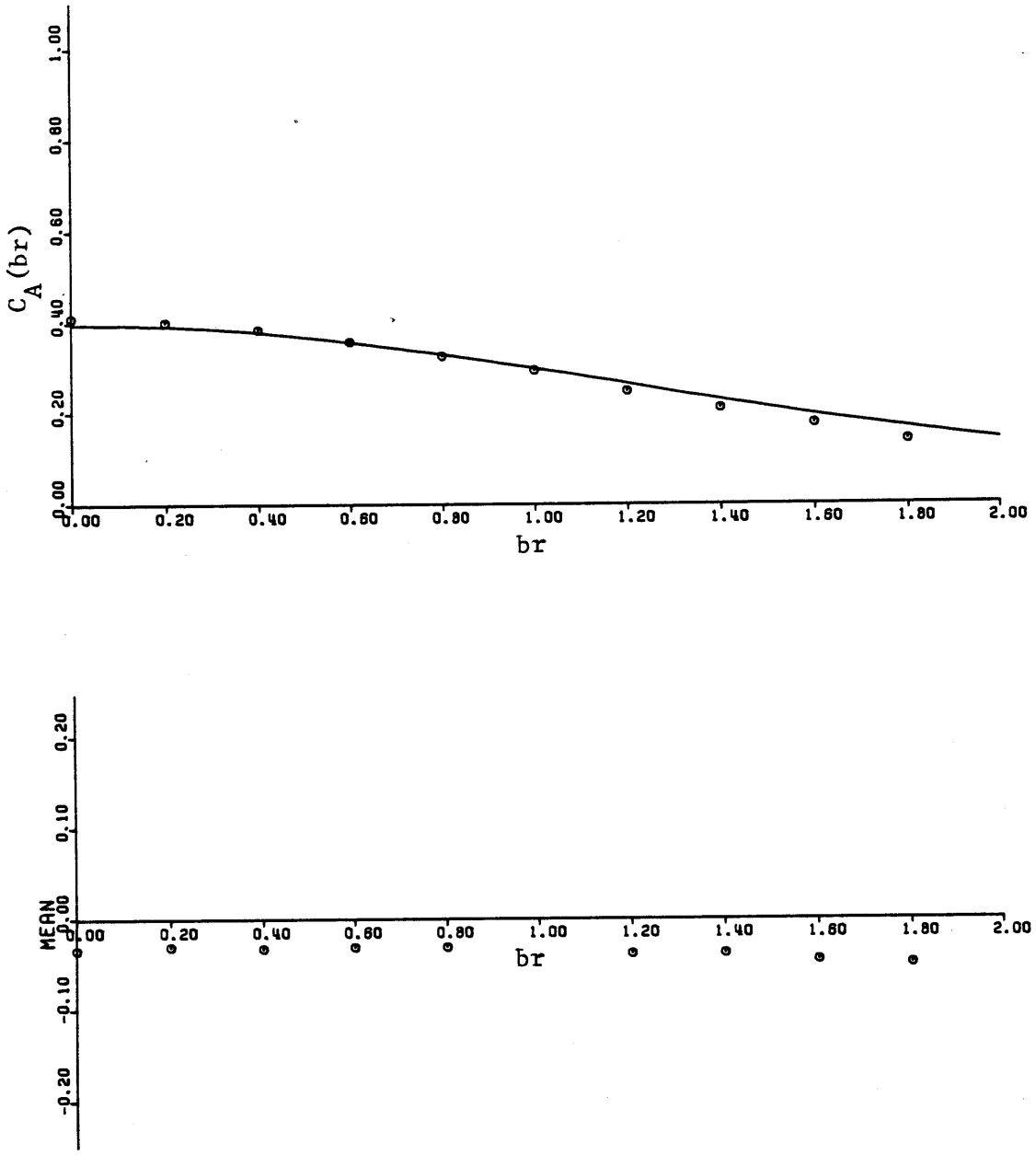

Figure 5.9 Theoretical and sample covariance function and mean of the areal average process: $b^2 L_x L_y = 4.0$.

(2.32). In the simulations the line process was generated with a discretization interval $\Delta\zeta = 0.10$, M = 50 harmonics, and a frequency discretization $\Delta\omega = 0.80$. We used 16 lines, and NS = 200 experiments were performed. The comparison between the theoretical covariance and the sample values taken from the 200 direct simulations are compared in Figures 5.8 and 5.9, for $bL_x = bL_y = 0.5$ and $bL_x = bL_y = 2.0$, respectively.

These figures show that the sample statistics are very close to the theoretical ones. Generally there is less scatter than found for the point process with an equivalent sample size (Figures 3.9 - 3.12), because of the reduction in the variance of the areal average process.

The cost, in CPU time, for the generation of the areal average process via TBM is equivalent to the cost of the generation of the point process. Each area corresponds in cost to one point--with a multiplier only a fraction above one to account for the slightly more complicated algorithm used.

5.4 Review of some other areal average simulation methods

Two other methods proposed for the direct simulation of the process of areal averages are reviewed in this section. The methods were proposed by Lenton and Rodriguez-Iturbe (1977) and Wilson (1979). The method of Lenton and Rodriguez is simular to Mejia and Rodriguez's method for the generation of isotropic point processes (see Section 2.4). The method proposed by Wilson consists of two steps: first, calculation of the covariance matrix of the areal average process between the

areas to be simulated; and second, decomposition of this matrix for generation of the process. A brief review of these models is given here.

5.4.1 Spectral method (Lenton and Rodriguez-Iturbe, 1977)

The simulated field at point $\underline{x}$, is given by an equation of the type:

$$z_s(\underline{x}) = \sigma\sqrt{\frac{2}{N}} \sum_{k=1}^{N} |H(\underline{\omega}_k)| \cos(\underline{\omega}_k \underline{x} + \phi_k) \qquad (5.30)$$

where $H(\underline{\omega})$ is the characteristic function of the area defined by (5.20), $\underline{\omega}_k$ is a random vector having probability density function given by the spectral density function of the point process, ω_k is a random angle uniformly distributed between 0 and 2π, and σ^2 is the variance of the point process. It is assumed that the process has zero mean and the spectral density function of the point process is known. The random vector $\underline{\omega}_k$ can be written as:

$$\underline{\omega}_k = (\omega_k \cos\theta_k, \omega_k \sin\theta_k)$$

where ω_k is a random variable having probability density function equal to the radial spectral density function of the point process, and θ_k is a random angle uniformly distributed between 0 and 2π.

The process defined by (5.30) is ergodic only as $N \to \infty$. In this model, as in Mejia and Rodriguez' model we generate randomly on the plane frequency vectors. In order to describe the frequency spectrum accurately the number of harmonics, N, chosen should be quite large. In practical applications the number of harmonics N = 500 or greater should give a satisfactory approximation.

5.4.2 Matrix decomposition method (Wilson, 1979)

A modification of the model proposed by Wilson (1979) is given here. In this model we assumed that the covariance matrix of the areal average process between the areas of the field we want to simulate is known. This covariance matrix can be calculated as an expected value using (5.9). Let $\underline{z}$ define the vector of the areal average process, which is assumed to be a zero mean process, and $\underline{P}_{zz}$ the corresponding theoretical covariance matrix which we want to preserve.

We define a process described by:

$$\underline{z} = \underline{B}\,\underline{w} \tag{5.31}$$

In the above equation $\underline{z}$ is a column vector of the values of the areal average process for the areas we simulate. $\underline{w}$ is an uncorrelated column vector of white noise having zero mean and covariance matrix given by:

$$P_{w\,w} = E[\underline{w}\,\underline{w}'] = \underline{I} \tag{5.32}$$

where $\underline{w}'$ is the transpose of vector $\underline{w}$, and $\underline{I}$ is the identity matrix.

Multiplying (5.31) by $\underline{z}'$ gives

$$\underline{z}\,\underline{z}' = \underline{B}\,\underline{w}\,\underline{z}'$$

Taking expected values we get: $E[\underline{z}\,\underline{z}'] = E[\underline{B}\,\underline{w}\,\underline{z}']$, or:

$$\underline{P}_{zz} = \underline{B}\,\underline{P}_{wz} \tag{5.33}$$

where $\underline{P}_{wz}$ is the covariance matrix between x and z. Multiplying (5.31) by $\underline{w}'$ yields:

$$\underline{z}\,\underline{w}' = \underline{B}\,\underline{w}\cdot\underline{w}'$$

which, taking expected values, gives the cross-covariance matrix

$$\underline{P}_{zw} = \underline{B}\,\underline{P}_{ww} = \underline{B} \tag{5.34}$$

This can be written as

$$\underline{P}'_{zw} = \underline{B}' \tag{5.35}$$

Using the property $\underline{P}'_{zw} = \underline{P}_{wz}$, equation (5.33) leads to

$$P_{zz} = B\,P'_{zw} \tag{5.36}$$

From (5.35) we get

$$\underline{P}_{zz} = \underline{B}\,\underline{B}'$$

From this equation, where $\underline{P}_{zz}$ is the known theoretical covariance matrix of the areal average process, we can calculate matrix $\underline{B}$ by decomposition. Then equation (5.31) is used for the generation of the process.

With this model we first have to calculate the covariance matrix $\underline{P}_{zz}$ of the areal average process. As is seen in Figures 5.5 to 5.7, as the distance between two blocks increase then the areal average covariance tends to the point covariance function. This is a useful property as it is sufficient to calculate only the variance of the process and the covariances between the nearest areas. For areas further apart the approximation of the areal covariance function with the point covariance should be quite good.

5.5 Discussion

In this section we discuss questions as the accuracy and the cost of the different simulation methods for the generation of the areal average process.

Both the turning bands method (TBM) and the method of Lenton and Rodriguez-Iturbe (1977) preserve the theoretical covariance function as a limit when the number of lines, etc., or the number of harmonics tend to infinity. In practice though, it should be enough to take 6-16 lines in the turning bands method or 200-500 harmonics in Lenton and Rodriguez' method (see Section 3.6). In the matrix decomposition method the theoretical and the model covariance function are the same, but in this method we have to calculate the variance and covariances of the process of areal averages and depending on the method used for this calculation some errors may be introduced.

As in the isotropic point case, the cost of the turning bands method increases approximately proportionally to the square root of the number of simulated areas in the field. The cost of Lenton and Rodriguez' method is linearly proportional to the number of areas, while the cost of the decomposition method is proportional to at least the square of the number of areas. This means that as the number of areas in the field at which we generate increases, the turning bands method becomes more efficient in comparison to the other methods.

5.6 Summary and Conclusions

A brief summary of this chapter is in order. In Section 5.2 we

derived some formulas for the calculation of the covariance function as well as the spectral density function of the areal average process. In Appendix E we calculated this spectral density function for some useful geometries. In Section 5.3 we found the covariance function of the areal average process in the case of rectangular regions, and give some examples of the direct simulation of this process using the turning bands method for generation of anisotropic processes. Finally we presented two other direct methods, along with discussion of comparison, in terms of accuracy and cost.

We conclude that the turning bands method well preserves the theoretical covariance function of the areal average process and in terms of cost will be cheaper than the other methods particularly for a large number of generated areal values.

CHAPTER 6

SIMULATION OF TWO DIMENSIONAL NON-STATIONARY INTRINSIC RANDOM FIELDS

6.1 Introduction

Intrinsic random fields described by a polynomial generalized covariance function (GC-k, see Section 2.3) can be easily simulated by the turning bands method (Matheron, 1973). Recall that if we differentiate an Intrinsic Random Function of order k(IRF-k), k + 1 times we produce a stationary process (Delfiner, 1976). Then, two IRF's $Y(\underline{x})$ and $Z(\underline{x})$ are regarded as equivalent (same GC) if $Z(\underline{x}) = Y(\underline{x}) + P_k(\underline{x})$ where $P_k(\underline{x})$ is a k^{th} order polynomial. To simulate an IRF-k, a realization is generated of the zero mean function $Y(\underline{x})$ with a given GC-k. Then the polynomial $P_k(\underline{x})$ with random coefficients is added. In practice we usually perform conditional simulations, so that the addition of $P_k(\underline{x})$ becomes meaningless, as it is subtracted during the conditioning step. Thus it suffices at this point to generate realizations of fields $Y(\underline{x})$ with a given GC-k having zero mean.

The turnings band method (TBM) is easily adopted for the generation of random fields with a given isotropic GC-k function of polynomial type K(r). On the turning bands lines a corresponding GC-k function $K_1(\zeta)$ is found which is also of polynomial type (Matheron, 1973). Then simple techniques for the generation of polynomial type unidimensional intrinsic processes can be used. In the following we present the basic derivation for the procedure, along with several examples of simulation of non-stationary random fields with a polynomial GC-k function. Our attention is focused on two-dimensional simulation. Three dimensional fields are simulated in an analogous way.

6.2 Derivation of the Unidimensional GC Function

If we perform line simulations with GC-k $K_1(\zeta)$, then the corresponding two dimensional GC-k $K(r)$ is given by (3.24), where the covariances are replaced by generalized covariances (Matheron, 1973):

$$K(r) = \frac{2}{\pi} \int_o^r \frac{K_1(\zeta)}{\sqrt{r^2-\zeta^2}} \, d\zeta \tag{6.1}$$

Take the special case of $K_1(\zeta) = \zeta^{2p+1}$, and find the equivalent $K(r)$:

$$K(r) = \frac{2}{\pi} \int_o^r \frac{\zeta^{2p+1}}{\sqrt{r^2-\zeta^2}} \, d\zeta$$

$$= \frac{r^{2p+1}}{\pi} \int_o^r \frac{\eta^p}{\sqrt{1-\eta}} \, dn$$

$$= \frac{r^{2p+1}}{\pi} \, B(p+1, 1/2) \tag{6.2}$$

$B(-,-)$ is a Beta function:

$$B(p+1 \, , \, 1/2) = \frac{\Gamma(p+1) \, \Gamma(1/2)}{\Gamma(p+3/2)} = \frac{\sqrt{\pi} \; p!}{\Gamma(p+3/2)} \tag{6.3}$$

This, for this special case $K(r)$ becomes

$$K(r) = \frac{p! \; r^{2p+1}}{\sqrt{\pi} \quad \Gamma(p+3/2)} \tag{6.4}$$

Comparing this special K(r) to the polynomial R^2 GC-k of (2.43) leads to the general relationship for undimensional GC-k:

$$K_1(\zeta) = \sum_{p=o}^{k} \frac{(-1)^{p+1}\alpha_p}{(2p+1)!}\ \zeta^{2p+1} \tag{6.5a}$$

$$= \sum_{p=o}^{k} (-1)^{p+1}\ \left(\frac{a_p}{\beta_{2p}}\right)\ \zeta^{2p+1} \tag{6.5b}$$

$$= \sum_{p=o}^{k} (-1)^{p+1}\ b_p\ \zeta^{2p+1} \tag{6.5c}$$

where, invoking (2.42), new coefficient b_p is defined by

$$b_p = \frac{\alpha_p}{(2p+1)!} = \frac{a_p}{\beta_{2p}} = \frac{\sqrt{\pi}\ \Gamma(p+3/2)}{p!}\ a_p \tag{6.6}$$

For a polynomial GC model with k = 0, 1 and 2 given by (2.44) the corresponding polynomial $K_1(\zeta)$ is:

$$k = 0 \quad K_1(\zeta) = -b_o\zeta \tag{6.7a}$$

$$k = 1 \quad K_1(\zeta) = -b_o\zeta + b_1\ \zeta^3 \tag{6.7b}$$

$$k = 3 \quad K_1(\zeta) = -b_o\zeta + b_1\ \zeta^3 - b_2\zeta^5 \tag{6.7c}$$

where

$$b_o = \frac{\pi}{2}\ a_o \quad ; \quad b_1 = \frac{3\pi}{4}\ a_1 \quad ; \quad b_2 = \frac{15\pi}{16}\ a_2 \tag{6.8}$$

The restrictions on the coefficients in R^2 are taken from (2.44d). Thus given a polynomial GC-k in R^2, of the form of (2.43), we have derived equivalent GK-k's along the turning bands lines in (6.7).

6.3 Generation of the Unidimensional Intrinsic Process

Matheron (1973) proposed a simple simulation model for the intrinsic line process. The unidimensional process $Y(\zeta)$ on line i is described by:

$$Y(\zeta) = c_o\, W(\zeta) + c_1 \int_o^{\zeta} W(\xi)\, d\xi + \ldots. + c_k \int_o^{\zeta} \frac{(\zeta-\xi)}{(k-1)!}^{k-1} W(\xi)\, d\xi \qquad (6.9)$$

where c_p are real coefficients and $W(\xi)$ is an intrinsic random function of order zero having GC-0 of $K_1(h) = -h$, where h is the increment (always taken positive).

The Wiener process, also called the Brownian motion process, is an intrinsic process of order zero that can be used to generate $W(\zeta)$. The first order differences of this process are stationary. The discrete version of the Wiener process is given by:

$$W(\zeta + h) = W(\zeta) + g\, U(\zeta) \qquad (6.10)$$

in which h is the increment and $U(\zeta)$ is a uniformly distributed number between [-0.5 , + 0.5]. The variance of the difference $[W(\zeta + h) - W(\zeta)]$ is:

$$\text{var}[W(\zeta + h) - W(\zeta)] = g^2/12 \qquad (6.11)$$

The generalized covariance $K_1(h)$ for this zero order process, or any higher order instrinsic process, must satisfy the relationship (Delfiner, 1976):

$$\text{var}\left[\sum_{i=1}^{N} \lambda_i \, W(\zeta_i)\right] = \sum_{i=1}^{N} \sum_{j=1}^{N} \lambda_i \, \lambda_j \, K_1(\zeta_i - \zeta_j) \qquad (6.12)$$

where N is the number of discretized points i, j = 1,N along the lines. For k = 0 the λ_i obey $\sum_{i=1}^{N} \lambda_i = 0$ (see Delfiner, 1976). One possible set of λ's meeting this criterion is $\lambda_\mu = +1$ for $\zeta_\mu = \zeta + h$, $\lambda_\nu = -1$ for $\zeta_\nu = \zeta$, and $\lambda_m = 0$ for $\zeta_m \neq \zeta+h$ or ζ. Then $\sum_{i=1}^{N} \lambda_i = 0$ and (6.12) simplifies to:

$$\text{var}[W(\zeta + h) - W(\zeta)] = -2 \, K_1(h) \qquad (6.13)$$

Comparing (6.13) and (6.11) leads to

$$g^2 = -24 \, K_1(h) \qquad (6.14)$$

for $K_1(h) = -h$ we get

$$g = \sqrt{24h} \qquad (6.15)$$

The Weiner process is generated from (6.10) with this value for g, where h is the increment $\Delta\zeta$ of the discretized line process (i.e., width of the turning bands).

For higher order intrinsic processes Matheron's (1973) representation (6.9) is used. The coefficients c_o, c_1 , ... c_k are related to b_o, b_1, ...b_k on page 467(watch out for change in notation!). For k = 2 equation (6.9) gives

$$Y(\zeta) = c_o \, W(\zeta) + (c_1 + c_2\zeta) \cdot \int_o^\zeta W(\xi) \, d\xi \; - c_2 \int_o^\zeta \xi \, W(\xi) \, d\xi \qquad (6.16)$$

In order to calculate the integrals we discretize the segments between the points i where values are generated (see Figure 6.1). The

trapezoidal rule is used to numerically calculate the integrals:

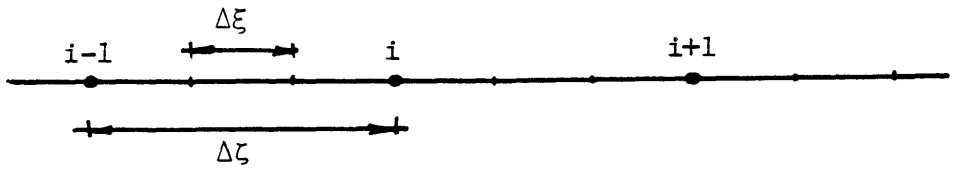

Figure 6.1 Schematic representation of numerical integration of unidimensional polynomial process

$$\left.\begin{aligned} I_1(\zeta) &= I_1\ (\zeta - 1) + \frac{w(\zeta\text{-}1) + w(\zeta)}{2}\,\Delta\xi \\ I_2(\zeta) &= I_2\ (\zeta - 1) + \frac{(\zeta\text{-}1)\ w(\zeta\text{-}1) + \zeta\ w(\zeta)}{2}\,\Delta\xi \end{aligned}\right\} \qquad (6.26)$$

where:

$$\left.\begin{aligned} I_1(\zeta) &\approx \int_o^\zeta w(\xi)\ d\xi \\ I_2(\zeta) &\approx \int_o^\zeta \xi w(\xi)\ d\xi \end{aligned}\right\} \qquad (6.27)$$

Obviously the approximation of the integrals will be better as $\Delta\xi$ becomes smaller or $\lambda = \frac{\Delta\xi}{\Delta\zeta}$ becomes large. It is noted that λ should be a positive

integral. The simulated values $y_s(\zeta)$ are calculated only at the discrete points, i-1, i, i+1 at discretization distances $\Delta\zeta = \lambda\ \Delta\xi$.

Chiles (1977) proposed another technique which uses many lines (of the order of 180) but a far less accurate model for the stimulation of the unidimensional processes $Y(\zeta)$, than the one proposed above. The comparison in accuracy and cost between those models though is still an open question.

6.4 Examples and discussion

Some examples of generation of IRF or orders k = 0, 1, and 2 having zero mean are given in Figures 6.2, 6.3, and 6.4. The dimensions of the simulated area are Xmax = 3.0 and Ymax = 2.4. The number of columns is NX = 50 the number of rows NY = 40 making N = 2000 simulated points. The number of lines was L = 12 the discretization along the lines $\Delta\zeta = 0.02$ and the parameter λ was set $\lambda = 1$. Figure 6.2 shows a realization of an IRF - 0 with $K(r) = -r$. The interpretation is that first order differences of this field will yield a stationary process. Figure 6.3 shows a realization of a field with GC-1 of $K(r) = r^3$. Second order differences of this field will yield a stationary process. Finally in Figure 6.4 a realization of a field with GC-2 given by $K(r) = -r^5$ is shown. Third order differences of this field will produce stationarity. Obviously if in the above realizations we had added one polynomial of k^{th} degree with arbitrary coefficients this polynomial would be filtered out by taking k+1 order differences and the remaining would be a stationary field.

Conditional simulations of IRF are obtained as in the case of stationary fields (see Chapter 2).

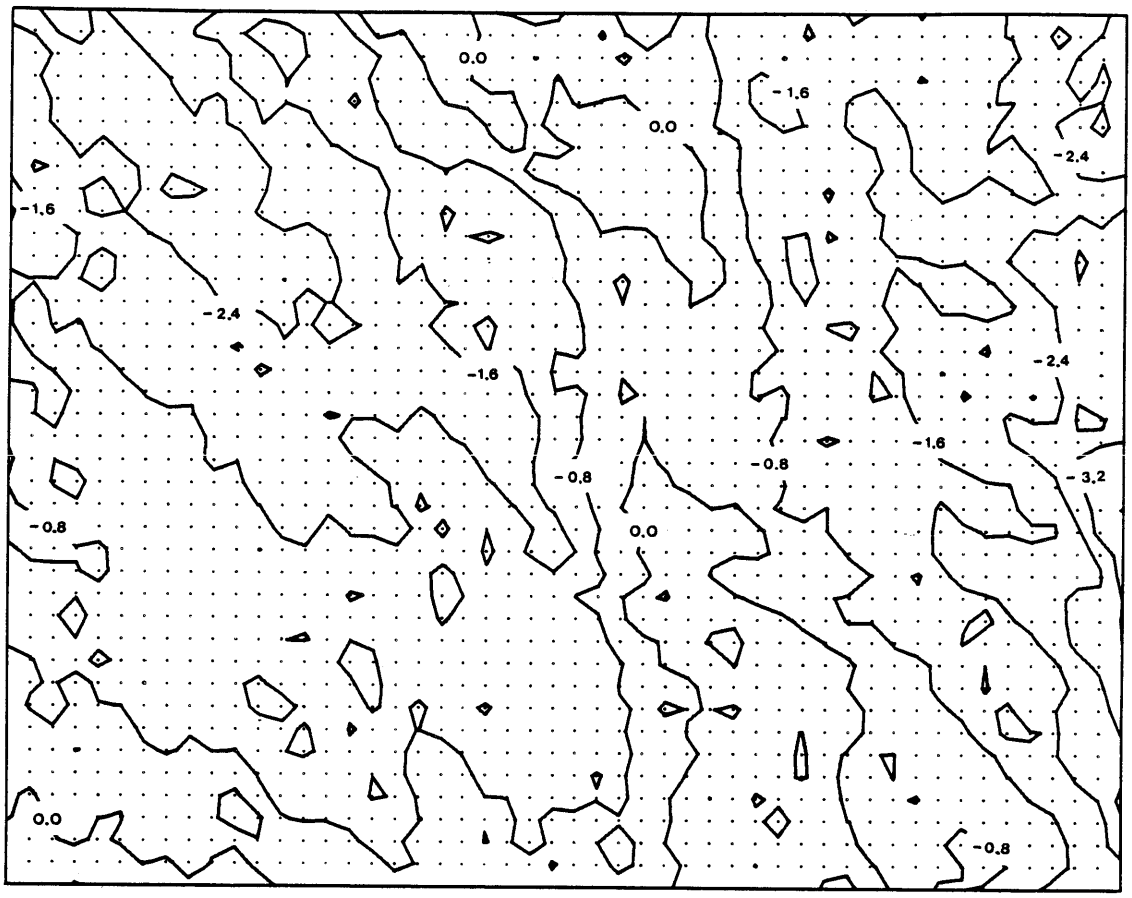

Figure 6.2 An example realization of an IRF-0 with K(r) = -r generated with the TBM.

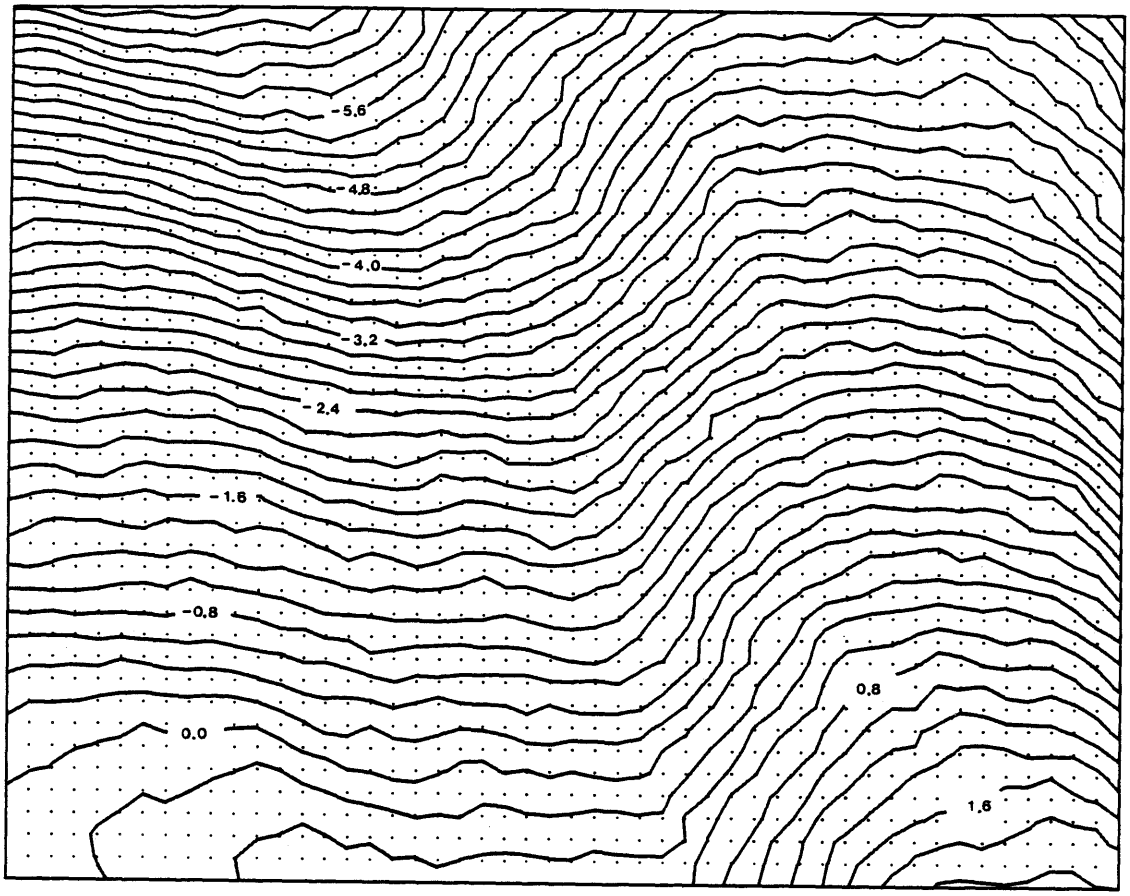

Figure 6.3 An example realization of an IRF-1 with $K(r) = r^3$ generated with the TBM.

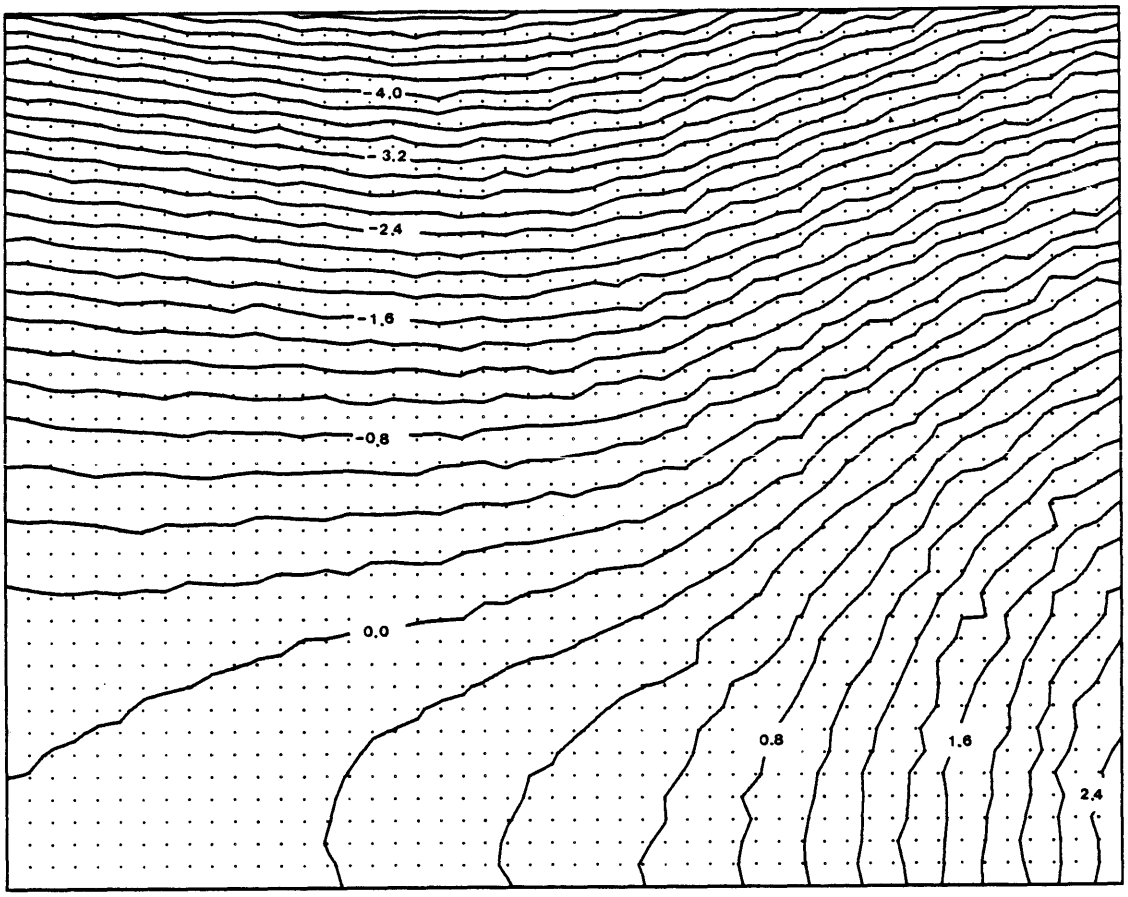

Figure 6.4 An example realization of our IRF-2 with $K(r) = -r^5$ generated with the TBM.

Orfeuil (1972; see examples in Matheron, 1973) was the first to generate IRF's using the turning bands method. The techniques described in this chapter are essentially the same as those used by him and Matheron.

Anisotropic intrinsic fields are not explicitly handled in this approach. Matheron (1973) argues that in practical cases of natural anisotropy the polynomial GC can adequately take it into account. Anisotropy introduced by spatial averaging is another matter.

Spatial averages of intrinsic fields can be simulated by taking the weighted average of point values (see Journel and Huijbregts, 1978). The direct use generation of these averaged intrinsic fields, say using a TBM-anistropic spectral line process, has not been previously attempted. We attempted to do this, following an approach similar to Chapters 4 and 5 for stationary processes, but found the calculations intractible. Further effort along these lines is warranted.

CHAPTER 7

SUMMARY, CONCLUSIONS, AND RECOMMENDATIONS

7.1 Summary and Conclusions

In this report we have presented the turning bands method (TBM) for the simulation of random fields, with special emphasis on two dimensional processes. In hydrology the turning bands method can be applied to the synthetic generation of a field of hydraulic conductivities or other aquifer properties or for the simulation of the rainfall depth over an area. In mining TBM can be used to simulate ore or energy resource deposits. It also has applications in the fields of ocean engineering, structural engineering, geotechnical engineering, etc.

In Chapter 2 we presented basic denfinitions and developed the equations describing a random function or random field of both stationary and intrinsic type. Then, we briefly reviewed existing stationary field simulation models from the literature.

In Chapter 3 the turning bands method for simulation of stationary two or three dimensional isotropic random fields was presented. In the two dimensional case, two different new approaches were proposed. One approach is based on the simulation of the line process using a spectral method, while in the other approach the line process is generated directly from the unidimensional covariance function as a moving average (MA) process. The unidimensional spectral method permits, for the first time, the TBM simulation of any properly posed covariance function, and as shown later in Chapter 4, is easily extended to the direct generation of anisotropic fields. The moving average unidimensional process is slightly

less expensive to use, but only certain covariance functions can be modeled. Examples of the TBM generation were given, comparing theoretical and sample statistics and demonstrating the accuracy of the method. A theoretical error analysis of the TBM was performed, backed up with examples, that illustrated the rapid covergence of the TBM with the number of lines. Sensitivity analyses were performed for the discretization of the unidimensional spectral generation, resulting in guidelines for the selection of model parameters. Finally, we compared the turning bands method to the other simulation methods in terms of cost and accuracy. We found that the cost of the TBM increases with the square root of the number of points simulated, while with the other methods, the cost increases linearly with the number of points. Consequently, the TBM offers very significant cost reductions for the generation of random field. The TBM is ergodic and converges rapidly; it is as accurate as the best available alternative and considerably less expensive!

In Chapter 4 we proposed a new technique for the generation of a two dimensional stationary anisotropic processes, using a modification of the turning bands method. In this case, we allowed the unidimensional covariance function, as well as the corresponding line process spectral density function, to depend on the direction of the line. After the mathematical development, an example of simulation of a two dimensional process having anisotropic exponential covariance function was given. By comparing the theoretical and sample statistics, we demonstrated the utility of this new technique.

In Chapter 5 we reviewed the basic definitions applying the areal average processes, in which the underlying continuous field is stationary. We discussed variance and covariance reduction due to averaging and presented graphs showing the theoretical covariances for several averaging geometries. We observed that the reduced covariance between areas can damp out quickly, relative to the size of the areas, suggesting the possibility of approximating areal average covariance by point covariance in some instances. A formula was derived for the claculation of the spectral density function of areal average processes. It was applied to particular geometries in Appendix E. The areal averages process was then simulated using Chapter 4's TBM for generation of anisotropic process. An example of the application of the proposed method for the case of square and rectangular areas was given, with a very favorable comparison between the theoretical and sample statistics.

In Chapter 6 we presented the TBM method for the simulation of non-stationary random fields of intrinsic type, having polynomial generalized covariance functions. The unidimensional simulations were generated by a Weiner (Brownian Motion) process. The procedure described is basically the same one proposed by Matheron [1973] and implemented by Orfeil [1972]. Examples were given for intrinsic random functions of order $k = 0, 1, 2$.

In conclusion, the turning bands method is an accurate, cost-effective and versatile method for the simulation of random fields. It is at least as accurate as other existing methods, and far less expensive. It can be directly extended, as we have shown, to the generation of anisotropic process, areal average processes, and particular cases of non-stationary processes. Using the spectral method for the line method for the line process, it can model any properly posed covariance function in the stationary case. For these reasons we expect that, in the future, the TBM will become a commobly used random field simulation method in hydrology and other fields.

Note: All of the simulations described in this report were coded in FORTRAN-IV and run on an IBM 360-168 at MIT. The code is described in Mantoglou and Wilson (1981).

7.2 Recommendations for future research

During the development of this work, a number of attractive adeas came up, but were not pursued due to time and space limitations. We give a brief description of some of these in the following paragraphs.

1. It would be interesting for us to apply the proposed method to the stochastic modeling of a real field problem. We would then follow the steps described below.
   (a) Obtain the theoretical statistics from field data (measurements).
   (b) Perform unconditional simulations.

(c) Condition the simulations such that simulation values at the points of measurements are the measured value.

(d) For problems such as groundwater flow, apply these conditioned parameters to a numerical model (for example; AQUIFEM, Townely and Wilson, 1980) to otain system outputs such as piezometric head, flow etc.

(e) Repeat steps b to c (or d) several times. We can then calculate the statistics of the output..

This has already been done for some cases by the Fontainbleau group [e.g., Journel and Huijbreghts, 1978; Delhomme, 1979], but others need this experience.

2. An extension of the proposed anisotropic method (Chapter 4) could be made for the generation of three dimensional anisotropic fields. This extended method then could be applied for generation of block values in three dimensional fields; mining deposits, petroleum reservoirs, aquifers, etc.
3. A more thorough comparison of the TBM to the method of Shinozuka and Jan (1972) in terms of accuracy and cost would be useful.
4. It would be interesting to apply and compare Wilson's (1979) model for areal average generation, and as a prerequisite, to solve the problem of variance covariance reduction, etc.
5. Although we encountered little success in doing so, it is probably worth some added effort to develop a direct simulator for areal averages of an intrinsic random field. This requires the consideration of anisotropic intrinsic fields.

REFERENCES

Abramovitz, M. and Stegun, I. A. (1965) Handbook of Mathematical Functions, Dover Publications, Inc., New York.

Chiles, J. P. (1979) "Geostatique Des Phenomenes Non Stationaries," in France, These de Docteur-Ingenieur, Univ. de Mancy, Nancy, France, 152 pages.

Delfiner, P. (1976) "Linear Estimation of Non-Stationary Spacial Phenonmena" Advanced Geostatistics in the Mining Industry, Proceedings of the Advanced Study Institute, University of Rome, Italy, October 13-25, 1975.

Delhomme, J. P. (1979) "Spatial Variability and Uncertainty in Groundwater Flow Parameters: A Geostatistical Approach," WRR, Vol. 15, No. 2, pg. 269-280.

Dettinger, M. P. and Wilson, J. L. (1981) "A First Order Analysis of Uncertainty in Numerical Models of Groundwater Flow," Part L. Mathematical Development, Part II. Applications with a Finite Difference Model," WRR, Vol. 17, No. 1, pg. 149-161.

Freeze, A. (1975) "A Stochastic-Conceptual Analysis of One-Dimensional Groundwater Flow in Nonuniform Homogeneous Media," WRR, Vol. 11, No. 5, pg. 725-741.

Gelb, A. (1974) "Applied Optimal Estimation," the MIT Press, Cambridge, Mass. 374 pages.

Gradshteyn, I. S. and Ryzhik, I. M. (1965) "Table of Integrals, Series and Products," Academic Press, New York.

Journel, A. G. (1974) "Geostatistics for Conditional Simulation of Ore Bodies," Economic Geology, Vol. 69, pp. 673-687.

Journel, A. G. and Huijbregts, Ch. I. (1978) "Mining Geostatistics," Academic Press, Inc., New York.

Kafritsas, J., Some applications of random field theory in Geotechnical Engineering, M. S. Thesis in Civil Engineering, MIT, May 1980

Lenton, R. L. and Rodriguez-Iturbe, I. (1974) "On the Collection, the Analysis and the SYnthesis of Spatial Rainfall Data," Tech. Report 194, R. M. Parsons Laboratory for Water Resources and Hydrodynamics, Massachusetts Institute of Technology, Cambridge, Mass.

Lenton, R. L. and Rodriguez-Iturbe, I (1977) "A Multidimensional Model for the Synthesis of Processes of Areal Rainfall Averages", WRR, Vol. 13, No. 3, pg. 605-612.

Matern, B. (1960) "Spatial Variation", Medd. Statens Skogsforsknigsinst., 49 (5).

Matheron, G. (1973) "The Intrinsic Random Functions and Their Applications, Adv. Appl. Prob. 5, pg. 439-468.

Mejia, J. and Rodriguez-Iturbe, I. (1974) "On the Synthesis of Random Fields from the Spectrum: An Application to the Generation of Hydrologic Spatial Processes," WRR, Vol. 10, No. 4, pg. 705-711.

Orfeuil, J. P. "Simulation du Wiener-Levy et de ses Integrals," Interual Rpt, Center de Morphologie Mathematique, Fontainebleau, 1972.

Rhenals-Figueredo, A. E. and Rodriguez-Iturbe, I. (1974) "Bidimensional Spectral Analysis of Rainfall Events," Tech. Report 193, R. M. Parsons Laboratory for Water Resources and Hydrodynamics, Massachusetts Institute of Technology, Cambridge, Mass.

Rice, S. O. (1954) "Mathematical Analysis of Random Noise," Selected Papers on Noise and Stochastic Processes (Editor: N. Wax), Dover Publications, Inc., New York, pp. 180-181.

Shinozuka, M., and Jan. C. M. (1972) "Digital Simulation of Random Processes and Its' Applications," Journal of Sound and Vibration, 25 (1), pg. 111-128.

Shoenberg (1938) "Metric Spaces and Completely Monotone Functions," Ann. Math., 39, pp. 811-841.

Smith, L. and Freeze, A. (1979a) "Stochastic Analysis of Steady State Groundwater Flow in a Bounded Domain. 1. One-Dimensional Simulations," WRR, Vol. 15, No. 3, pg. 521-528.

Smith, L. and Freeze, A. (1979b) "Stochastic Analysis of Steady State Groundwater Flwo in a Bounded Domain. 2. Two-Dimensional Simulations," WRR, Vol. 15, No. b, pg. 1543-1559.

Townley, L. R. and Wilson, J. L. (1980) "Description of and User's Manual for a Finite Element Aquifer Flow Model AQUIFEM-1," Technology Adaptation Program Reprot No. 79-3, Massachusetts Institute of Technology, Cambridge, Mass.

Vanmarcke, E. (1977) "Probabilistic Modeling of Soil Profiels," J. of Geotechnical Eng. Div. GT11, pp. 1227-1247.

Veneziano, D. A. (1978) "Random Processes for Engineering Applications," Course Notes, Massachusetts Institute of Technology.

Wilson, J. L. (1979) "The Synthetic Generation of Areal Averages of a Random Field," Socorro Workshop on Stochastic Methods in Subsurface Hydrology, April 26-27.

APPENDIX A

In this appendix we calculate the one dimensional covariance functions $C_1(\zeta)$ corresponding to two dimensional covariance models of the exponential and Bessel type.

A.1 Exponential model: $C(r) = \sigma^2 e^{-br}$

The spectral density function of the unidimensional process is given by (3.35) as

$$S_1(\omega) = \frac{\sigma^2}{2} \frac{\omega}{b^2[1 + \frac{\omega^2}{b^2}]^{3/2}} \tag{A.1}$$

The corresponding covariance function is given by (3.55) as

$$C_1(\zeta) = \frac{\sigma^2}{b^2} \int_o^\infty \cos(\omega\zeta) \frac{\omega}{[1 + \frac{\omega^2}{b^2}]^{3/2}} d\omega \tag{A.2}$$

By recognizing that

$$\frac{1}{b^2} \frac{\omega}{[1 + \frac{\omega^2}{b^2}]^{3/2}} = - \frac{d}{d\omega} \left[\frac{1}{(1 + \frac{\omega^2}{b^2})^{1/2}}\right]$$

The integral (A.2) becomes

$$C_1(\zeta) = -\sigma^2 \int_o^\infty \cos(\omega\zeta) \{\frac{d}{d\omega} \left[\frac{1}{[1 + \frac{\omega^2}{b^2}]^{1/2}}\right]\} d\omega =$$

$$= -\sigma^2 \{\cos(\omega\zeta) \frac{1}{[1 + \frac{\omega^2}{b^2}]^{1/2}} \Big|_o^\infty +$$

$$+ \int_o^\infty \zeta \sin(\omega\zeta) \frac{1}{[1 + \frac{\omega^2}{b^2}]^{1/2}} d\omega\} =$$

$$= -\sigma^2 \left[-1 + b\zeta \int_o^\infty \sin(\omega\zeta) \frac{1}{[b^2 + \omega^2]^{1/2}} d\omega\right] \qquad (A.3)$$

The integral

$$I = \int_o^\infty \sin(\omega\zeta) \frac{1}{[b^2 + \omega^2]^{1/2}} d\omega$$

is given in Gradshteyn and Ryzhik (1965, p. 419) as:

$$I = \frac{\pi}{2} [I_o(b\zeta) - L_o(b\zeta)]$$

where I_o is a Bessel function of order zero, and L_o is a modified Struve function of order zero. Thus (A.3) can be written as

$$C_1(\zeta) = \sigma^2 \{1 - \frac{\pi}{2} [I_o(b\zeta) - L_o(b\zeta)]\} \qquad (A.4)$$

The functions $I_o(x)$ and $L_o(x)$ are given by the following series:

$$I_o(x) = \sum_{k=0}^{\infty} \frac{1}{(k!)^2} (\frac{x}{2})^{2k}$$

$$L_o(x) = \sum_{k=0}^{\infty} \frac{1}{[\Gamma(k + 3/2)]^2} (\frac{x}{2})^{2k+1}$$

4.2 Bessel model: $C(r) = \sigma^2 br\, K_1(br)$

From (3.36) we have:

$$C_1(\zeta) = \frac{2\sigma^2}{b^2} \int_o^\infty \cos(\omega\zeta)\, \frac{\omega}{[1 + \omega^2/b^2]^2}\, d\omega =$$

$$= -\sigma^2 b^2 [\cos(\omega\zeta)\, \frac{1}{[b^2 + \omega^2]} \Big|_o^\infty + \int_o^\infty \frac{\zeta \sin(\omega\zeta)}{[b^2 + \omega^2]}\, d\omega] =$$

$$= -\sigma^2 b^2 \, [-b^2 + \zeta \int_o^\infty \frac{\sin(\omega\zeta)}{[b^2 + \omega^2]}\, d\omega] \qquad (A.5)$$

The integral

$$I = \int_o^\infty \frac{\sin(\omega\zeta)}{[b^2 + \omega^2]}\, d\omega$$

is given in Gradshteyn and Ryzhik (1965, pg. 406) as:

$$I = \frac{1}{2b} [e^{-b\zeta} Ei(b\zeta) - e^{b\zeta} Ei(-b\zeta)]$$

so that (A.5) becomes

$$C_1(\zeta) = \sigma^2 \{1 - \frac{b\zeta}{2} [e^{-b\zeta} Ei(b\zeta) - e^{b}\, Ei(-b\zeta)]\} \qquad (A.6)$$

where Ei is the exponential integral function. The exponential integral has the following series representation:

$$Ei(x) = \gamma + \ell n|x| + \sum_{k=1}^{\infty} \frac{x^k}{k!k}$$

where $\gamma = 0.577215.....$ is Euler's constant.

APPENDIX B

In this appendix we calculate the two dimensional covariance functions C(r) corresponding to unidimensional covariance functions of the hole or the exponential type.

B.1 Hole type: $C_1(\zeta) = \sigma^2(1-a\zeta)e^{-a\zeta}$

The two dimensional covariance function will be given by:

$$C(r) = \frac{2}{\pi}\int_o^r \frac{C_1(\zeta)}{\sqrt{r^2-\zeta^2}}\,d\zeta = \frac{2\sigma^2}{\pi}\int_o^r \frac{(1-a\zeta)}{\sqrt{r^2-\zeta^2}}\,e^{-a\zeta}\,d\zeta =$$

$$= \frac{2\sigma^2}{\pi}\left\{\int_o^r \frac{e^{-a\zeta}}{\sqrt{r^2-\zeta^2}}\,d\zeta - a\int_o^r \frac{\zeta e^{-a\zeta}}{\sqrt{r^2-\zeta^2}}\,d\zeta\right\} \qquad (B.1)$$

These integrals are evaluated in Gradshteyn and Ryzhik (1965) as:

$$\Pi_1 = \int_o^r \frac{e^{-a\zeta}}{\sqrt{r^2-\zeta^2}}\,d\zeta = \frac{\pi}{2}\,[I_o(ar)-L_o(ar)] \qquad (B.2a)$$

$$\Pi_2 = \int_o^r \frac{\zeta\, e^{-a\zeta}}{\sqrt{r^2-\zeta^2}}\,d\zeta = r - \frac{\pi}{2}\,r\,[I_1(ar)-L_1(ar)] \qquad (B.2b)$$

so that (B.1) becomes

$$C(r) = \sigma^2\{I_o(ar)-L_o(ar) + ar[I_1(ar)-L_1(ar) - \frac{2}{\pi}]\} \qquad (B.3)$$

where I_o, I_1 are Bessel functions of order zero and one respectively, and L_o, L_1 are Struve functions of order zero and one respectively.

The functions I_1 and L_1 are given by the following series:

$$I_1(x) = \sum_{k=0}^{\infty} \frac{(x/2)^{2k+1}}{k!(k+1)!}$$

$$L_1(x) = \left(\frac{x}{2}\right)^2 \sum_{k=0}^{\infty} \frac{(x/2)^{2k}}{\Gamma(k + 3/2)\Gamma(k + 5/2)}$$

The series representations of functions I_o, L_o are given in Appendix A.

B.2 Exponential type $C_1(\zeta) = \sigma^2 e^{-a\zeta}$

In this case we have:

$$C(r) = \frac{2\sigma^2}{\pi} \int_o^r \frac{e^{-a\zeta}}{\sqrt{r^2-\zeta^2}}\, d\zeta = \frac{2\sigma^2}{\pi} I_1 = \sigma^2[I_o(ar)-L_o(ar)]$$

where I_1 is given by (B.2a) and I_o, L_o are defined above.

APPENDIX C

In this appendix we derive the spectral density function of an anisotropic two dimensional field having exponential covariance function given by:

$$C(\underline{h}) = C(x,y) = \sigma^2 \exp[-(h_1^2x^2 + h_2^2y^2)^{1/2}] \tag{C.1}$$

where σ^2 is the variance of the process and h_1, h_2 are positive parameters.

The spectral density function of the two dimensional process is given by:

$$S(\underline{\omega}) = \frac{1}{(2\pi)^2} \int_{R^2} C(\underline{h}) e^{-i\underline{\omega h}} \, d\underline{h} \tag{C.2}$$

where $\underline{h} = (x,y)$, $\underline{\omega} = (\omega_1, \omega_2)$ and $d\underline{h} = dxdy$. Equation (C.2) is then written as:

$$S(\omega_1,\omega_2) = \frac{\sigma^2}{4\pi^2} \int_{-\infty}^{+\infty}\int_{-\infty}^{+\infty} \exp[-(h_1^2x^2+h_2^2y^2)^{1/2}]\exp[-i(\omega_1x+\omega_2y)]dxdy$$

$$= \frac{\sigma^2}{4\pi^2} \int_{-\infty}^{+\infty} \exp(-i\omega_1x)\{\int_{-\infty}^{+\infty} \exp[-(h_1^2x^2+h_2^2y^2)^{1/2}]\exp(-i\omega_2y)dy\}dx \tag{C.3}$$

Because the function $\exp[-(h_1^2x^2+h_2^2y^2)]$ is an even function with respect to y, the integral inside the brackets { } becomes:

$$I = \int_{-\infty}^{+\infty} \exp -(h_1^2x^2+h_2^2y^2)^{1/2} \exp(-i\omega_2 y)dy =$$

$$= 2\int_{o}^{\infty} \exp -(h_1^2x^2+h_2^2y^2)^{1/2} \cos(\omega_2 y)dy =$$

$$= 2\int_{o}^{\infty} \exp\left[-h_2\left(\frac{h_1^2}{h_2^2}x^2+y^2\right)^{1/2}\right]\cos(\omega_2 y)dy$$

From Gradshteyn and Ryzhik(1965, pg. 482)

$$I = \frac{2h_2 \frac{h_1}{h_2} x}{\sqrt{h_2^2+\omega_2^2}} K_1\left(\frac{h_1}{h_2} x \sqrt{h_2^2+\omega_2^2}\right) \qquad (C.4)$$

so that (C.3) becomes:

$$S(\omega_1,\omega_2)= \frac{\sigma^2 h_1}{2\pi^2\sqrt{h^2+\omega^2}} \int_{-\infty}^{+\infty} \exp(-i\omega_1 x)\ x\ K_1\left(\frac{h_1}{h_2}\sqrt{h_2^2+\omega_2^2}\ x\right)dx \qquad (C.5)$$

Because the Bessel function K_1 is an odd function, the function $x\ K_1(ax)$ should be even. Thus (C.5) can be written as:

$$S(\omega_1,\omega_2)= \frac{\sigma^2 h_1}{\Pi^2\sqrt{h_2^2+\omega_2^2}} \int_{o}^{\infty} x\cos(\omega_1 x)\ K_1\left(\frac{h_1}{h_2}\sqrt{h_2^2+\omega_2^2}\ x\right)dx \qquad (C.6)$$

From Gradshteyn and Ryzhik(1965, pg. 749) we get, for this integral:

$$\int_o^\infty x \cos(\omega_1 x)\ K_1\left(\frac{h_1}{h_2}\sqrt{h_2^2+\omega_2^2}\ x\right)dx =$$

$$= \frac{\pi}{2}\ \frac{1}{\left[\frac{h_1^2}{h_2^2}\ (h_2^2 + \omega_2^2) + \omega_1^2\right]^{3/2}}\ \frac{h_1}{h_2}\sqrt{h_2^2+\omega_2^2}$$

Simplifying the relationship expressed in (C.6):

$$S(\omega_1,\omega_2)= \frac{\sigma^2}{2\pi^2}\ \frac{1}{h_1 h_2\ \left(1 + \frac{\omega_1^2}{h^2} + \frac{\omega_2^2}{h_2^2}\right)^{3/2}} \qquad (C.7)$$

For $\omega_1 = \omega \cos\theta$, $\omega_2 = \omega \sin\theta$, and because $S_{1,\theta}(\omega) = \pi\omega S(\underline{\omega})$, we finally obtain:

$$S_{1,\theta}(\omega) = \frac{\sigma^2}{2}\ \frac{\omega}{h_1 h_2\left[1 + \omega^2\left(\frac{\cos^2\theta}{h_1^2} + \frac{\sin^2\theta}{h_2^2}\right)\right]^{3/2}} \qquad (C.8)$$

APPENDIX D

In this appendix we derive the relationship between the geometric function $H(\underline{\omega})$ of an area A, for a rotation of the area with angle β, and the function $H_o(\underline{\omega})$, which corresponds to zero rotation. The definition of the axis of zero rotation is arbitrary and is conveniently chosen such that the evaluation of the integral (5.20) defining the characteristic function is easy.

In the case of the triangle at Figure D.1 for example, it is convenient to define the x^o axis of zero rotation parallel to side AB of the triangle. Then the Cartesian system x^o, y^o will be oriented at an angle β to the original x,y system (see Figure D.2). For a triangle we can define the angle of rotation β as:

$$\beta = \arctan \frac{y_B - y_A}{x_B - x_A} \tag{D.1}$$

where x_A, y_A and x_B, y_B are the coordinates of the points A and B of the triangle in the original system. We note that the corners A,B,C of the triangle are taken such that they form a counterclockwise set. The point P is an arbitrary but specific point inside the area. It might be convenient to take P as the centroid of the area.

We derive now the relation between $H(\underline{\omega})$ corresponding to rotation angle β and $H_o(\underline{\omega})$ corresponding to zero rotation. For example, let the region be the triangle defined in Figure D.2. If we make the transformation:

$$\underline{z} = \underline{w} e^{-i\beta} \tag{D.2}$$

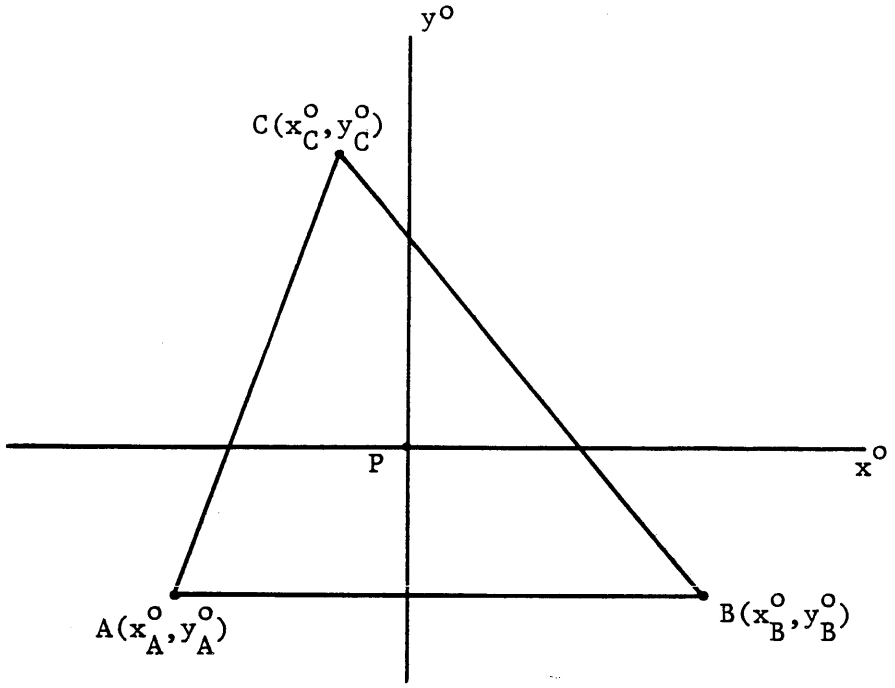

Figure D.1 Definition sketch of triangle ABC in $(x^o y^o)$ coordinate system.

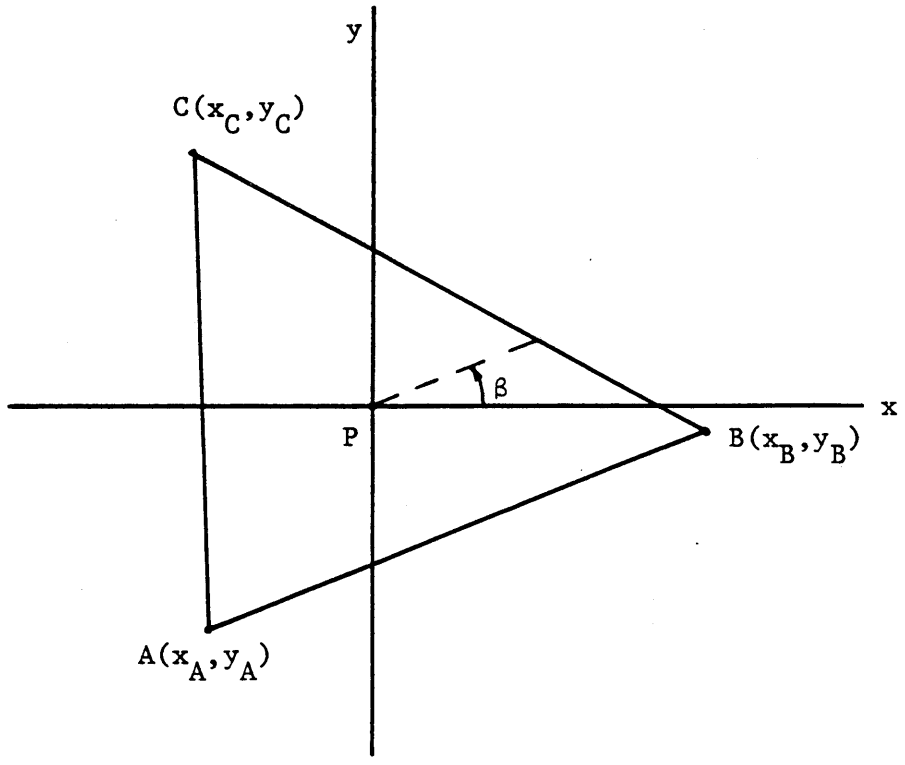

Figure D.2 Triangle ABC in (x,y) coordinate system.

where $\underline{w} = (x,y)$ is in the original domain and $\underline{z} = (x^o,y^o)$ is in the transformed domain, the triangle ABC will be mapped into another triangle $A_oB_oC_o$ of the same geometry but having side A_oB_o taken as a vector parallel to the x^o axis. The triangle $A_oB_oC_o$ is defined to have zero rotation $\beta = 0$, so that it then corresponds to the characteristic function $H_o(\underline{\omega})$.

Let $H(\underline{\omega})$ be the characteristic function for the triangle ABC. We get from (5.20)

$$H(\underline{\omega}) = \int_{R^2} e^{-i\underline{\omega}\underline{w}} f_o(\underline{w})d\underline{w} \tag{D.3}$$

The probability density function of $\underline{w}$ is given by:

$$f_o(\underline{w}) = \frac{1}{A} \tag{D.4}$$

where A is the area of the region. Substituting (D.4) and (D.2) into (D.3) we get:

$$H(\underline{\omega}) = \frac{1}{A} e^{i\beta} \int_{R^2} e^{-i\underline{\omega}e^{i\beta}\underline{z}}d\underline{z} \tag{D.5}$$

The characteristic function $H_o(\underline{\omega})$ is defined as:

$$H_o(\underline{\omega}) = \frac{1}{A} \int_{R^2} e^{-i\underline{\omega}\underline{z}}d\underline{z} \tag{D.6}$$

Thus (D.5) becomes:

$$H(\underline{\omega}) = e^{i\beta} H_o(\underline{\omega} e^{i\beta}) \tag{D.7}$$

or

$$|H(\underline{\omega})|^2 = |H_o(\underline{\omega} e^{i\beta})|^2 \tag{D.8}$$

This equation relates the characteristic functions between two areas of the same geometry and relative rotation of angle β.

Using this relation we need to calculate the function $H_o(\underline{\omega})$ only once. Then if the area rotates we use (D.8) to calculate $H(\underline{\omega})$ for the rotated areas. This would be useful, for example, in generating areal averages over triangular finite elements of the field of permeabilities in groundwater models.

We note here that (D.8) is valid for any geometry of averaging region. The example of the triangle was taken only for illustration purposes.

APPENDIX E

In this appendix we are going to derive expressions for the characteristic function $|H_o(\underline{\omega})|^2$ for some useful geometries: squares, rectangles and triangles.

Rectangles (and squares)[1]

We derive first $|H_o(\underline{\omega})|^2$ in the case of a rectangular (or square) region with sides L_x and L_y, respectively (see Figure E.1). The point P is chosen as the centroid of the area. The characteristic function $H_o(\omega)$ is given by (5.20):

$$H_o(\underline{\omega}) = \int_{R^2} e^{-i\underline{\omega}\underline{w}} f_o(\underline{w}) d\underline{w} \qquad \text{(E.1)}$$

where:

$$f_o(\underline{w}) = \begin{cases} \frac{1}{A} & \text{if } \underline{w} \text{ in region A} \\ 0 & \text{elsewhere} \end{cases}$$

Equation (E.1) then is written as:

$$H_o(\underline{\omega}) = \frac{1}{A} \int_A e^{-i\underline{\omega}\underline{w}} d\underline{w} = \frac{1}{A} \int_{-L_y/2}^{L_y/2} \int_{-L_x/2}^{L_x/2} e^{-i(\omega_1 x + \omega_2 y)} dxdy =$$

$$= \frac{1}{A} \int_{-L_y/2}^{L_y/2} e^{-i\omega_2 y} dy \int_{-L_x/2}^{L_x/2} e^{-i\omega_1 x} dx =$$

[1] A different derivation can be found in Matheron (1960) or in Lenton (1974; with some errors).

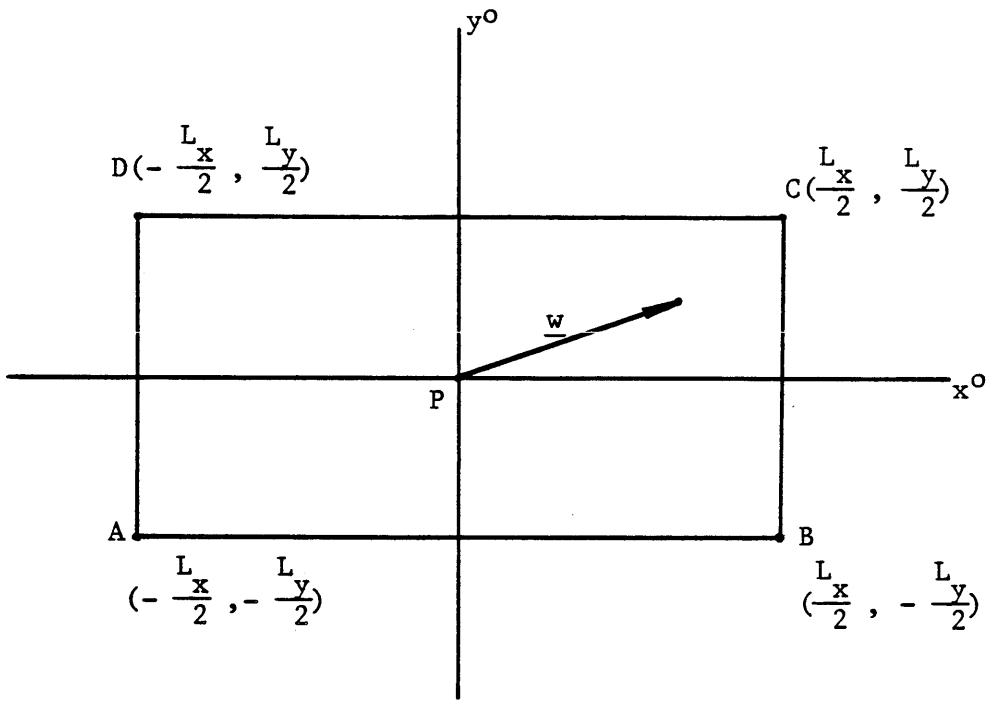

Figure E.1 Rectangular (ABCD) in coordiante system (x^o,y^o).

$$= \frac{1}{A}\left[-\frac{1}{i\omega_2}\left(e^{-i\omega_2 L_y/2} - e^{i\omega_2 L_2 y/2}\right)\right]\left[-\frac{1}{i\omega_1}\left(e^{-i\omega_1 L_x/2} - e^{i\omega_1 L_x/2}\right)\right] =$$

$$= -\frac{4}{A\omega_1\omega_2}\sin\left(\frac{\omega_1 L_x}{2}\right)\cdot\sin\left(\frac{\omega_2 L_y}{2}\right) \qquad (E.2)$$

but $A = L_x \cdot L_y$, so that

$$H_o(\underline{\omega}) = -\frac{4}{L_x L_y \omega_1 \omega_2}\sin\left(\frac{\omega_1 L_x}{2}\right)\sin\left(\frac{\omega_2 L_y}{2}\right) \qquad (E.3)$$

The function $|H(\underline{\omega})|^2$ then is given by

$$|H_o(\underline{\omega})|^2 = \frac{16}{L_x^2 L_y^2 \omega_1^2 \omega_2^2}\sin^2\left(\frac{\omega_1 L_x}{2}\right)\cdot\sin^2\left(\frac{\omega_2 L_y}{2}\right) \qquad (E.4)$$

for a rectangle. For a square $L_x = L_y$.

Triangles

We derive now the function $|H_o(\underline{\omega})|^2$ in the case of a triangle region (Figure E.2). It is assumed that the side AB is taken as a vector is parallel to x^o axis and the point P represents a characteristic point inside the region (for example the centroid of the triangle). For axes x^o, y^o passing through P the characteristic function $H_o(\underline{\omega})$ is given by:

$$H_o(\underline{\omega}) = \int_{R^2} e^{-i\underline{\omega}\underline{w}} f_o(\underline{w})\,d\underline{w} \qquad (E.5)$$

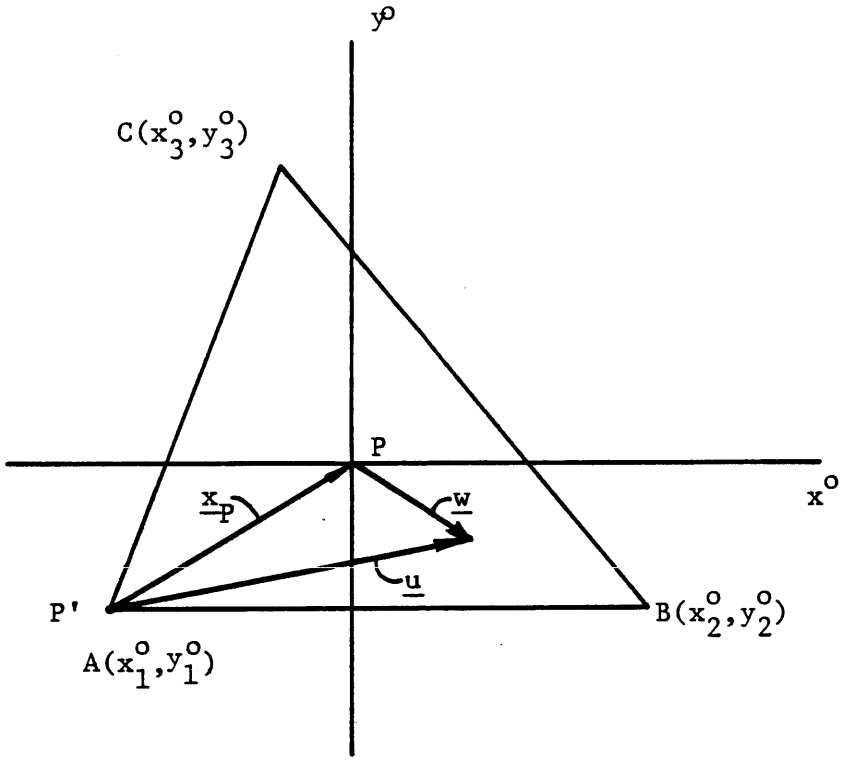

Figure E.2 Triangle ABC in coordinate system (x^o, y^o).

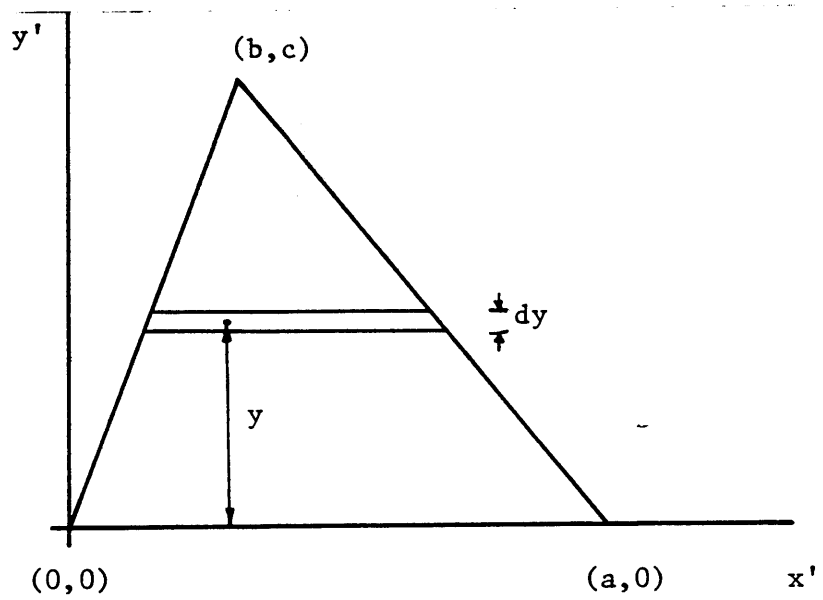

Figure E.3 Triangle ABC in coordinate system (x', y').

where $\underline{w}$ is the vector distance from origin P. If we define a new origin P' to coincide with the corner A of the triangle, and a new system of orthogonal axes x', y' parallel to original axes x^o, y^o, we can write (Figure E.3):

$$\underline{w} = \underline{u} - \underline{x}_p \tag{E.6}$$

where $\underline{x}_p$ is the vector with origin P' ending at point P, and $\underline{u}$ is a vector with origin $\underline{P}'$, corresponding to the point $\underline{w}$ in the original coordinate system. (E.6) gives:

$$d\underline{w} = d\underline{u} \tag{E.7}$$

We also know that $f_o(\underline{w}) = f'_o(\underline{u})$ where:

$$f'_o(\underline{u}) = \begin{cases} \frac{1}{A} & \text{if } \underline{u} \\ 0 & \text{elsewhere} \end{cases}$$

In the new system with origin at $P' \equiv A$ and axes x'y', see Figure E.3, (E.5) becomes:

$$H_o(\underline{\omega}) = \int_{R^2} e^{-i\underline{\omega}(\underline{u}-\underline{x}_p)} f'_o(\underline{u}) d\underline{u} = \frac{1}{A} e^{i\underline{\omega}\underline{x}_p} \int_A e^{-i\underline{\omega}\underline{u}} d\underline{u} \tag{E.8}$$

The coordinates of the corner A=P' in the new axes are (0,0). Let the coordinates of B and C be (a,0) and (b,0) respectively. The integral on the right-hand side of (E.8) is

$$I = \int_A e^{-i\omega \underline{u}} \, d\underline{u} \tag{E.9}$$

$$= \int_A [\cos(\omega_1 x' + \omega_2 y') - i \sin(\omega_1 x' + \omega_2 y')] dx' dy' \tag{E.10}$$

We define:

$$I_R = \int_A \cos(\omega_1 x' + \omega_2 y') dx' dy' \tag{E.11a}$$

$$I_M = \int_A \sin(\omega_1 x' + \omega_2 y') dx' dy' \tag{E.11b}$$

So that (E.10) can be simply written as:

$$I = I_R - iI_M \tag{E.12}$$

The limits of integration are given in Figure E.3, so that:

$$I_R = \int_o^c \left\{ \int_{(\frac{b}{c})y'}^{a-(\frac{a-b}{c})y'} \cos(\omega_1 x' + \omega_2 y') \, dx' \right\} dy' \tag{E.13}$$

We call the integral inside the brackets Π_R and we get:

$$\Pi_R = \frac{\sin(\omega_1 x' + \omega_2 y')}{\omega_1} \Bigg|_{\frac{b}{c} y'}^{a - \frac{a-b}{c} y'}$$

$$= \frac{1}{\omega_1} \{\sin[\omega_1 (a - \frac{a-b}{c} y') + \omega_2 y'] - \sin[(\omega_1 \frac{b}{c} + \omega_2) y']\}$$

Thus (E.13) becomes

$$I_R = \int_o^c \Pi_R dy' = \frac{1}{\omega_1} \{ \frac{\cos\ \omega_1(a - \frac{a-b}{c}\ y') + \omega_2 y'}{\omega_1 \frac{a-b}{c} - \omega_2} +$$

$$+ \frac{\cos[(\omega_1 \frac{b}{c} + \omega_2)y']}{\omega_1 \frac{b}{c} + \omega_2} \Big|_o^c \}$$

$$= \frac{c}{\omega_1} \{ \frac{\cos[b\omega_1 + c\omega_2] - \cos(a\omega_1)}{(a-b)\omega_1 - c\omega_2} + \frac{\cos[b\omega_1 + c\omega_2] - 1}{b\omega_1 + c\omega_2} \}$$

$$= \frac{c}{\omega_1} \{ \cos(b\omega_1 + c\omega_2) \ [\frac{a\omega_1}{[(a-b)\omega_1 - c\omega_2][b\omega_1 + c\omega_2]}] -$$

$$- \frac{\cos(a\omega_1)}{(a-b)\omega_1 - c\omega_2} - \frac{1}{b\omega_1 + c\omega_2} \} \qquad \text{(E.14)}$$

I_M is calculated similarly:

$$I_M = \int_o^c \{ \int_{\frac{b}{c} y}^{a - \frac{a-b}{c} y'} \sin(\omega_1 x' + \omega_2 y')\ dx' \} dy' \qquad \text{(E.15)}$$

Define the integral inside the brackets as Π_M , we get then:

$$\Pi_M = - \frac{\cos(\omega_1 x' + \omega_2 y')}{\omega_1} \Big|_{\frac{b}{c} y'}^{a - \frac{a-b}{c} y'} =$$

$$= - \frac{1}{\omega_1} \{ \cos[\omega_1(a - \frac{a-b}{c}\ y') + \omega_2 y'] - \cos[(\frac{b}{c}\ \omega_1 + \omega_2)y'] \}$$

Equation E.15 then becomes

$$I_M = \int_o^c \Pi_M dy' = \frac{1}{\omega_1} \{ \frac{\sin[\omega_1(a - \frac{a-b}{c} y') + \omega_2 y']}{\omega_1 \frac{a-b}{c} y' - \omega_2 y'} +$$

$$+ \frac{\sin[(\omega_1 \frac{b}{c} + \omega_2)y']}{\frac{b}{c}\omega_1 + \omega_2} \Big|_o^c \} =$$

$$= \frac{c}{\omega_1} \{ \frac{\sin b\omega_1 + c\omega_2 - \sin(a\omega_1)}{(a-b)\omega_1 - c\omega_2} + \frac{\sin b\omega_1 + c\omega_2}{b\omega_1 + c\omega_2} \}$$

$$= \frac{c}{\omega_1} \{ \sin b\omega_1 + c\omega_2 \quad \frac{a\omega_1}{[(a-b)\omega_1 - c\omega_2][b\omega_1 + c\omega_2]} -$$

$$- \frac{\sin(a\omega_1)}{(a-b)\omega_2 - c\omega_2} \} \qquad (E.16)$$

Using (E.8), (E.9), (E.13), (E.14) and (E.16) we get

$$H_o(\underline{\omega}) = \frac{1}{A} \{\cos(\omega_1 x_1^o + \omega_2 y_1^o) - i \sin(\omega_1 x_1^o + \omega_2 y_1^o)\} (I_R - iI_M)$$

Then:

$$|H_o(\underline{\omega})|^2 = \frac{1}{A^2} \{ [\cos(\omega_1 x_1^o + \omega_2 y_1^o) I_R - \sin(\omega_1 x_1^o + \omega_2 y_1^o) I_M]^2 +$$

$$+ [\cos(\omega_1 x_1^o + \omega_2 y_1^o) I_M + \sin(\omega_1 x_1^o + \omega_2 y_1^o) I_R]^2 \} \qquad (E.17)$$

In (E.14) and (E.16) we substitute:

$$a = x_2^o - x_1^o$$

$$b = x_3^o - x_1^o$$

$$c = y_3^o - y_1^o$$

We have then:

$$I_R = \frac{y_3^o - y_1^o}{\omega_1} \{\cos [(x_3^o - x_1^o)\omega_1 + (y_3^o - y_1^o)\omega_2] \cdot$$

$$\frac{(x_2^o - x_1^o)\omega_1}{[(x_2^o - x_3^o)\omega_1 - (y_3^o - y_1^o)\omega_2][(x_3^o - x_1^o)\omega_1 + (y_3^o - y_1^o)\omega_2]} -$$

$$- \frac{\cos[(x_2^o - x_1^o)\omega_1]}{(x_2^o - y_3^o)\omega_1 - (y_3^o - y_1^o)\omega_2} - \frac{1}{(x_3^o - x_1^o)\omega_1 + (y_3^o - y_1^o)\omega_2} \} \qquad \text{(E.18)}$$

$$I_M = \frac{y_3^o - y_1^o}{\omega_1} \{\sin [(x_3^o - x_1^o)\omega_1 + (y_3^o - y_1^o)\omega_2] \cdot$$

$$\frac{(x_2^o - x_1^o)\ \omega_1}{[(x_2^o - x_3^o)\omega_1 - (y_3^o - y_1^o)\omega_2][(x_3^o - x_1^o)\omega_1 + (y_3^o - y_1^o)\omega_2]} -$$

$$- \frac{\sin\ (x_2^o - x_1^o)\omega_1}{(x_2^o - x_3^o)\omega_1 - (y_3^o - y_1^o)\omega_2} \} \qquad \text{(E.19)}$$

From (E.17), (E.18) and (E.19) we calculate $|H_o(\omega_1, \omega_2)|^2$ easily.